SAPIENZA
Università di Roma
Facoltà di Scienze Matematiche Fisiche e Naturali

DOTTORATO DI RICERCA
IN GENETICA E BIOLOGIA MOLECOLARE

XXX Ciclo
(A.A. 2016/2017)

IMPORTIN BETA REGULATES MITOSIS VIA DISTINCT MOLECULAR MECHANISMS

Annalisa Verrico

Docente guida
Dr. Patrizia Lavia

Tutore
Prof. Maria Eugenia Schininà

Coordinatore
Prof. Fulvio Cruciani

"Qualunque decisione tu abbia preso per il tuo futuro, sei autorizzato, e direi incoraggiato, a sottoporla ad un continuo esame, pronto a cambiarla, se non risponde più ai tuoi desideri."

Rita Levi-Montalcini

ACKNOWLEDGMENTS

My PhD project was carried out in Dr. Patrizia Lavia's laboratory at the Institute of Molecular Biology and Pathology-CNR (National Research Council of Italy), c/o University "La Sapienza", Rome, and was supported by AIRC (Associazione Italiana per la Ricerca sul Cancro). I want to express my gratitude to Patrizia, that has been my supervisor during my PhD work and also during my bachelor and master degree thesis. I want to thank her, for being my scientific guide and inspiration on how a scientist should work to produce the best he can. I have appreciated her scientific knowledge and I feel lucky to have been part of her laboratory. Finally, I want to thank her because she continuously represented a referring point that contributed to my scientific and personal growth.

A special thank goes to all members of the lab that I have met during these years. I am particular grateful to Maria Giubettini and Valeria de Turris, that have contributed to my initial training. I also want to thank Paola, Michela, Jessica, Federica, Lia, Elena, and Francesco for the stimulating and pleasant environment.

I also want to thank Dr. Giulia Guarguaglini, for her training and help with microscopy.

I want to thank my PhD Tutor, Dr. Maria Eugenia Schininà, for her availability to discuss and for their interesting and motivating suggestions, and Dr. Laura Di Francesco, for her support and essential help for proteomic experiments.

Finally, I want to thank Dr. Alessandro Rosa (Department of Biology and Biotechnology "Charles Darwin", University "Sapienza" of Rome) for his availability in generating the plasmid constructs used in this work.

INDEX

GLOSSARY

CHD4: chromodomain helicase DNA binding protein 4
CPC: chromosomal passenger complex
CRM1: chromosomal maintenance 1
Dox: Doxycycline
ER: endoplasmic reticulum
FG: phenyl-glycine
gamma-TuRC: tubulin ring complex
GEF: guanine nucleotide exchange factor
GTP: guanosine triphosphate
HAUS: homologous to augmin subunits
HURP: hepatoma up-regulated protein
IF: Immunofluorescence
K-fibre: kinetochore fibre
KMN: KNL1 MIS12 NDC80
KNL1: kinetochore null protein 1
KPNB1: Karyopherin Beta 1/ Importin beta 1
KT: kinetochore
MAP: microtubule-associated protein
MCAK: mitotic centromere-associated kinesin
MCRS1: microspherule protein 1
MEF: mouse mutant embryonic fibroblast
MIP: Maximum Intensity Projection
MIS12: mis-segregation 12
MT: microtubule
MTOC: MT-organizing centres
NDC80: nuclear division cycle 80
NE: nuclear envelope
NEB: nuclear envelope breaks down
NES: nuclear export signal
NLS: nuclear localization signal
NPC: nuclear pore complex
NUP: nucleoporins
NuRD: nucleosome-remodeling deacetylase
NuSAP: nucleolar and spindle-associated protein

OP18: oncoprotein 18
PIAS: protein inhibitor of activated of STAT
PLA: proximity ligation assay
RAN: RAs-related Nuclear protein
RANBP1: RAN binding protein1
RANBP2/NUP358: RAN-binding protein 2/Nucleoporin 358
RANGAP: GTP-hydrolysis activating factor for RAN
RCC1: Regulator Of Chromosome Condensation 1
RRSU: RANBP2-RANGAP1-SUMO-UBC9
SAF: spindle assembly factor
SENP: Sentrin specific proteases
SIM: SUMO interaction motif
Ska: spindle and kinetochore-associated
SUMO: small ubiquitin-related modifier
TOP2A: Topoisomerase II alpha
TPX2: targeting protein for Xklp2
WB: Western blotting

SUMMARY

Importin beta is the main vector for protein nuclear import in interphase and a global regulator of mitosis. Its functions reflect its ability to interact with, and regulate, different pathways during the cell cycle, operating as a major effector of the GTPase RAN. Importin beta is overexpressed in many cancer types characterized by high genetic instability. In this project, I have investigated Importin beta mitotic functions in mammalian cells, using multiple and complementary approaches.

In the first part of my PhD project, I aimed to obtain a global view of Importin beta mitotic interactors, which were previously only known from studies of individual factors. Endogenous Importin beta was co-immunoprecipitated from cells synchronised in mitosis, then proteome-wide mass spectrometry analysis was performed. Both known and new interactors of Importin beta were identified. In order to validate the newly identified protein-protein interactions, I developed an automated protocol for proximity ligation assays (PLA) to detect the spatial and temporal windows of interactions *in situ*. Interestingly, many Importin beta partners in our mitotic interactome list hint at unexpected pathways via which Importin beta might regulate mitosis.

In parallel, I sought to gain new information on downstream molecular pathways regulated by Importin beta. To that aim, I generated a stable cell line that can be induced to overexpress EGFP-tagged Importin beta under tetracycline control. With this biological tool I have investigated Importin beta mitotic roles.

A major Importin beta interactor is RANBP2, a large nucleoporin (NUP) residing at nuclear pore complexes (NPCs) in interphase; in mitosis it localizes at microtubules (MTs), and a fraction accumulates at kinetochores (KTs) after MT/KT attachment. RANBP2 has SUMO (small ubiquitin-related modifier) ligase and stabilizing activities, and regulates protein SUMO conjugation.

RANBP2, together with SUMO-RANGAP1 (the GTP-hydrolysis activating factor for the GTPase RAN) and Ubc9 (a SUMO E2 enzyme), form a multimeric SUMO-E3-ligase complex, called RRSU. Using the PLA technique, I found that RANBP2 interactions with Importin beta are abundant in prometaphase and are downregulated in metaphase. Importin beta overexpression prevents RANBP2 recruitment at KTs in metaphase. In turn, this prevents SUMO-modification of Topoisomerase II alpha (TOP2A). Impaired accumulation of SUMO-TOP2A at centromeres in Importin beta- overexpressing cells was associated with chromosome mis-segregation. Thus, Importin beta influences KT functions by regulating RANBP2 localization and interactions at KTs, and hence modulating the SUMOylation of downstream targets such as TOP2A.

Importin beta interaction with NUPs involves its NUP-binding domain, mapping in the 45-462 region. To understand the functional roles of this domain in mitosis, I generated stable cell lines for two Importin beta mutants: (i) I178A/Y255A Importin beta, defective for NUP-binding; (ii) 45-462 Importin beta, which only contains the NUP-binding region. I found however that the 45-462 region alone is unstable and subjected to proteasome-mediated degradation. Henceforth, the NUP binding region was studied in the cell line expressing Importin beta^{I178A,Y255A}. In functional assays, overexpression of Importin beta^{WT}, but not NUP-binding defective mutant, dramatically increases MT destabilization. Instead, MT reassembly was similarly impaired and/or delayed by both WT and I178A/Y255A Importin beta. Thus, Importin beta acts in distinct pathways, i.e. MT dynamic instability and MT growth, respectively dependent and independent on the NUP-binding domain.
Proteomic analysis in mitotic cells using the GFP trap method identified both common and specific partners for Importin beta^{WT} and I178/Y255 mutant. An interesting difference emerged regarding the protein HURP (Hepatoma Up Regulated Protein,

involved in kinetochore-fibres stabilization), an Importin beta binding partner selectively lost in the co-IP of Importin beta$^{I178A/Y255A}$. I found that Importin beta^{WT} overexpression (but not I178A/Y255A mutant) alters HURP localization, preventing its accumulation on kinetochore-fibres, suggesting that Importin beta-dependent MT destabilization is likely associated with HURP displacement.

Overall, the results of this project clarify mitotic roles of Importin beta at the level of KTs and MTs in mitosis. They identify specific roles mediated by RANBP2 and HURP, and indicate that elevated concentrations of Importin beta, such as found in cancers, disrupts mitotic control.

INTRODUCTION

Mitotic cell division is a crucial step during cell life, and ensures the generation of two identical daughter cells. In this process two main specialized structures are assembled to orchestrate chromosome congression and segregation in daughter cells:

(i) the mitotic spindle, made up of highly dynamic polymers of tubulin, the microtubules (MTs), to which several motor proteins associate;
(ii) the kinetochores (KTs), multimeric protein structures assembled at the centromeric region of chromosomes, with which MTs establish stable interactions.

Each chromosome, via its KT, must bind MTs: more specifically, sister chromatids bind MTs emanating from opposite spindle poles in order to equally partition the genetic information into the newly forming cells. MT dynamics and correct attachment to KTs are highly regulated processes: if errors occur, chromosome mis-segregation will take place and aneuploid cells may be generated. Aneuploidy is a recognised hallmark of cancer associated with poor prognosis (*Holland and Cleveland, 2012*).

The RAN GTPase network, with its regulators, transport vectors and nucleoporins (NUPs) regulate nucleo-cytoplasmic transport of proteins in interphase and take on a new role as regulators of the mitotic apparatus when the nuclear envelope breaks down (NEB) and transport ceases.

In my PhD Thesis I have investigated the mitotic roles of Importin beta (also known as Karyopherin Beta 1, KPNB1), the main vector for protein import in interphase nuclei. Importin beta was previously found to perturb mitosis when overexpressed, but how exactly it operates in mitotic cells is only partially understood. The work carried out in this Thesis identifies at least two pathways through which Importin beta affects mitosis: (i) it regulates KT functions; (ii) it regulates MT functional properties.

1. Importin beta, a multifunctional protein with multiple roles in cell life.

1.1. Structural studies and the dissection of Importin beta's function in nucleocytoplasmic transport

Eukaryotic cells are compartmentalised and have specific transport systems for communication between the cytoplasm, membranous organelles and the nucleus. Nucleo-cytoplasmic transport system is essential to connect functionally nucleus and cytoplasm. Transport of molecules in and out of the nucleus takes place through nuclear pore complexes (NPCs), very large protein complexes (about 60 MDa) that regularly fenestrate the nuclear membrane (*Sorokin et al., 2007*). Small cargoes (<40 kDa) diffuse rapidly through the NPC; larger molecules, instead, require an active mechanism, that involves soluble nuclear transport receptors, belonging to the Importin- (also called karyopherin) beta family. The prototype member of this family, and focus of this Thesis, is Importin beta-1 (for simplicity it will be referred to as Importin beta only).

Importin beta is a major effector of the GTPase RAN (RAs-related Nuclear protein) and a highly conserved member of the superfamily of nuclear transport receptors. It was originally identified as the main transport vector for protein import in interphase nuclei. Given the importance of this process in delivering nuclear factors in a regulated manner during cell life (e.g. DNA replication and repair factors, transcription factors, epigenetic and chromatin- modifying factors), that discovery was awarded the Nobel Prize for Biomedicine to G. Blobel in 1999.

In nuclear import, Importin beta acts via different adaptors, belonging to the Importin alpha transport receptor family. In the most classical import pathway, Importin alpha recognizes proteins bearing a nuclear localization signal (NLS), assembling in the "import complex" [Importin beta/Importin alpha/NLS-containing cargo] (*Görlich et al, 1995)*. In the direct import pathway, Importin beta interacts directly with NLS-cargoes, without the

alpha adaptors. Once the import complex has assembled in cytoplasm, Importin beta traverses the nuclear envelope (NE) by binding with nucleoporins. In the nucleus, the import complex dissociates to release the cargoes. This process is highly regulated, and a major role is played by the GTPase RAN. RAN is present in the GTP-loaded form in the nucleus, due to the association of the RAN guanine nucleotide exchange factor (GEF), termed RCC1 (Regulator of Chromosome Condensation 1), with chromatin. RANGTP has high affinity for Importin beta: its binding to Importin beta dissociates the import complex, hence releasing cargoes free in the nucleoplasm (*Izaurralde et al, 1997*). RANGTP and Importin beta then exit the nucleus. They dissociate in the cytoplasm, after RANGTP hydrolysis by RANGAP (GTP-hydrolysis activating factor for RAN), which resides in the cytoplasm). A schematic view of the import process is given in **Figure 1.**

Importin beta functions in nuclear import are possible due to its modular structure. It is composed of 19 HEAT repeats, arranged in a superhelical spiral ("HEAT" is an acronym for four proteins in which this repeat structure is found: Huntingtin, elongation factor 3 (EF3), protein phosphatase 2A (PP2A), and the yeast kinase TOR1).

These repeats arrange in Importin beta structure and constitute three functional domains (**Figure 2**) (*Strom and Weis, 2001*):

- the N-terminal domain harbours the sites of interaction with RANGTP (HEATs 1-8, residues 1-364) (*Kutay et al., 1997; Cingolani et al., 1999*).
- the central region contains multiple binding sites for phenyl-glycine (FG and FxFG)-rich repeats, present in NUPs (HEATs 5-7, residues 152-352) (*Chi et al., 1997*).
- the C-terminal region harbours the binding domain for Importin alpha adaptors, and hence NLS protein (HEATs 7-19, residues 331-876) (*Kutay et al., 1997, Cingolani et al., 1999*).

Interaction studies using Importin beta truncated forms were instrumental to dissect Importin beta structure and function.

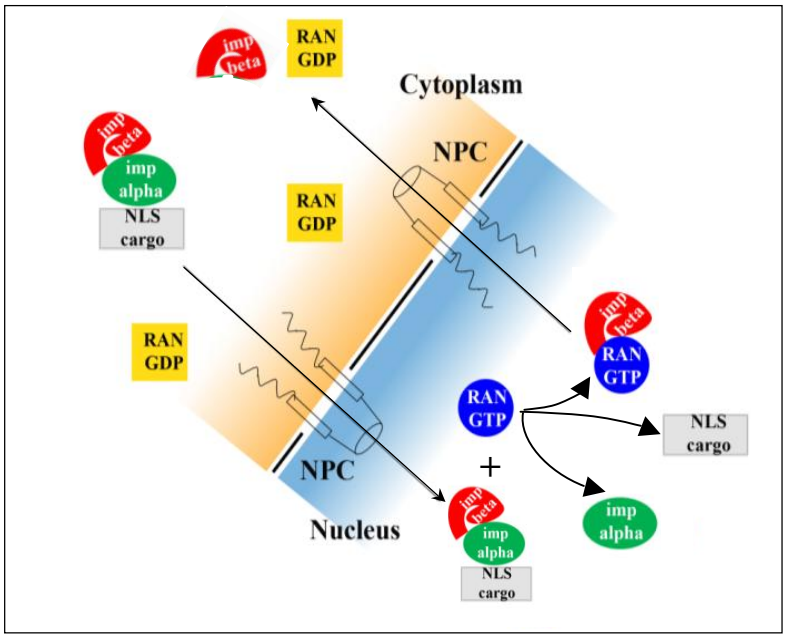

Figure 1: Schematic view of RAN/Importin beta dependent nuclear import. Import complexes assemble in the cytoplasm and are composed of an import cargo (NLS-cargo, grey square), an Importin alpha receptor (green filled circle) and Importin beta (red shaped). Importin beta then drives the entire complex across the nuclear pore complex (NPC) (symbolized by an arrow). RANGTP (blue filled circles) is highly enriched in the nucleus: therein it binds Importin beta and releases free cargo. RANGTP/Importin beta exit the nucleus together (reverse arrow) and dissociate in the cytoplasm, where RANGTP is hydrolyzed to RANGDP (orange square) so that the free pool of Importin beta is re-established.

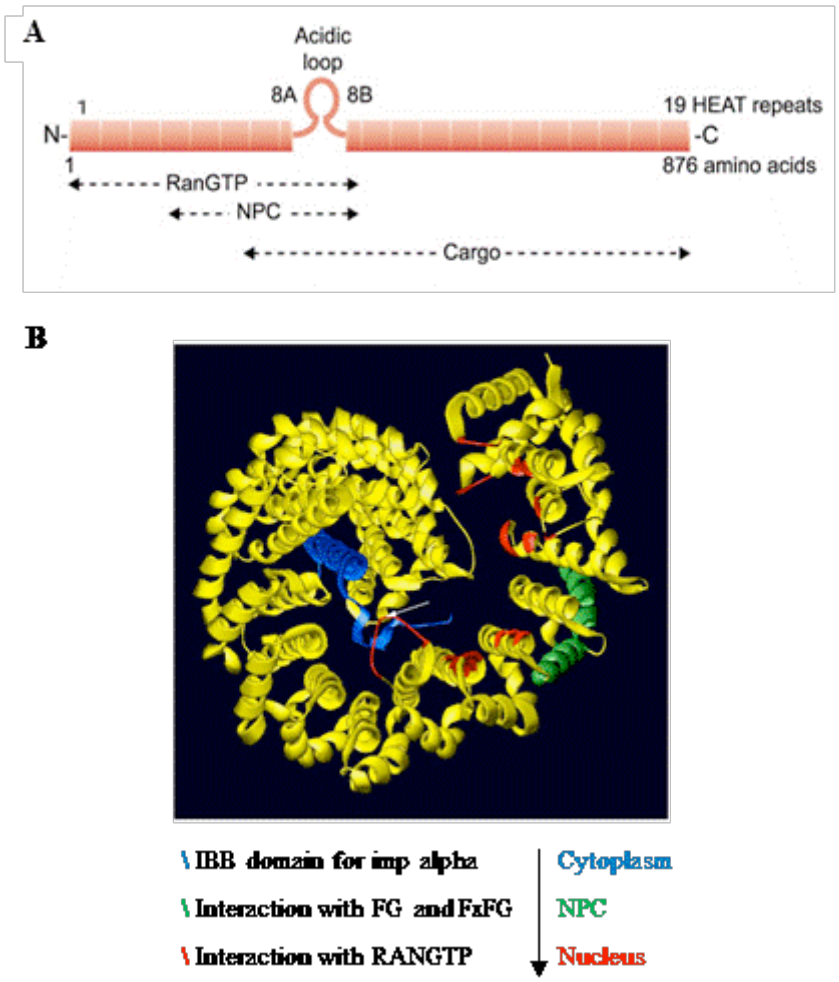

Figure 2: Representation of Importin beta functional domains and structure. A. Importin beta linear map: the binding regions for protein partners are indicated. **B.** 3D-representation of Importin beta structure; the colored domains show the position at which the indicated classes of interactors bind Importin beta (modified from *Ström and Weis, 2001*).

These studies showed that deletion of residues 1-45 impairs RAN binding on Importin beta. In addition, deletion of a small C-terminal region (1-771) prevented Importin alpha binding. Finally, the mutant 45-462 binds neither RAN, nor Importin alpha, but still binds NUPs.

The NUP-binding domain was further dissected in structural studies: in particular, site-directed mutagenesis showed that residues I178 and Y255 are crucial for NUP binding (*Bayliss et al., 2000*).

Subsequent in vitro studies showed the existence of additional NUP-binding sites nearer the C-terminal domain (between HEAT repeats 14 and 16); although these latter sites have weaker affinity for NUPs compared to the N-terminal sites, they are still required for the passage of Importin beta through NPCs (*Bednenko et al., 2003, Otsuka et al., 2008*). Indeed, in a structural model proposed by *Bednenko et al. (2003),* Importin beta is propelled to traverse the NPC via a succession of continuously alternating binding of the N- and the C-terminal domains with progressive NUPs, in a manner that drives and facilitates the translocation of import complexes through the NPCs. Together these data indicate that there is an intrinsical "polarity" in the organisation of Importin beta domains, which corresponds to the directionality of the import process.

The import process depends on the ability of Importin beta to establish specialised interactions, using distinct domains, in different compartments of the cell. The production of crystals for many of these interactions *(Vetter et al., 1999; Cingolani et al., 1999; Bayliss et al., 2000; Cingolani et al., 2002*) has revealed that Importin beta undergoes twisted conformational changes when the N-terminal domain is complexed with RANGTP. These studies indicate that Importin beta has evolved a mechanism of mutually exclusive interactions with either RANGTP, or with Importin alpha: this mechanism ensures the assembly of stable import

complexes (in which Importin beta binds Importin alpha) in the cytoplasm, from which RANGTP is absent, and an efficient release in the nucleus, where RANGTP is highly abundant.
In conclusion, Importin beta regulation of protein import in nuclei underlies its control of fundamental processes, such as DNA replication, DNA repair, transcriptional and epigenetic control of gene expression (*Chook and Süel, 2011; Kimura et al., 2014*).

1.2. Importin beta: beyond nucleocytoplasmic transport

Beyond its established role in nucleo-cytoplasmic transport, Importin beta is also known to regulate the localization and activity of factors implicated in mitotic spindle organization and function after nuclear envelope breakdown (NEB) (*Forbes et al., 2015*). In addition, at the end of mitosis, it regulates the reorganization of the NE, NPCs and nuclear structure (*Schellhaus et al., 2016; Ungricht et al., 2017*).
Early indications of a possible mitotic role came from the observation that Importin beta localizes at the mitotic spindle (**Figure 3**). Indeed, after NEB, Importin beta and alpha are recruited to mitotic spindle, associating with MTs via dynein, a motor protein (*Ciciarello et al., 2004*). When associated with MTs, Importin beta still interacts with partner proteins and inhibits their unscheduled activity. Analogous to the mechanism operating in nuclear import, RANGTP binding to Importin beta releases those proteins in a free, biologically active form, thus enabling relevant mitotic events to take place.

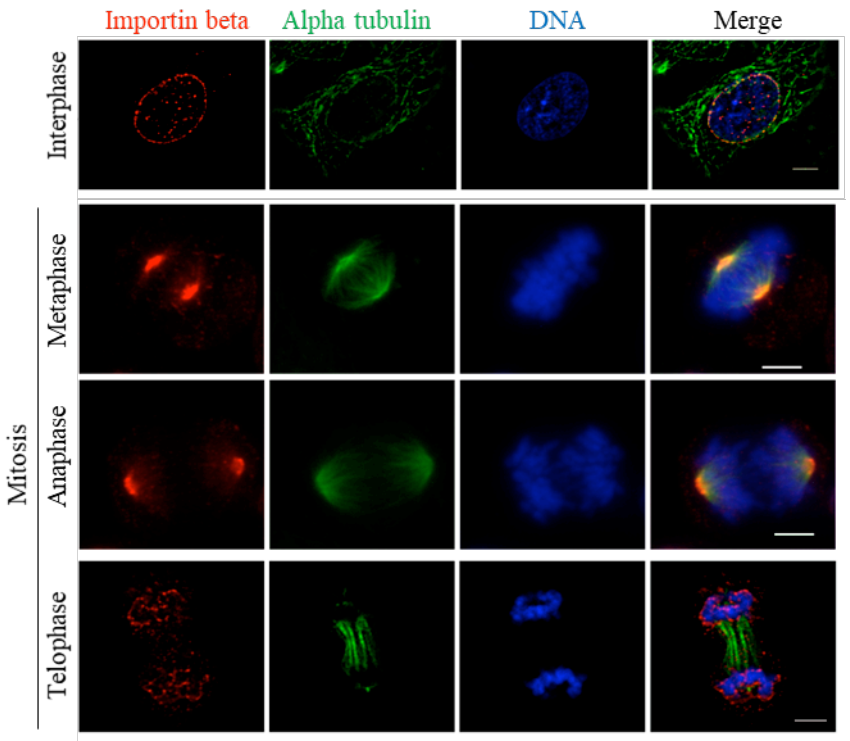

Figure 3. Importin beta localization. Localization of Importin beta, detected by immunofluorescence, in HeLa cells. Importin beta (red) accumulates in the nucleus and around the nuclear envelope in interphase, to be then recruited at mitotic spindle microtubules and poles until anaphase; later in telophase it relocalizes around the segregating chromatin, where the nuclear envelope will reform. Bars, 5 µm.

A well-known class of "mitotic cargoes comprises spindle assembly factors (SAFs), factors that promote the assembly (or nucleation) of microtubules into a bipolar spindle at mitosis and spindle pole-organizing factors. Among microtubule-associated proteins (MAPs), the best known are TPX2 and NuMA, operating at spindle poles, as well as Xnf7, HURP, Maskin, and NuSAP, which associate with MTs. Other SAFs include kinesins (XCTK2, Kid), which affect the spindle dynamic activity, spindle matrix proteins (Lamin B, Rae) and also some NPC proteins (Nup107-160, Nup98, ELYS/Mel28) (**Figure 4**) (reviewed in *Kalab and Heald 2008; Forbes et al., 2015*).

Spindle Assembly Factors (SAFs)	
MAPs	TPX2, NuMA, Xnf7, HURP, Maskin, NuSAP
Kinesins	XCTK2, Kid
Spindle matrix proteins	Lamin B, Rae1
K-fiber stabilization	MCRS1
Tumor suppressor	Adenomatous polyposis Coli (Apc)
Chromatin remodeling ATPases	CHD4, ISWI
Multiple cellular functions	Nucleophosmin, Survivin, Cdk11
NPC proteins	Nup107-160 complex, Nup98, ELYS/Mel28
NPC Assembly Factors	
Importin beta and/or transportin regulated Nups	Nup107-160 complex, ELYS, FG Nups (Nup358, Nup214, Nup153, Nup98, Nup62, Nup50)
Ran Modulation Factors	
	RCC1, RanGAP, RanBP1*, RanBP2, Sumo

Figure 4: Targets of Importin beta/RAN regulation of mitotic spindle assembly. Adapted from *Forbes et al., 2015.*

Because the hypothesized mechanism of action of Importin beta in mitotic control is that it inhibits factors that are then released by RANGTP (reviewed in *Kalab and Heald 2008; Forbes et al., 2015*), it is clear that a very important role is exerted by the regulators of the GTP status on RAN: RCC1 and RANGAP. RCC1, the RANGEF, is involved in the regulation of onset of chromosome condensation in the S phase, and binds both to the nucleosomes and double-stranded DNA (*Ohtsubo et al., 1989*): thus, in mitosis, it generates RANGTP near chromosomes. RANGTP is also enriched in the centrosome area, where it is recruited by the protein AKAP450 (*Keryer et al., 2003*) and along the growing MTs (*Tedeschi et al., 2007*). The opposite player, RANGAP, promotes GTP hydrolysis on RAN. Together with its partners, RANBP1 (RAN binding protein1) and RANBP2 (RAN binding protein 2), RANGAP localizes on the mitotic spindle and, in part, at KTs after MT attachment (*Roscioli et al., 2012; Joseph et al., 2002*).
The asymmetric distribution of RAN regulators implies that mitotic factors will be preferentially activated in the MT area nearer to chromosomes and at centrosomes, where the RANGTP concentration is high, whereas they will be preferentially inhibited away from the mitotic apparatus, and subjected to a finely tuned balance of inhibitory (Importin beta) and releasing (RANGTP) activities along the spindle (*Ciciarello et al., 2007: Clarke an Zhang 2008; Kalab and Heald 2008; Roscioli et al, 2010; Forbes et al., 2015; Cavazza and Vernos, 2016*).
Despite of the wealth of localization studies, our mechanistic understanding of mitotic control by the RANGTP/Importin beta system remains limited.

2. The RAN network in mitotic spindle formation

As recalled, the formation of a proper mitotic spindle is necessary for a successful mitotic division. At the onset of mitosis, the duplicated centrosomes, which act as the major (but not unique)

MT-organizing centres (MTOC), move apart in opposite directions and begin to nucleate MTs. Growing and highly dynamic MTs start forming aster-like structures. These highly dynamic MTs project randomly in all directions in the cytoplasm, until they find a chromosome, in a process defined "search-and-capture" (*Heald and Khodjakov, 2015*).
It has also been demonstrated that animal cells experimentally deprived of their centrosomes can still assemble a functional mitotic spindle, the nucleation of which is driven by KTs (*Debec et al., 1995; Khodjakov et al., 2000*). However, mathematical simulations suggest that the search-and-capture mechanism, alone, could not account for the short time required for spindle assembly in most animal cells if it was not aided by positioning mechanisms emanating from chromosomes and orchestrated, at least in part, by RANGTP (*Wollman et al., 2005*). Not surprisingly, other mechanisms, independent on centrosomes, are involved in the formation of spindle MTs.
Indeed, two main mechanisms drive acentrosomal MT assembly in dividing cells: the first one is dependent on chromosomes, the second is dependent on nucleation of pre-existing MT themselves (reviewed by *Meunier and Vernos, 2016*). These different mechanisms are linked to one another in a sequence of events that ultimately lead to the formation of kinetochore MTs, often referred to as KT-fibres (K-fibres) within the bipolar spindle.

2.1 The chromosome-dependent mechanism of MT nucleation

Central to this mechanism is the signalling network mediated by the GTPase RAN (*Ciciarello et al., 2007; Clarke and Zhang 2008; Kalab and Heald, 2008*).
KTs contain a fraction of the export receptor CRM1 (Chromosomal maintenance 1), a RANGTP effector also belonging to the superfamily of nuclear transport receptors. KTs can thus assemble trimeric complexes with factors containing nuclear export sequences and RANGTP. The formation of such

complexes has been shown to be essential for MT nucleation from KTs (*Arnaoutov et al., 2005; Torosantucci et al., 2008*). Indeed, KTs drive MT growth in a RANGTP- and CRM1-dependent manner, following gamma-TuRC (tubulin ring complex) recruitment to the kinetochore by the Nup107-160 nucleoporin complex (*Mishra et al., 2010)*.
The polymerized MTs are then stabilized in the vicinity of KTs via a phosphorylation-dependent mechanism involving Aurora B in the chromosomal passenger complex (CPC) (reviewed by *Weaver and Walczak 2015*). The CPC resides at KTs in metaphase. Here Aurora B, the catalytic component of the complex, phosphorylates and inactivates MT-destabilizing factors, including MCAK (mitotic centromere-associated kinesin) and OP18 (oncoprotein 18). This creates a local environment around the KTs acting as a "hot spot" for MT stabilization (*Tulu et al., 2006*). MTs are therefore preferentially stabilized in the KT area.
An additional mechanism for acentrosomal MT assembly involves the octameric augmin complex termed HAUS (homologous to augmin subunits) (*Goshima et al., 2008; Lawo et al., 2009; Hsia et al., 2014*). This complex is recruited to both i) MT arrays that are being nucleated and stabilized through the RANGTP and CPC pathways, and ii) "canonical" centrosome-nucleated MTs. Gamma-TuRC is recruited to nucleated MTs and induces extra-nucleation and branching of a new MT *(Petry et al., 2011; Uehara et al., 2009)*. This amplification mechanism drives the rapid increase of the MT mass within the spindle. Moreover, augmin co-immunoprecipitates with TPX2 (targeting protein for Xklp2) (*Petry et al., 2013*), a RANGTP-dependent "SAF" *(Carazo-Salas et al. 1999)*. This suggests a potential direct link between RANGTP-dependent and augmin-dependent MT assembly pathways. The newly “branched” MTs are then captured and stabilized at KTs through their interaction with KT-associated proteins.
To summarize (**Figure 5**), RANGTP triggers the initial activation of MT nucleation and stabilization around mitotic chromosomes.

The chromosomal and centrosomal MTs are then stabilized in the proximity of the KTs. Concomitantly, MTs act as a template for augmin-dependent MT nucleation, providing an efficient mechanism for MT amplification around chromosomes (*Meunier and Vernos, 2016*). These evidences highlight the crucial role of KTs both for MT nucleation and MT stabilization. The RAN GTPase emerges as a key regulator in both processes.

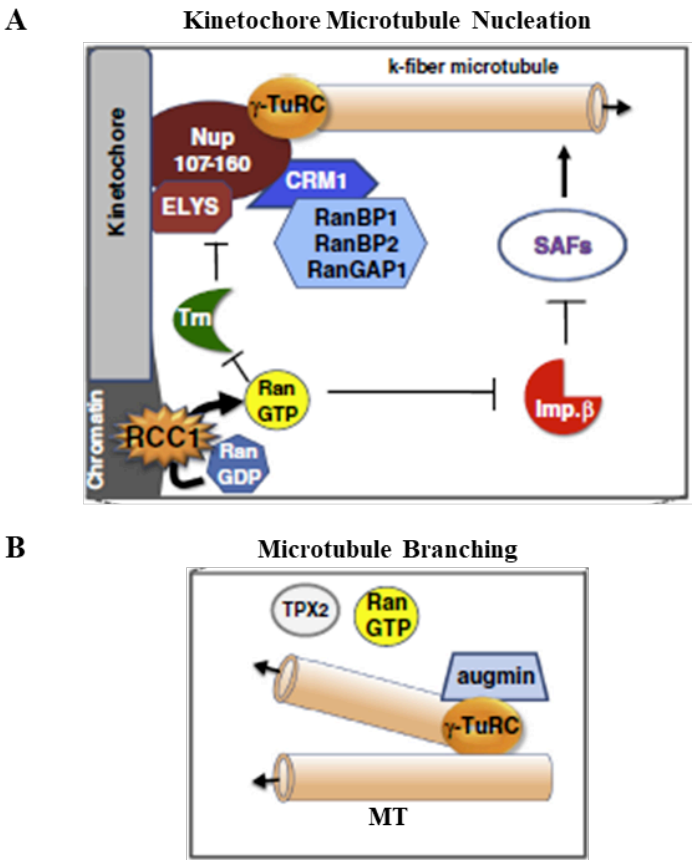

Figure 5: RAN network regulation of MT nucleation. The kinetochore-driven MT nucleation **(A)** and MT branching **(B)** pathways are here exemplified. Adapted *from Forbes et al., 2015***.**

2.2. K-fibre stabilization

The RANGTP pathway, in addition to triggering chromosomal microtubule assembly, is also involved in control of K-fibre dynamic properties by loading specific factors on MTs.
Several factors, controlled by Importin beta/RAN, stabilize K-fibres. Among those:
- CHD4 (chromodomain helicase DNA binding protein 4), a chromatin-remodeling ATPase and a catalytic subunit of the NuRD (nucleosome-remodeling deacetylase) complex. It is a RANGTP-regulated MAP that localizes to spindle MTs, essential for spindle assembly and involved in K-fibre stability (*Yokoyama et al., 2013*).
- NuSAP (nucleolar and spindle-associated protein) binds MTs in mitosis, regulating the formation of asters and long MTs, and showing MT-stabilizing activity (*Ribbeck et al., 2006 and 2007*).
- MCRS1 (microspherule protein 1) is also involved in K-fibre stability. It localizes to the spindle poles in early mitosis, accumulating to K-fibre minus ends. Interestingly, it binds directly to Importin beta (without an alpha adapter), and was demonstrated to stabilize MTs by preventing MCAK depolymerase activity (*Meunier and Vernos, 2011*).
- HURP (hepatoma up-regulated protein) is another direct cargo of Importin beta. In mitosis, it localizes predominantly to K-fibres. It displays a strong MT-bundling activity and contributes to K-fiber stabilization. Indeed, HURP depletion destabilizes K-fibers and delays chromosome congression (*Sillje 2006*).
In addition to these factors, the RANBP2/RANGAP complex also contributes to K-fiber stabilization: their recruitment to KTs after MT attachment is required for the formation of normal kinetochore fibres and faithful chromosome segregation (*Arnaoutov et al., 2005*). The importance of this complex at KTs will be discussed later.

3. The role of SUMOylation in mitosis

SUMO proteins are small ubiquitin-like modifiers that become covalently conjugated to cellular proteins carrying the consensus motif ψ-K-X-E (ψ, any hydrophobic amino acid, e.g. A, I, L, M, P, F, V or W; X, any amino acid residue) (*Zhao et al., 2009*).
Protein conjugation with SUMO (small ubiquitin-related modifier) peptides is a post-translational modification of growing importance in cell division (reviewed by *Wan et al., 2012; Flotho and Werner, 2012; Eifler and Vertegaal, 2015*). Indeed, SUMO addition modifies the interaction surfaces of proteins and, therefore, can modulate their interaction profile, localisation or function. SUMOylation was found to be essential for multiple cellular events, e.g transcription (*Hay, 2006*), DNA repair (*Moschos and Mo, 2006; Morris, 2010; Dou et al., 2011*), DNA recombination (*Potts, 2009*) and, of interest to this work, mitotic chromosome segregation (*Wan et al., 2012*).
In order to achieve protein SUMOylation, several actors act sequentially:

- the SUMO E1 activating enzyme SAE1/UBA2 (SUMO-activating enzyme subunit 2, or Ubiquitin-like 1-activating enzyme 2),
- the single SUMO conjugating enzyme Ubc9, acting as an E2 ligase in the conjugation pathway,
- several E3 ligases, which catalyze the conjugation of SUMO peptides on target proteins. These include PIAS (protein inhibitor of activated of STAT) family members, RANBP2, and a few other E3 ligases.

All these steps finally lead to addition of SUMO peptides, enabling the interaction of the SUMOyalted protein with a new partner, bearing SUMO interaction motifs (SIMs) (*Johnson, 2004*).

As for many post-translational modifications, SUMOylation is reversible. SUMO proteases, called SENPs (Sentrin specific proteases) remove SUMO peptides from target proteins, some of which are required for proper chromosome segregation (*Cubeñas-*

Potts et al., 2013). Several studies have revealed the importance of SUMO modification in KT function. In particular, SUMOylation involves centromeric proteins (Borealin, Topoisomerase II alpha), inner and outer kinetochore proteins (CENP-H, CENP-I, Nuf2) and proteins of the fibrous corona (BubR1, CENP-E, RANGAP). For a schematic view of SUMO-substrates at KT see **Figure 6**.

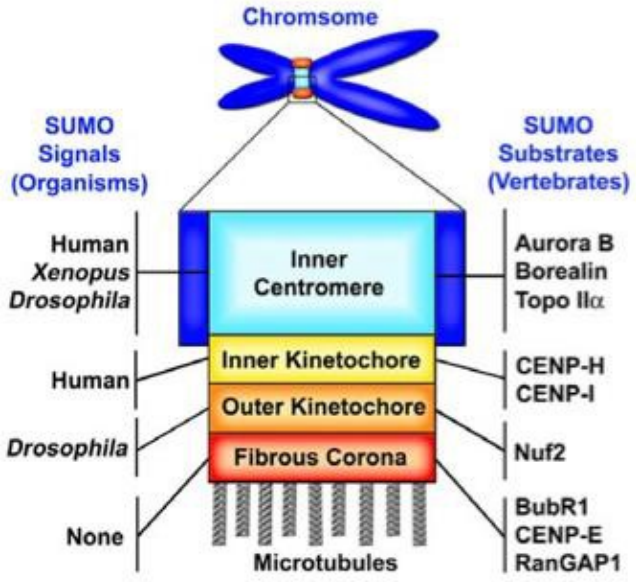

Figure 6: SUMO substrates at kinetochores. Known SUMO targets are shown in association with their exact localization at the inner centromere, the inner and outer KTs and at the fibrous corona. From *Wan et al., 2012*

A well-characterized SUMOylation substrate is Topoisomerase II alpha (TOP2A) (*Bachant et al., 2002; Azuma et al., 2003*). During mitosis TOP2A localizes from chromosome arms to the centromeres of sister chromatids (*Christensen et al., 2002; Tavormina et al., 2002*), where it decatenates DNA to enable chromosome segregation (*Lee and Bachant, 2009*). SUMOylation plays a critical role in regulation of TOP2A-mediated decatenation

of centromeric DNA (*Ryu et al., 2010; Porter and Farr, 2004*): PIAS gamma is required for SUMO2/3 modification on TOP2A in *Xenopus* extracts (*Azuma et al., 2005*). SUMOylation inhibits TOP2A function and prevents the premature resolution of centromeric DNA until anaphase (*Ryu et al., 2010*). RANBP2 has been found to act as the SUMO E3 ligase for TOP2A in mice. Indeed, in mouse embryonic fibroblast (MEF) cells with reduced expression of RANBP2, TOP2A is defective for SUMOylation and fails to localize at mitotic inner centromeres (*Dawlaty et al., 2008*). Although evidence is still sparse, these data indicate that the timely conjugation (and deconjugation) of specific proteins with SUMO peptides plays an important function in centromere/KT biology and hence in chromosome segregation.

4. RANBP2 and the RRSU complex in the regulation of KT functions.

4.1 The RRSU complex as a SUMOylation platform

RANBP2, also known as NUP358 (nucleoporin of 358 kDa), is the largest nucleoporin and resides at the cytoplasmic face of the NPC. When the NE disassembles at mitotic onset, RANBP2 localizes at mitotic spindle, and a fraction is recruited to the outer KTs at metaphase (*Salina et al., 2003*) (**Figure 7**). RANBP2 has a modular structure (*Wu et al., 1995; Yokoyama et al., 1995*) that includes:

- four RAN-binding domains;
- phenyl/glycine (FG)-rich regions to which Importin beta can bind during protein import across the NPC;
- a zinc-finger region and a cyclophilin-homologous domain, with a still unclear function (**Figure 8)**.

As introduced above, RANBP2 is also endowed with SUMO E3-type ligase activity (*Pichler et al., 2002*). Overlapping with the SUMO ligase domain is the SIM domain, which mediates RANBP2 interaction with SUMO-conjugated proteins; this

binding is crucial for the stabilization of the SUMOylated form of these proteins (*Werner et al., 2012*).
A major RANBP2 target is RANGAP1: RANBP2 associates with and stabilises SUMOylated RANGAP1 (SUMO-RANGAP1), tethering it to NPCs in interphase (*Matunis et al., 1996, 1998; Mahajan et al., 1997*), while unconjugated RANGAP1 remains soluble in the cytoplasm. In turn, RANGAP1 association with RANBP2 reinforces its SUMO E3 activity: RANBP2 and RANGAP1 are actually viewed as components of a multimeric SUMO ligase unit that also includes the E2 SUMO-conjugating enzyme UBC9. This multimeric complex is known as the RRSU (RANBP2-RANGAP1-SUMO-UBC9) complex (*Werner et al., 2012*).

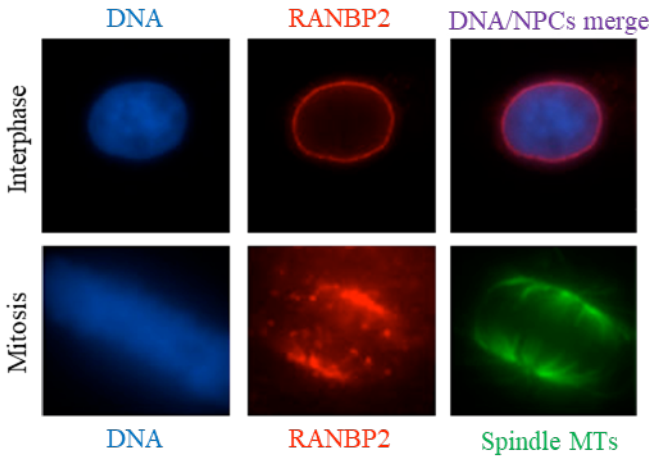

Figure 7. RANBP2 localization in human HeLa cells. Top row: RANBP2 distribution in interphase; note the punctuate red staining around the nucleus (blue), which identifies the regular distribution of nuclear pore complexes (NPC)s. Bottom row: in metaphase, RANBP2 co-localizes with mitotic MTs and KTs. (From *Di Cesare and Lavia, 2014*).

Figure 8. Schematic of RANBP2 domains. Black boxes 1-4 identify four RAN-binding domains; Cy indicates a cyclophilin-like domain, vertical dashes mark the position of FG-repeats that interact with transport receptors (modified from *Werner et al., 2012*).

4.2 The RRSU complex functions at KTs

RANBP2 and SUMO-RANGAP1 associate throughout the cell cycle (*Swaminathan et al., 2004*). The RRSU complex may serve as a source of SUMO-E3-ligase activity at KTs; because SUMO-specific isopeptidases also reside at centromeres and KTs (*Zhang et al., 2008; Cubeñas-Potts et al., 2015*), it is likely that cycles of SUMOylation and deSUMOylation modulate proteins in KT-directed mitotic processes that ultimately govern chromosome segregation (*Wan et al., 2012*).
The RRSU complex appears at KTs after MT attachment and affects at least two cycles therein:

- SUMOylation of KT-associated proteins, governed by the SUMO-E3-ligase activity of RANBP2;
- the GTP-bound status of RAN, governed by its GTP-hydrolysis activating factor RANGAP; the GTP turn-over on RAN is critical to regulate KT-driven MT growth (*Torosantucci et al., 2008*).

4.3 RRSU interacts with nuclear transport receptors in all cell cycle stages.

Both RANBP2 and RANGAP1 interact with nuclear transport receptors during nuclear transport cycles. As described, RANBP2

interacts with Importin beta via its FG-rich domains when import complexes traverse NPCs to reach the nucleus.
In mitosis, Importin beta associates with the spindle MTs; both RANBP2 and SUMO-RANGAP co-immunoprecipitate with it and co-localise on mitotic MTs.
RANBP2 and RANGAP1 also interact with CRM1, and the KT-associated CRM1 fraction is required to localise SUMO-RANGAP1 and RANBP2 therein (*Arnaoutov et al., 2005*).

The RRSU complex has been recently reported to facilitate the disassembly of export complexes (*Ritterhoff et al., 2016*): indeed, RANGAP1-dependent RANGTP hydrolysis at NPCs initiates export complex disassembly and release of the NES (nuclear export signal) cargo. In mitosis, RANBP2 localizes at MT-attached KTs (*Joseph et al., 2004*), in a CRM1-dependent manner. Therein, the RRSU complex may facilitate the release of KT proteins harbouring NES signals, in analogy with the export process.

5. Importin beta overexpression and cancer

5.1 Importin beta overexpression affects mitosis

Several works indicate that altered expression of Importin beta in human cells causes complex mitotic abnormalities. Indeed, experimental induction of either down-modulation (*Hashizume et al., 2013*) or increased expression of Importin beta (*Nachury et al., 2001; Ciciarello et al., 2004; Kalab et al., 2006; Roscioli et al., 2012*) yields an array of mitotic abnormalities, including multipolar spindles and chromosome mis-segregation *(Nachury et al., 2001; Ciciarello et al., 2004; Kalab et al., 2006*), as well as inhibition of RANGAP1 recruitment at KTs (*Roscioli et al., 2012*). In addition, Importin beta overexpression also affects nuclear membrane reassembly by preventing the fusion of the endoplasmic reticulum (ER) membrane vesicles and tubules that normally form

the double nuclear membrane (*Harel et al., 2003*). It also impairs nuclear pore assembly, leading to a nuclear envelope structure devoid of nuclear pores (*Walther et al., 2003*).
While the regulatory role of Importin beta on NE reassembly at mitotic exit clearly precludes the re-establishment of nuclear import, Importin beta-dependent mitotic abnormalities are observed even under experimental conditions in which nuclear import is not overtly affected; this indicates therefore that mitosis is most sensitive to altered Importin beta levels.

5.2 Importin beta and cancer

Given the role of Importin beta in nuclear trafficking and in mitotic division, it is no surprise that its deregulated expression associates with pathogenesis.

Indeed, Importin beta is overexpressed in many cancer types that generally display high genomic instability, including: cervical (*van der Watt et al., 2009*), gastric (*Zhu et al., 2016*) and hepatocellular carcinoma (*Yang 2015*), as well as diffuse large B-cell lymphoma (*He et al., 2016*), myeloma (*Yan 2015*) and head and neck cancers (*Martens-de Kemp et al., 2013*). Some studies have highlighted the underlying mechanism underlying Importin beta overexpression. A well characterized mechanism was described in cervical cancer, in which Importin beta overexpression is due to HPV-dependent dysregulation of the E2F/Rb pathway (E2F constitutive activity). Since the Importin beta-1 gene promoter is a transcriptional target of E2F, this leads to abnormally high protein levels in cancer compared to normal cells (*van der Watt et al., 2008*). Excess Importin beta in cells has two important consequences, one affecting nuclear transport, the other one on mitotic cell division.

First, elevated expression of transport receptors in transformed cells correlates with dysregulation of protein transport across the NE: this mechanism could be devised by cancer cells to cope with

the increased metabolic and proliferative demands. Dysregulation of protein import might allow the increased entry of proteins with oncogenic functions, for example ERK1/2, c-Myc and E2F (reviewed in *Stelma et al., 2016*).
Second, as previously described, Importin beta overexpression affects mitotic division, being this cell cycle stage the most sensitive target process. This generates chromosome mis-segregation and may cause the onset of genetic instability, a hallmark of cancer.

It has been reported that cancer types in which Importin beta is overexpressed, depend on its expression for their proliferation and survival: Importin beta inhibition actually leads to massive apoptosis. Importin beta has therefore been proposed as a therapeutic target in those cancer types (*van der Watt et al., 2013*) and inhibitors are being developed, e.g. Importazole (*Soderholm et al., 2011*) and INI-43 (*van der Watt et al., 2016*).

Interestingly, other members of the nuclear transport pathway are also dysregulated in cancer. Importin alpha and CRM1 are frequently found to be both overexpressed in the same cancer types in which Importin beta is also upregulated (*Stelma et al., 2016*).

Interestingly, a recent study found that the loss of RANBP2 (with which Importin beta interacts) is lethal to a subset of BRAF-like colon cancers (*Vecchione et al., 2016*). Remarkably, RANBP2 confers a "vulnerability" to those cancers, by rendering them sensitive to the MT-targeting drug vinorelbine (*Vecchione et al., 2016*). That observation, if generalised, opens up the very interesting perspective that Importin beta overexpression might sensitize certain cancer types to particular mitosis-targeting chemotherapeutic drugs.

AIM OF THE WORK

The aim of this project was to clarify the roles of Importin beta in the control of mitotic division, in particular in the regulation of MT functional properties and KT functions.
As recalled in the introduction, Importin beta has roles beyond nuclear-cytoplasmic transport: it is involved in control of mitotic spindle assembly (*Ciciarello et al., 2004*; reviewed in *Forbes et al., 2015*) and NE reconstitution at mitotic exit (*Schellhaus et al., 2016; Ungricht et al., 2017*). Our group has shown that Importin beta overexpression, in addition to spindle defects, also induces faulty chromosome congression and segregation, (*Roscioli et al., 2012; Gilistro et al., 2017*), suggesting roles also in control of KT functions.

Together these data indicate that Importin beta exerts a global control over mitotic events; however, how it controls these multiple activities is only partially understood. Gaining that knowledge is important in light of the fact that Importin beta is abnormally expressed in several tumours that display high genetic instability (*van der Watt et al., 2009*; *Zhu et al., 2016*; *Yang 2015*; *He et al., 2016*; *Yan 2015*; *Martens-de Kemp et al., 2013*).

The standing question, therefore, is how can Importin beta control different pathways in mitosis?

Importin beta mitotic interactors are known only from studies of specific individual partners, but a global view is lacking. To fill this gap, one goal of my PhD project was the identification of Importin beta mitotic interactors in a systematic manner.

In parallel, I sought to elucidate the mitotic pathways through which Importin beta exerts its control, exploiting stable and inducible cell lines engineered for Importin beta overexpression. The results shed light on two major processes:

i) the mechanisms through which Importin beta controls the functional state of KTs: proximity ligation and functional assays show that Importin beta regulates the timing of RANBP2 localization at KTs, and hence the–timely modulation of the SUMOylation of KT-associated substrates.

ii) Importin beta control of MT functional properties: by combining proteomic and functional assays, we clarified that Importin beta acts on at least two MT-regulatory pathways, i.e. MT stability and MT growth, that are differentially sensitive to mutations in the NUP-binding region and hence to the differential binding of specific factors.

The dysfunctions at the MT or KT level generated by Importin beta overexpression might ultimately underlie errors in chromosome segregation and the onset of aneuploidy.

RESULTS

1. Dissection of the Importin beta-1 mitotic interactome.

Importin beta's modular structure enables it to establish interactions with different partners in interphase transport.
In this work we were interested to identify Importin beta mitotic interactors. To that aim, we devised the workflow schematized in **Figure 9**. In preliminary experiments we compared various conditions for efficient Importin beta immunoprecipitation and mitotic cell population enrichment, based on
i) thymidine-dependent block of the DNA replication and release,
ii) inhibition of the Eg5 kinesin and arrest in prophase and release, or
iii) inhibition of cdk1 at the G2/M transition and release (data not shown).
The cell cycle synchronization protocol that proved most effective is presented in **Figure 10**. We used the Cdk1-inhibitor RO3306, which arrests cells at the G2/M boundary. The inhibitor is reversible, and when removed from the culture media (wash-out), cells rapidly enter mitosis.
For Importin beta co-IP, mitotic cell extracts were prepared from RO3306-synchronized and released HeLa cells, collected by mechanical shake off at mitotic round up, then incubated with Importin beta antibody for co-IP under non denaturing conditions. The co-IP material was then processed by Orbitrap MS analysis. An extended list (272 proteins) was obtained (not reported extensively for space reasons), which includes known as well novel Importin beta interactors (*Di Francesco and Verrico et al., 2018*).

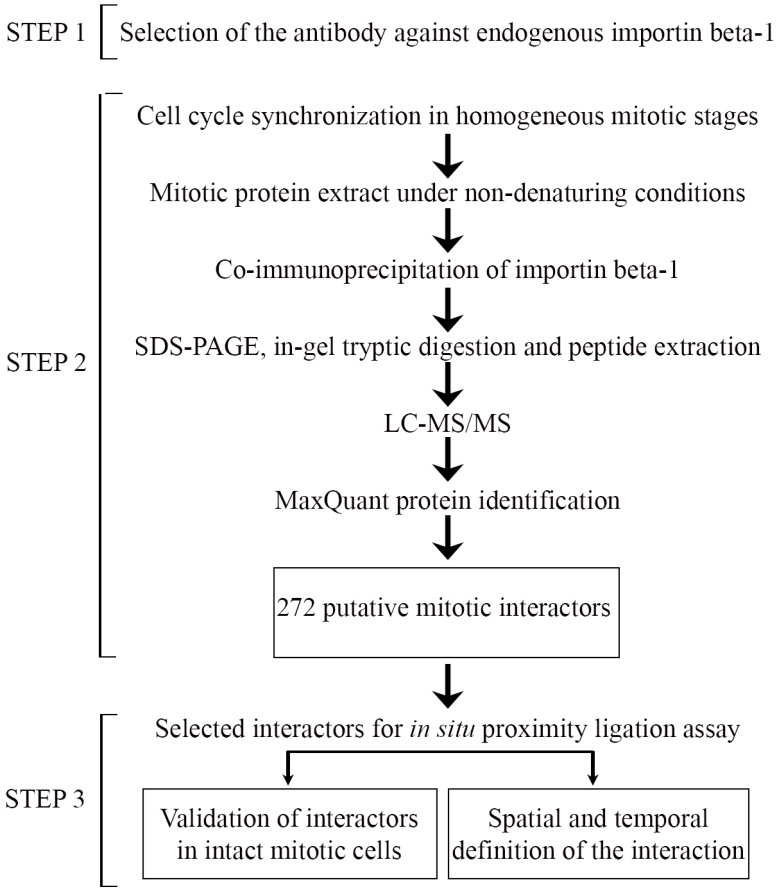

Figure 9: Schematics of the three-step interactomic workflow for the identification of mitotic Importin beta interactors. After selection of the Importin beta antibody (step 1), co-immunoprecipitating mitotic partners are identified and profiled in step 2; in step 3, selected partners are then validated by an automated acquisition of is-PLA images (see Materials and Methods) .

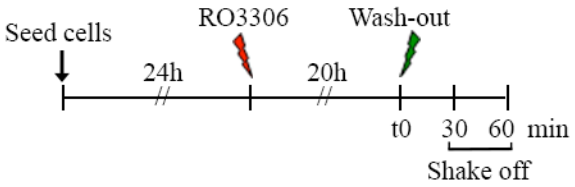

Figure 10: Cell cycle synchronization protocol for preparation of mitotic cell extract. Cells are arrested at the G2/M boundary by the addition of the Cdk1-inhibitor (RO3306), then released by changing the culture medium. After wash-out, cells rapidly enter mitosis (30 - 60 minutes), to be then collected by mechanical shake-off.

We analysed the profile of our identified Importin beta mitotic interactors and compared our list to that obtained from the Mitocheck database. The latter was built after a genome-wide siRNA-based screening and phenotypic analysis of mitotic phenotypes (http://www.mitocheck.org/gene.shtml): that comparison confirmed that most interactors identified in our experiments actually play roles in mitosis (195 of our 272 hits were annotated in Mitocheck), as their inactivation is associated with aberrant mitotic phenotypes. Among the 272 partners, we checked roles in mitosis by Pubmed search, reporting for each of them whether the association with Importin beta was already known (Pubmed data and Biogrid protein interaction database). The results of this search are presented in **Table 1**. We grouped Importin beta mitotic interactors according to their function/ontogenetic protein group. Some interesting results emerged:

1) One first group includes nuclear import and RAN GTPase network components, including components of the RRSU complex (RANBP2, SUMO-conjugated RANGAP1, and UBC9/UBE21).

2) We also identified the major spindle component, tubulin, together with mitotic spindle-binding proteins (NuSAP and HURP), and the mitotic checkpoint protein BUB3.

3) Besides factors that were already known to bind Importin beta, we also identify novel factors belonging to other ontogenic pathways. These include components of signalling pathways, and, somehow unexpectedly, a high proportion of factors involved in some aspect(s) of RNA biology: nucleolar proteins, hnRNPs, ribosomal proteins, and RNA-splicing and processing proteins. Mitotic roles are growingly emerging for many protein of these groups, consistent with the finding that RNAs are part of the mitotic apparatus (*Alliegro, 2011*). Some of the RNA-binding proteins were previously known to be involved in mitotic spindle regulation (RBM14, clathrin, HNRPU, RPS3, PRP19), centrosome function (Prdx1, RBM14, Plectin), regulation of MT/KT interactions (Nucleolin, HNRPU, ERH) and also mitotic exit (KHDRBS1/SAM68, IQGAP). These proteins, beside their main function, play roles at various steps of mitotic progression, and can thus be regarded as moonlighting proteins. Importantly, most of them were not previously reported to interact with Importin beta before. Their identification in the Importin beta mitotic interactome hints at unexpected pathways via which Importin beta might regulate mitosis.

				Interaction with importin beta-1	
Group / pathway	Protein ID	Gene name	Protein names	Pubmed	Biogrid
Nuclear import	Q14974	KPNB1	Importin subunit beta-1	Yes	Yes
	P52292	KPNA2	Importin subunit alpha-1	Yes	Yes
	O95373	IPO7	Importin-7	Yes	Yes
RAN GTPase network	P62826	RAN	GTP-binding nuclear protein Ran	Yes	Yes
	P46060	RANGAP1	Ran GTPase-activating protein 1	Yes	Yes
	P43487	RANBP1	Ran-specific GTPase-activating protein 1	Yes	Yes
SUMO modification	P49792	RANBP2	E3 SUMO-protein ligase RanBP2	Yes	Yes
	P63279	UBE2I	SUMO-conjugating enzyme UBC9	Yes	Yes
Mitotic spindle	P07437	TUBB	Tubulin beta chain	Yes	Yes
	Q9BXS6	NUSAP1	Nucleolar and spindle-associated protein	Yes	Yes
	Q15398	HURP	Hepatoma up-regulated protein	Yes	Yes
Mitotic checkpoint	O43684	BUB3	Mitotic checkpoint protein BUB3	Yes	Yes
Signal transduction	P62258	YWHAE	14-3-3 protein epsilon	Yes	Yes
Heat shock / chaperones	P08238	HSP90AB1	Heat shock protein HSP 90-beta	Yes	No
	P14625	HSP90B1	Endoplasmin	Yes	No
Nucleolus	P19338	NCL	Nucleolin	Yes	Yes
Ribosome	P23396	RPS3	40S ribosomal protein S3	Yes	No
Ribonucleoproteins	P07910	HNRNPC	Heterogeneous nuclear ribonucleoproteins C1/C2	Importin alpha-1	No
	P61978	HNRNPK	Heterogeneous nuclear ribonucleoprotein K	Yes	No
	Q00839	HNRNPU	Heterogeneous nuclear ribonucleoprotein U	Yes	No

Table 1: Importin beta mitotic interactors: highlights

				Interaction with importin beta-1	
Group / pathway	Protein ID	Gene name	Protein names	Pubmed	Biogrid
RNA binding	Q9UMS4	PRPF19	Pre-mRNA-processing factor 19	No	No
	Q01844	EWSR1	RNA-binding protein EWS	No	No
	Q96PK6	RBM14	RNA-binding protein 14	No	No
	Q07666	KHDRBS1	KH domain-containing, RNA-binding, signal transduction-associated protein 1	Yes	No
	P84090	ERH	Enhancer of Rudimentary Homolog	No	No
	Q86V81	ALYREF	THO complex subunit 4	No	No
RNA helicases	P17844	DDX5	Probable ATP-dependent RNA helicase DDX5	No	No
	Q92841	DDX17	Probable ATP-dependent RNA helicase DDX17	Yes	No
Elongation factor	P13639	EEF2	Eukaryotic Elongation Factor 2	No	No
Histones	Q92522	H1FX	Histone H1x	No	No
Cytoskeleton	Q15149	PLEC	Plectin	No	No
	P63261	ACTG1	Actin, cytoplasmic 2	No	No
	P60709	ACTB	Actin, cytoplasmic 1	No	No
	P46940	IQGAP1	Ras GTPase-activating-like protein IQGAP1	No	No
Vesicular transport	Q00610	CLTC	Clathrin heavy chain 1	Functional	No
	Q92734	TFG	Protein TFG (Trk-fused gene)	No	No
Redox metabolism	Q06830	PRDX1	Peroxiredoxin-1	No	No

Table 1 (continues).

At this point, we chose to validate a subset of the identified interactors, using a methodology that would enable us to visualise where and when the interactions take place. We decided to develop an *in situ* proximity ligation assay (*is*-PLA) protocol to validate Importin beta mitotic interactors. The PLA assay detects protein interactions *in situ* in intact cells, their localization on specific structures and their dynamics during cell cycle stages (see Materials and Methods for details). Moreover, we developed a protocol for automated microscopy acquisition and analysis of PLA signals (described in Materials and Methods).

To control the specificity of the technique we performed a negative control of the PLA assay after incubation of native HeLa cells (not transfected with GFP) with antibodies directed against GFP and Importin beta: no PLA signal was detected (**Figure 11A**), indicating that no aspecific amplification occurred.
We next selected RAN and RANBP2, among proteins listed in **Table 1**, as well-established Importin beta interactors in all cell cycle stages (positive controls). The results in **Figure 11B and Figure 11C** indicate that PLA depicts genuine interactions between Importin beta and its partners. We next tested Importin beta interaction with the mitotic spindle checkpoint factor BUB3, which monitors the stabilization of correct ("end-on") MT attachments to KTs. That interaction was studied in biochemical terms (*Jiang et al., 2015*), yet has never been visualized in intact cells. Our assays show that interactions of Importin beta with BUB3 can be visualized by PLA in mitotic cells until chromosome segregation onset. These data depict for the first time the timing of Importin beta/BUB3 interactions in mitotic cells and are consistent with biochemical models for Importin beta shielding of BUB3 from ubiquitination, and hence proteasome-dependent degradation, until anaphase onset (*Jiang et al., 2015*).

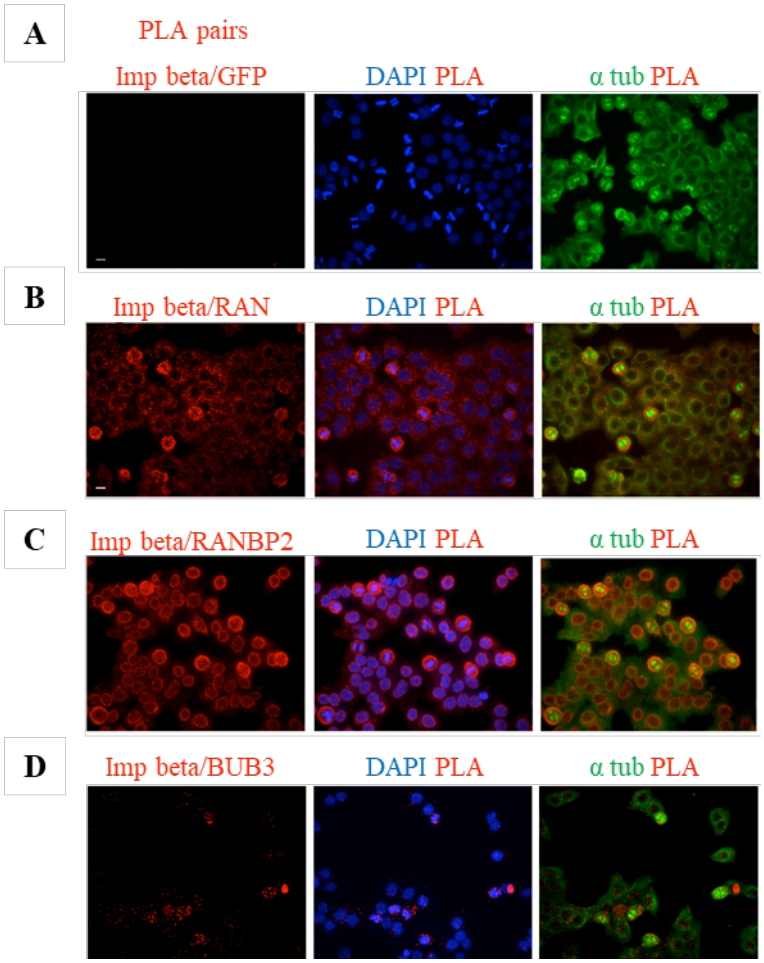

Figure 11: Detection of Importin beta containing PLA products. **A**. Negative control for is-PLA experiments: there are no visible PLA signals (RED) after incubation with antibodies for Importin beta and GFP in cells not expressing GFP. 40x panels show the PLA product reactions for Importin beta with RAN (**B**), RANBP2 (**C**) and BUB3 interactions (**D**); columns 2 and 3 show the superimposition of PLA signals (red) with DNA (DAPI, blue) and alpha tubulin (green), used as markers in the automated image acquisition. Bars 10μm.

Thus, the PLA method provides an effective validation tool for the co-immunoprecipitating mitotic partners identified in our proteome-wide approach. More generally, these results open up the interesting methodological perspective that validation of protein interactions from proteomic screenings may not only be achieved via Western blot (which requires high amounts of material and laborious procedures for protein extraction and immunoprecipitation) but also via PLA, which requires very little material and enables testing of multiple interactions in a short time.

2. Importin beta overexpression affects KT functions.

2.1 Generation of an inducible cell line for Importin beta overexpression.

To begin to unravel the mechanisms with which Importin beta acts in mitosis, it was of interest to study its effects under condition of overexpression. To this aim, I generated a HeLa cell line with stably integrated EGFP-tagged wild-type Importin beta, expressed under the control of a doxycycline (dox)-inducible promoter (see Materials and Methods for details). In time-lapse imaging assays, cells begin to express the exogenous EGFP-tagged protein already after 3-4 hours after dox administration. After 24 hours, all cells display the green fluorescence signal (**Figure 12A**). I also validated the expression of the inducible Importin beta-EGFP by Immunofluorescence **(B)**, Western Blot (**C**) and FACS **(D)** analysis. These independent techniques confirmed that: i) exogenous EGFP-tagged Importin beta protein is selectively expressed in dox-treated cells; ii) overall, exogenous Importin beta protein shows an increase by over 2-fold over the endogenous (24 hours induction) (**Figure 12C)**.

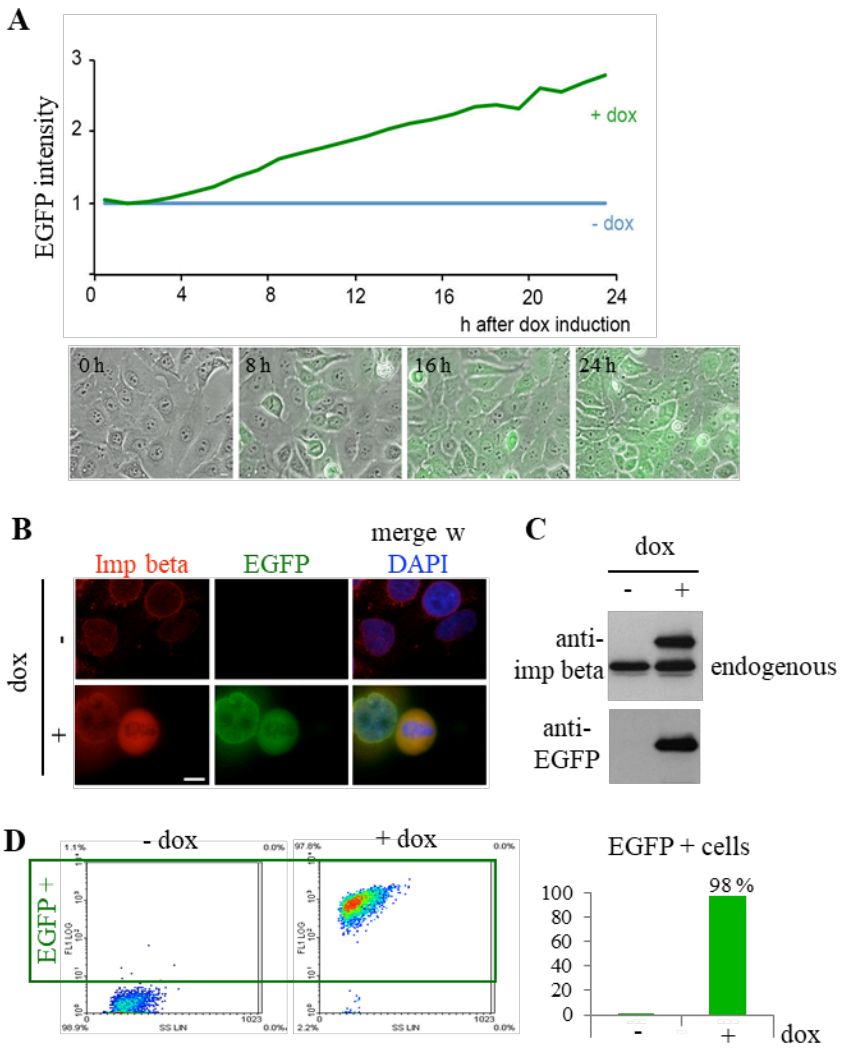

Figure 12: Generation of a HeLa cell line with stably integrated dox-inducible wild type Importin beta-EGFP expressing construct (details in Materials and Methods). A. Time-lapse panels from videorecording of Importin beta-EGFP after dox induction. Analysis of cell cultures after 24h of dox-induction by Immunofluorescence (**B**), Western Blot (**C**) and FACS (**D**) analysis. Bar, 10 μm.

The IF analysis revealed mitotic abnormalities in many Importin beta-induced cells. To identify and quantify these abnormalities, cells (fixed 14 hours after dox induction) were processed for IF to visualize chromosomes (DAPI), KTs (CREST antibody) and alpha-tubulin (specific antibody), and abnormalities (examples in **Figure 13A)** were counted in comparison to uninduced controls **(Figure 13B)**. We found that induction of Importin beta increased the amount of multipolar mitoses, and of metaphase cells with mis-aligned chromosomes, in a statistically significant manner compared to controls.

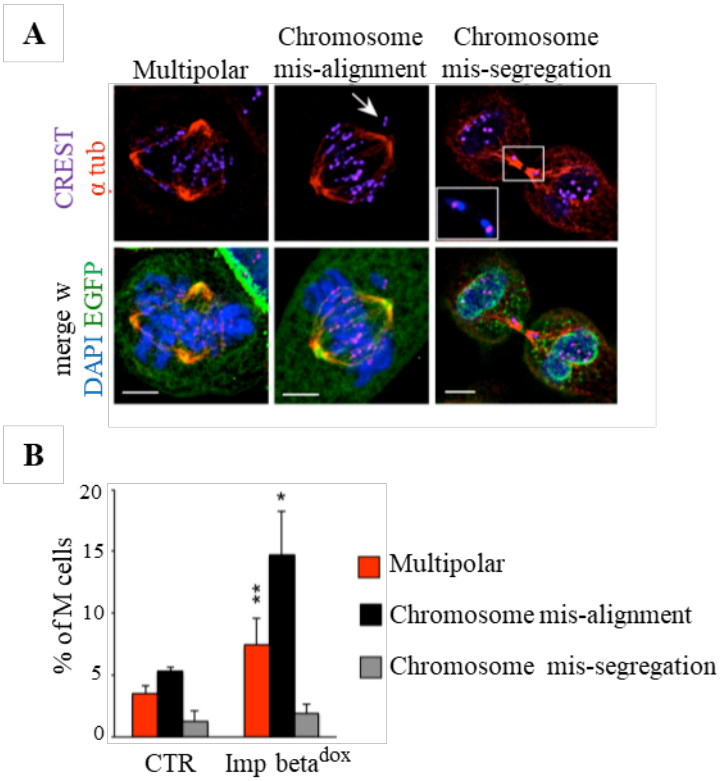

Figure 13: Importin beta overexpression induces mitotic abnormalities. A. IF panels exemplify mitotic abnormalities observed in fixed cell samples dox-induced for 14h. **B.** Quantification of mitotic abnormalities in uninduced-control (CTR) and Importin beta overexpressing cells. At least 500 cells in 2 independent experiments were analyzed. $\chi 2$ test, *p<0,05; **p<0,01. Bars, 5μm.

2.2. Importin beta regulates the timing of RANBP2 recruitment to KTs in mitotic cells.

The data in **Table 1** confirm previous data that identified RANBP2 as an abundant partner of Importin beta (*Roscioli et al., 2012*). RANBP2 localizes at mitotic MTs and a fraction accumulates at KTs after MT attachment (*Joseph et al., 2002*). As mentioned in the introduction, Importin beta and exportin-1/CRM1 also localize at MTs and KTs, respectively (*Ciciarello et al., 2004; Arnaoutov et al., 2005; Zuccolo et al., 2007*). Given the ability of Importin beta to interact with RANBP2, we asked whether it influenced the RRSU localization or functions in mitosis.

First, we examined RANBP2 interactions with transport factors by PLA during mitotic progression. Interactions of RANBP2 with Importin beta (**Figure 14A)**, as well as with CRM1 (**Figure 14C)**, are abundant at nuclear rim in interphase. When the NE breaks down, Importin beta and RANBP2 abundantly interact on MTs in prometaphase; quantification of PLA signals indicates that the interaction is then down-regulated in abundance from metaphase onwards (**Figure 14 B)**.

In contrast, RANBP2 interactions with CRM1 show an opposite pattern: they are low in PM, and increase in abundance at metaphase in the chromosome region (**Figure 14 D)**.

These experiments visualize the timing of RANBP2 interactions. Similar results were obtained by performing PLA reactions with RANGAP1 (data not shown).

Together the data suggest that RANBP2 "switches" partners before and after MT attachment to KTs, interacting with Importin beta along MTs in early mitosis until MT attach to KTs, at which point new interactions with CRM1 are established at KTs (*Gilistro et al., 2017*). This regulated recruitment appears to involve the entire RRSU complex.

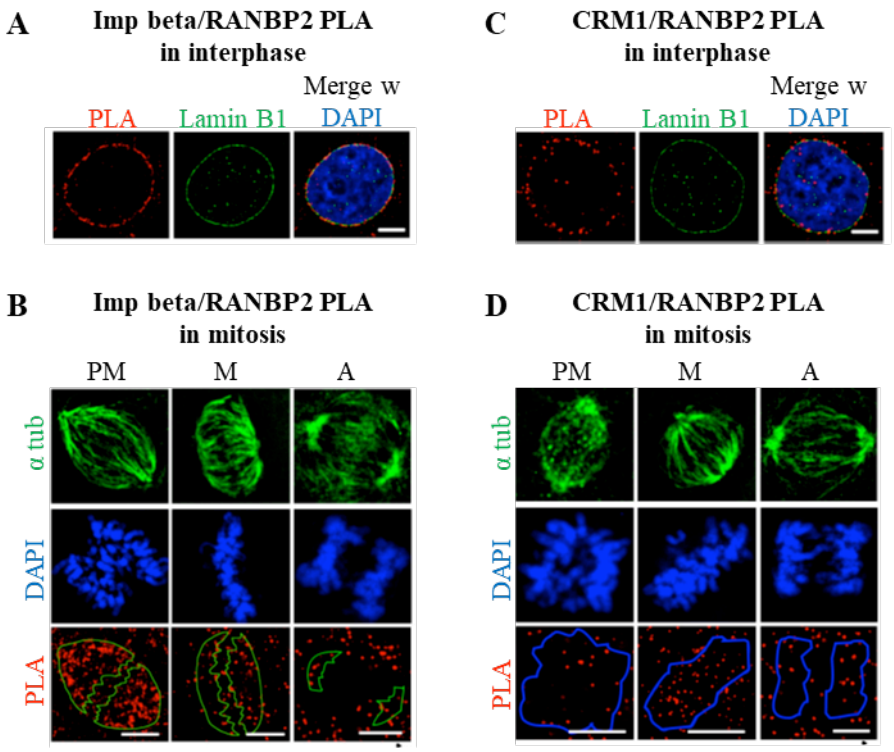

Figure 14: Spatial and temporal localization of RANBP2/Importin beta and RANBP2/CRM1 PLA products in mitosis. Panels show representative localization of PLA products. RANBP2/Importin beta interactions are revealed by PLA in interphase (**A**) and mitosis (**B**). RANBP2/CRM1 PLA products in interphase **(C)** and mitosis (**D**). Scale bars: 5 µm.

We wondered whether Importin beta overexpression influenced RANBP2 interaction patterns. We found that, in dox-induced cells, Importin beta-EGFP interaction with RANBP2 is prolonged compared to control cells; interestingly, the interaction persists in metaphase, when in normal conditions RANBP2 dissociates from Importin beta to bind CRM1 at KTs (**Figure 15**). Concomitantly, in Importin beta-induced cells, CRM1 and RANBP2 show fewer interaction signals when compared to control cells (**Figure 16**).

Together, these data suggest that Importin beta overexpression retains RANBP2 on spindle MTs in metaphase, preventing its recruitment at KTs by CRM1.

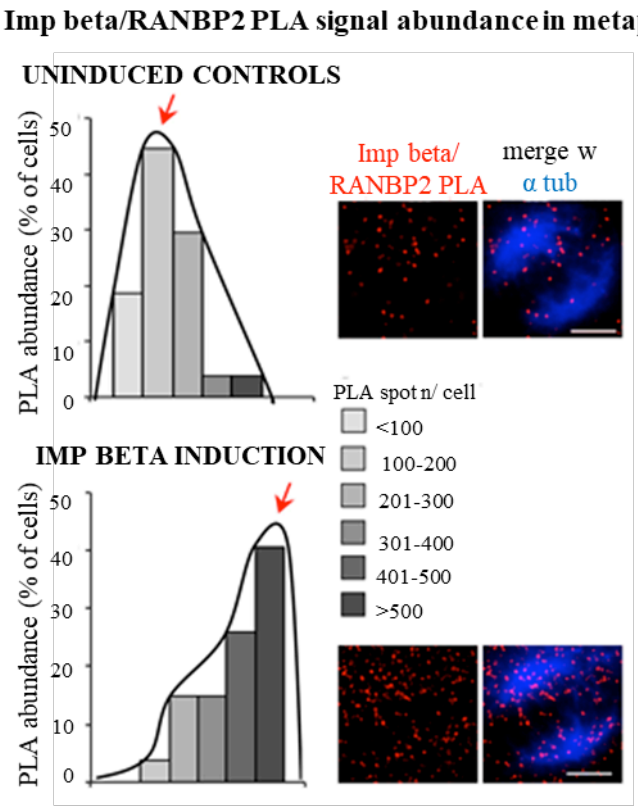

Figure 15: Importin beta overexpression results in increased interactions between RANBP2 and Importin beta at the spindle. The histograms represent the distribution of metaphases in discrete classes, according to their abundance of Importin beta/RANBP2 PLA signals, represented in the legend by shades of grey. The increase of signals in dox-induced compared to non induced cells is highly significant ($p<0.0001$ $\chi 2$ test). At least 130 metaphases per condition were analyzed in 3 independent experiments. Red arrows indicate modal classes. Bars: 5 μm.

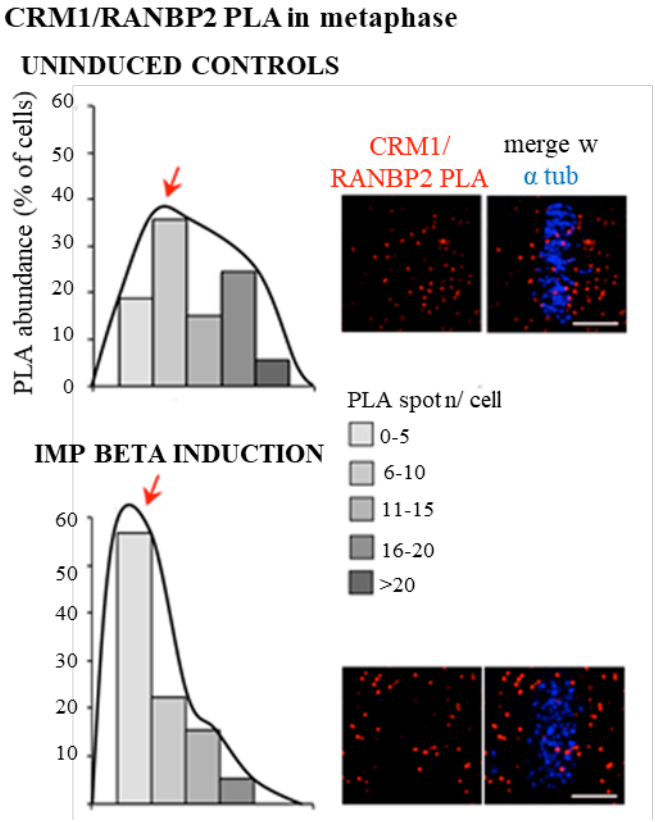

Figure 16: Importin beta overexpression results in decreased interactions between RANBP2 and CRM1 at KTs. The histograms represent the distribution of metaphases in discrete classes, according to their abundance of CRM1/RANBP2 PLA signals, represented in the legend by shades of grey. The decrease of PLA signals in dox-induced compared to non induced cells is highly significant ($p<0.005$ $\chi 2$ test). At least 215 metaphases per condition were analyzed in 4 independent experiments. Red arrows indicate modal classes. Bars, 5 μm.

2.3. Failure of RANBP2 localization at KTs in Importin beta induced cells hinders SUMO-TOP2A accumulation at centromeres.

Results described above delineate a scenario in which Importin beta excess prevents RANBP2 accumulation at KTs.
But what are the functional consequences of this activity?
As discussed in the introduction, RANBP2 is a unique nucleoporin, endowed with SUMO-E3-ligase activity. We were therefore interested in assessing the effects of Importin beta overexpression on RANBP2 SUMOylation substrates.
Among them, Topoisomerase 2 alpha (TOP2A) is fundamental in the decatenation of chromatids to enable segregation. TOP2A localizes to chromosomes in early mitosis (**Figure 17A**, upper row) and gradually concentrates at sister KTs in metaphase (**Figure 17A**, lower row). Parallel studies showed that a fraction of TOP2A is SUMOylated (*Azuma et al., 2005*) and that impaired SUMOylation affects the centromere decatenation function of TOP2A (*Dawlaty et al., 2008*). Importantly, TOP2A fails to accumulate at inner centromeres in animal models that express lowered RANBP2 levels, but this defect is rescued by overexpressing the SUMO-E3-ligase domain of RANBP2. These data suggest that regulation of sister centromere decatenation is exerted via SUMO-conjugation on TOP2A.
We asked whether SUMO-TOP2A was affected by Importin beta-dependent RANBP2 delocalization from KTs, besides being affected by its abundance.
First, we adapted the PLA protocol to detect intramolecular reactions between TOP2A and SUMO-2/3 peptides. Representative images in **Figure 17B** show the localization of SUMO-TOP2A, with an accumulation of SUMO-TOP2A PLA products at KTs in metaphase (quantified in the graph).
We then assessed whether Importin beta overexpression, which reduces RANBP2-CRM1 interactions at metaphase KTs, also affects the abundance of SUMO-TOP2A at centromeres. We

found that SUMO-TOP2A signals were indeed significantly reduced in Importin beta induced cells (**Figure 18)**.
These data indicate that Importin beta abundance regulates RANBP2 localization and interactions at KTs, hence modulating the state of SUMOylation of KT proteins such as TOP2A.

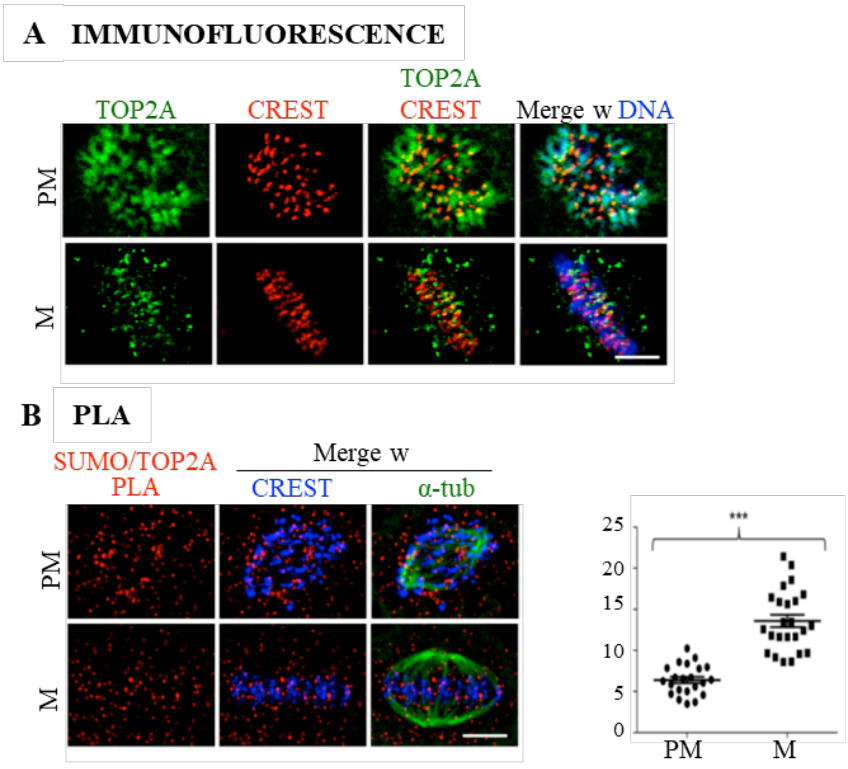

Figure 17: SUMO-conjugated Topoisomerase II alpha (SUMO-TOP2A) accumulates at centromeres in **metaphase. A.** TOP2A localization in prometaphase (PM) and metaphase (M). **B.** Exemplifying panels (left) of intramolecular PLA reactions detecting SUMO-TOP2A. The accumulation of SUMO-TOP2A PLA products at centromeres of metaphase chromosomes is quantified in the scatter plot (right panel), measuring the fraction of SUMO-TOP2A signals localized at CREST-stained KTs relative to the entire cellular pool, in prometaphase and metaphase cells. Unpaired t test, $p<0.0001$ (n= 22 prometaphases and 24 metaphases, two independent experiments)

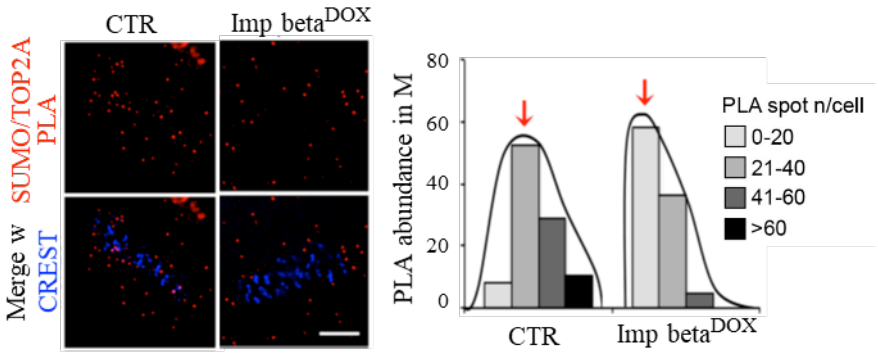

Figure 18. Importin beta overexpression prevents the accumulation of Topoisomerase II alpha (SUMO-TOP2A) at centromeres. Left, decreased accumulation of SUMO-TOP2A at metaphase KTs in Importin-beta-induced cells. The graphs on the right represent the distribution of metaphase cells in classes of abundance of PLA signals for SUMO-TOP2A at KTs: Importin-beta-overexpressing cultures display a significant decrease compared with controls ($P<0.0001$, $\chi 2$ test); n=40 scored metaphases per condition, two experiments. Arrows indicate modal classes. Scale bars: 5 μm.

3. Importin beta regulates MT functions.

The results thus far show that Importin beta influences KT functions via RANBP2. Deletion mapping delimited the NUP-binding region of Importin beta to the 45-462 region (*Kutay et al. 1997*). Structural biology studies revealed that the simultaneous mutation of two key residues in that region, i.e. isoleucin 178 and tyrosine 255, abolished nucleoporin binding (*Bayliss et al 2000*). I therefore generated ad hoc cell lines to analyse the role of the NUP-binding region in modulation of MT functions.

3.1 Dissecting Importin beta's NUP-binding region: generation of inducible cell lines for Importin beta derivatives.

To assess whether Importin beta effects on MTs are exerted via NUPs, I generated stably integrated, dox-inducibile cell lines using the same integration vector described above, expressing two Importin beta mutants:

- The double mutant I178A/Y255A, engineered by site-directed mutagenesis (*Roscioli et al., 2012*);
- A double Importin beta deletion at both the C- and N-termini (region 45-462), encompassing the NUP-binding domain.

The two Importin beta-derivatives may be seen as opposite mutations: the first one retains all functional regions of Importin beta, except for the NUP-binding capacity; the second one, instead, retains only the NUP-binding region.
I checked the expression of the EGFP chimaeric proteins by WB (**Figure 19)**. In both the Importin beta^{WT} and Importin beta$^{I178A/Y255A}$-expressing cell lines, the EGFP-tagged exogenous protein increased over 2-fold increase over the endogenous (24 hours induction). That was not seen for the Importin beta$^{45-462}$ mutant.

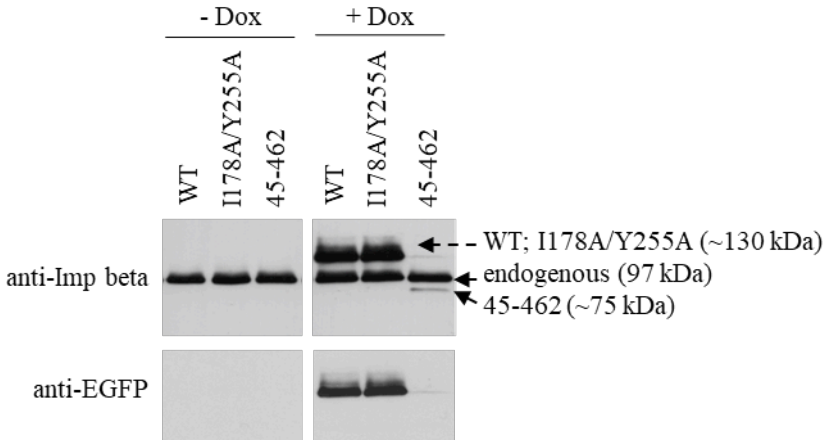

Figure 19: Immunodetection of importin beta derivatives in stable, dox-inducible cell lines. Visualization of the EGFP-tagged Importin beta after 24h of dox-induction by WB. After electrophoretic separation through 10% PAGE, WT- and I178/Y255-EGFP Importin beta migrate more slowly compared to the endogenous protein and are selectively recognized by anti EGFP-antibody. The 45-462 fragment, of faster migration, is barely visible.

3.2 The isolated Importin beta 45-462 region is unstable and subjected to proteasome-dependent degradation.

The failure to detect the Importin beta$^{45-462}$ was unexpected, because the vector scaffold used to clone Importin beta derivatives is the same for all cell lines, and the same transposase mediates the integration process. At least three possible explanations may account for the lack of expression of Importin beta$^{45-462}$: i) the integration occurred in a transcriptionally silent genomic locus, leading to inefficient expression of the exogenous fragment; ii), high instability of the 45-462 mRNA, or iii) the chimaeric protein is unstable.

To assess hypothesis i), I tested whether levels of expression varied after independent integration events, and generated three more independent cell lines for Importin beta$^{45-462}$. By Western blot analysis, however, all three cell lines still showed very low levels of the 45-462 mutant (**Figure 20A**), suggesting that the low expression of Importin beta$^{45-462}$ is unlikely to depend on a particular integration site. I next assessed if the protein was unstable by inhibiting the proteasome activity. The cell lines were induced with dox (8 hours) and, in the last 2 or 4 hours of induction, the proteasome inhibitor MG132 was added. As shown in **Figure 20B**, Importin beta$^{45-462}$, barely visible after dox induction, increased in abundance when the proteasome was inhibited in all three cell lines expressing the mutant (**Figure 20C**). I also generated independent cell lines for single truncation mutants lacking either the N-terminus, or the C-terminus: these constructs were efficiently expressed, and showed no significant variation after MG132 addition, similar to Importin beta^{WT} (data not shown). These experiments failed to identify a specific degradation signal in either the N-ter or the C-ter regions removed by the deletions, rather suggesting that the simultaneous deletion of both domains destabilizes the central region of Importin beta.
We therefore conclude that the region 45-462 of Importin beta, when expressed alone, is unstable. To the purpose of this work, therefore, the cell lines expressing that mutant could not be used. The importance of the NUP-binding domain was therefore studied in the cell line expressing Importin beta $^{I178A/Y255A}$, which is null for that binding.

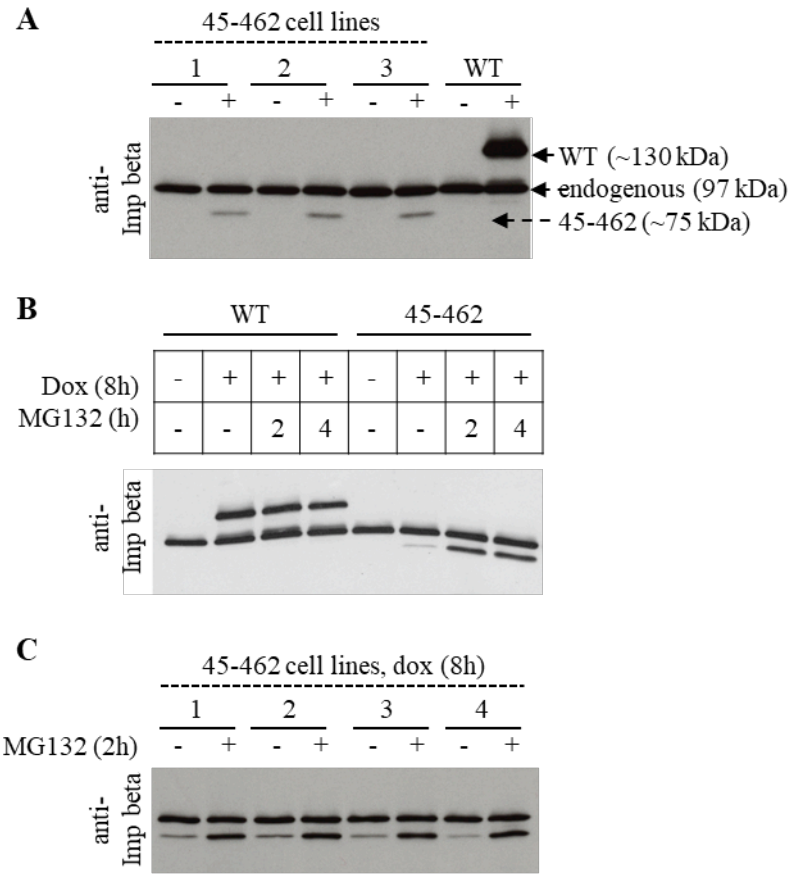

Figure 20: The 45-462 fragment is unstable and subjected to degradation. A. Induction of independently generated cell lines expressing EGFP-tagged Importin beta$^{45\text{-}462}$ (numbered 1-3) or EGFP-tagged Importin beta^{WT} after 24h of dox-induction. The WB panel clearly shows a faint signal for importin beta$^{45\text{-}462}$.
B. Proteasome inhibition with MG132 (2 or 4 h) in cell lines expressing WT and 45-462 Importin beta. When the proteasome is inhibited, Importin beta$^{45\text{-}462}$ level is close to that of importin beta^{WT}.
C. The stabilizing effect of the proteasome inhibitor was confirmed in all four cell lines expressing Importin beta$^{45\text{-}462}$.

3.3 Search for WT and NUP-binding defective Importin beta mitotic interactors.

At this point I compared cell lines expressing either Importin beta^{WT}, or the I178A/Y255A mutant, for various functional features. I first investigated patterns of protein interactions of both Importin beta versions. To that aim, I set up co-immunoprecipitation experiments using the GFP-TRAP method followed by proteomic analysis for both WT and I178A/Y255A Importin beta cell lines.
Dox-induced cell lines expressing Importin beta^{WT}-EGFP, Importin beta$^{I178A/Y255A}$-EGFP, or EGFP vector alone, were synchronized in late G2 by RO3306 treatment (Cdk1 inhibition); the medium was then washed out and cells were released into mitosis. Mitotic cells were collected by mechanical shake off (protocol in **Figure 21**). Protein extracts were prepared under non-denaturing conditions to preserve protein-protein interactions, then incubated with GFP-TRAP beads (also binding the EGFP variant of GFP, see Materials and Methods for details). The immunoprecipitate was then subjected to electrophoretic separation and processed for mass-spectrometry analysis.

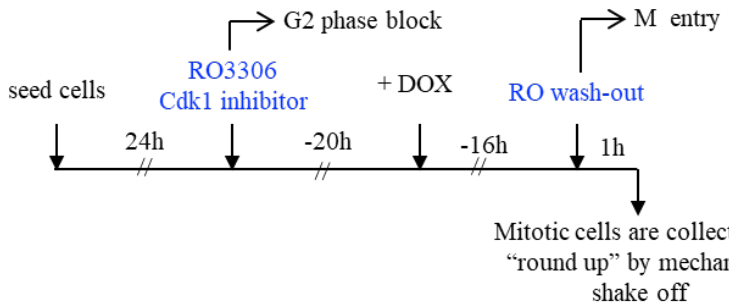

Figure 21: GFP-TRAP method for WT and I178/Y255 Importin beta co-immunoprecipitation. Cell cycle synchronization protocol for preparation of mitotic cell extract. Cells are arrested at the G2/M boundary by the addition of the Cdk1-inhibitor (RO3306), induced with dox, then released by changing the culture medium. After wash-out, cell rapidly enter mitosis (1h), then collected by shake-off.

A preliminary comparison of components in the co-IP of Importin beta^{WT}-EGFP (**Table 2**), and in the co-IP of the endogenous protein (**Table 1**), indicate that Importin beta^{WT}-EGFP reproduces the same interactions as the endogenous.

The identified interactors for WT and I178A/Y255A EGFP-tagged Importin beta versions are schematically visualized in the Venn diagram in **Figure 22**. For space reasons, in this Thesis only the most significant examples of identified mitotic partners are reported (**Table 2)**.
Briefly, I found:
- 128 partners, common to both WT and I178A/Y255A Importin beta, included RAN, RAN-binding proteins (including RANBP2 and its partners UBC9, RANGAP1 and SUMO peptides, components of a multimeric SUMO ligase complex, *Werner et al., 2012*), tubulins, ribonucleoproteins, certain histones and transcription factors. These results are consistent with data from the endogenous Importin beta mitotic interactome (*Di Francesco and Verrico et al., 2018*).
- 81 partners (highlighted in red) are selectively lost in the NUP-binding defective Importin beta co-IP. Among those, Importin beta$^{I178A/Y255A}$-EGFP does neither interact with NUP153 nor NUP50 (**Table 2**), as expected for the mutations introduced in the NUP-binding domain. In addition, some remarkable non-nucleoporin partners including HURP, BUB3, HNRPU and HNRPK, bind selectively Importin beta^{WT} but not the NUP-binding defective Importin beta$^{I178A/Y255A}$.

A

	Interactors(n)
Endogenous Imp beta	272
Imp beta WT-EGFP	251
Imp beta I178A/Y255A-EGFP	209

B

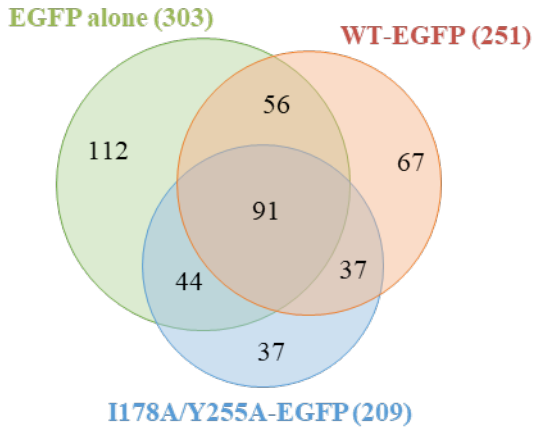

Figure 22: Overview of the importin beta interactome.
A. Interactors identified by MS/MS in the co-IP of endogenous Importin beta, Importin beta $^{WT\text{-}EGFP}$ and Importin beta $^{I178A/Y255A\text{-}EGFP}$. **B**. Interactors are grouped and represented in the Venn diagram; protein groups identified in control co-IP (EGFP alone) are also represented.

Group / pathway	Protein ID	Gene name	Protein names	Interaction with	
				Importin beta WT-EGFP	Importin beta I178A/Y255A-EGFP
Nuclear import	Q14974	KPNB1	Importin subunit beta-1	Yes	Yes
	P52292	KPNA2	Importin subunit alpha-1	Yes	No
	O95373	IPO7	Importin-7	Yes	No
Nucleporins	Q9UKX7	NUP50	Nuclear pore complex protein Nup50	Yes	No
	P49790	NUP153	Nuclear pore complex protein Nup153	Yes	No
RAN GTPase network	P62826	RAN	GTP-binding nuclear protein Ran	Yes	Yes
	P46060	RANGAP1	Ran GTPase-activating protein 1	Yes	Yes
	P43487	RANBP1	Ran-specific GTPase-activating protein 1	Yes	Yes
SUMO modification	P49792	RANBP2	E3 SUMO-protein ligase RanBP2	Yes	Yes
	P63279	UBE2I	SUMO-conjugating enzyme UBC9	Yes	Yes
	P61956	SUMO2	Small ubiquitin-related modifier 2	Yes	Yes
Mitotic spindle	P07437	TUBB	Tubulin beta chain	Yes	Yes
	Q15398	**HURP**	Hepatoma up-regulated protein	Yes	No
	Q9NQT8	**KIF13B**	Kinesin-like protein KIF13B	No	Yes
Mitotic checkpoint	O43684	**BUB3**	Mitotic checkpoint protein BUB3	Yes	No
	P06493	CDK1	Cyclin-dependent kinase 1	No	Yes
	Q96H22	CENPN	Centromere protein N	Yes	No
Signal transduction	P62258	YWHAE	14-3-3 protein epsilon	Yes	Yes
Heat shock / chaperones	P08238	HSP90AB1	Heat shock protein HSP 90-beta	Yes	Yes
Ribosome	P23396	RPS3	40S ribosomal protein S3	Yes	Yes
Ribonucleoproteins	P07910	HNRNPC	Heterogeneous nuclear ribonucleoproteins C1/C2	Yes	Yes
	P61978	HNRNPK	Heterogeneous nuclear ribonucleoprotein K	Yes	No
	Q00839	HNRNPU	Heterogeneous nuclear ribonucleoprotein U	Yes	No
RNA binding	Q01844	EWSR1	RNA-binding protein EWS	Yes	No
	P84090	ERH	Enhancer of Rudimentary Homolog	Yes	Yes
Elongation factor	P13639	EEF2	Eukaryotic Elongation Factor 2	Yes	Yes
Cytoskeleton	Q15149	PLEC	Plectin	Yes	No
	P63261	ACTG1	Actin, cytoplasmic 2	Yes	Yes
	P60709	ACTB	Actin, cytoplasmic 1	Yes	Yes
Vesicular transport	Q00610	CLTC	Clathrin heavy chain 1	Yes	Yes
Redox metabolism	Q06830	PRDX1	Peroxiredoxin-1	Yes	Yes

Table 2: Importin beta mitotic interactors: highlights

In parallel, the EGFP immunoprecipitate was processed for WB (**Figure 23A**). Eluted fractions (E2) were loaded in parallel with whole cell extracts (WCE) and supernatant (SUP) fractions. As **Figure 23A** shows, EGFP is effectively recovered: compare the EGFP protein signal intensity (27 kDa) in WCE and SUP; the same is observed with WT and I178A/Y255A Importin beta-EGFP (130 kDa). Blotting with anti-Importin beta antibody confirmed the recovery of the chimaeric protein (the 130 kDa band visible in WCE is absent in SUP and is collected in the E2). I next validated NUP153 (nucleoporin known to strongly bind Importin beta): as expected, NUP153 was recovered in the WT, but not in the I178A/Y255A Importin beta co-IP. In **Figure 23B,** RAN is abundant in both the WT and the I178A/Y255A Importin beta co-IP. Some RANBP2 and SUMO-conjugated RANGAP1 are found in the co-IP of Importin beta$^{I178A/Y255A}$. Quantification of the signal, normalized to the corresponding, WT and I178A/Y255A Importin beta, showed that RANBP2 in the co-IP of Importin beta$^{I178A/Y255A}$ amounted to 20% of the amount bound to Importin beta^{WT}, and SUMO-RANGAP1 signal in the co-IP of Importin beta$^{I178A/I255A}$ represented 50% of that bound to Importin beta^{WT}. Thus, binding to RANBP2 and SUMO-RANGAP1, though not being fully prevented, is strongly disfavoured by mutations at I178 and Y255.
Another interesting partner of Importin beta^{WT} is HURP: **Figure 23B** clearly shows that HURP co-immunoprecipitates only with the WT form but not with I178A/Y255A Importin beta mutant. Therefore, the two residues I178 and Y255 in Importin beta are crucial for HURP binding.

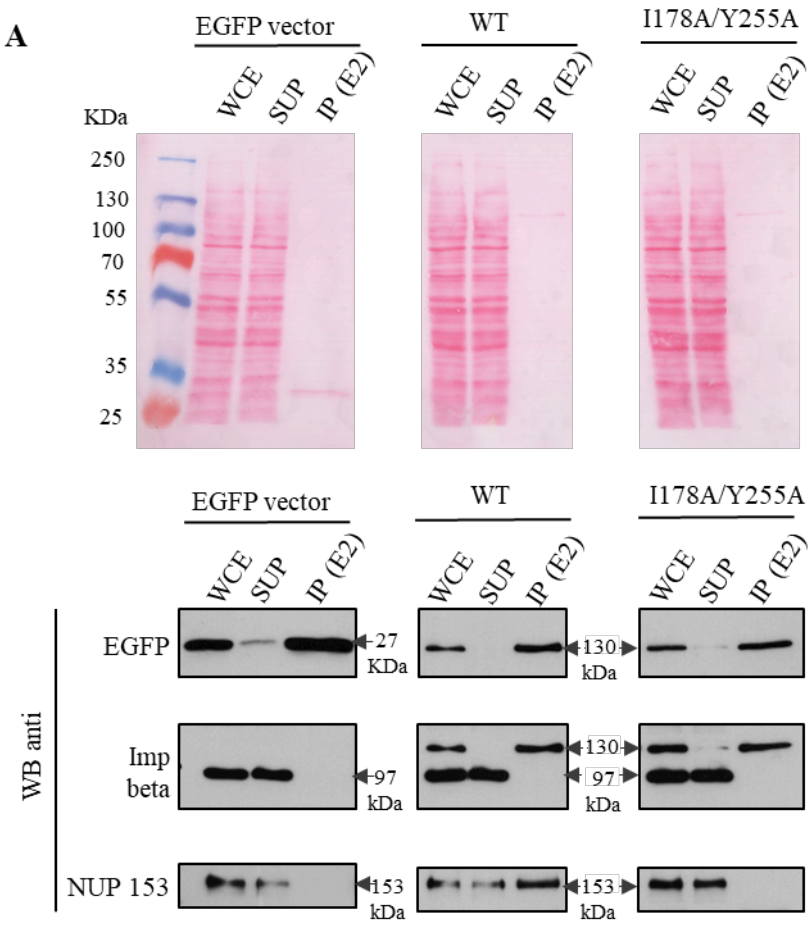

Figure 23: Validation of GFP TRAP interactors by WB. A. The eluted fraction (indicated as IP-E2) was loaded alongside with WCE (whole cell extract, 20 µg) and SUP (supernatant, 20 µg). Western blot with anti-GFP and Importin beta antibodies indicates that EGFP, Imp-WT-EGFP and Imp-I178/Y255-EGFP are effectively recovered. Hybridization with an anti-NUP153 antibody indicates that partners are efficiently co-IPed.

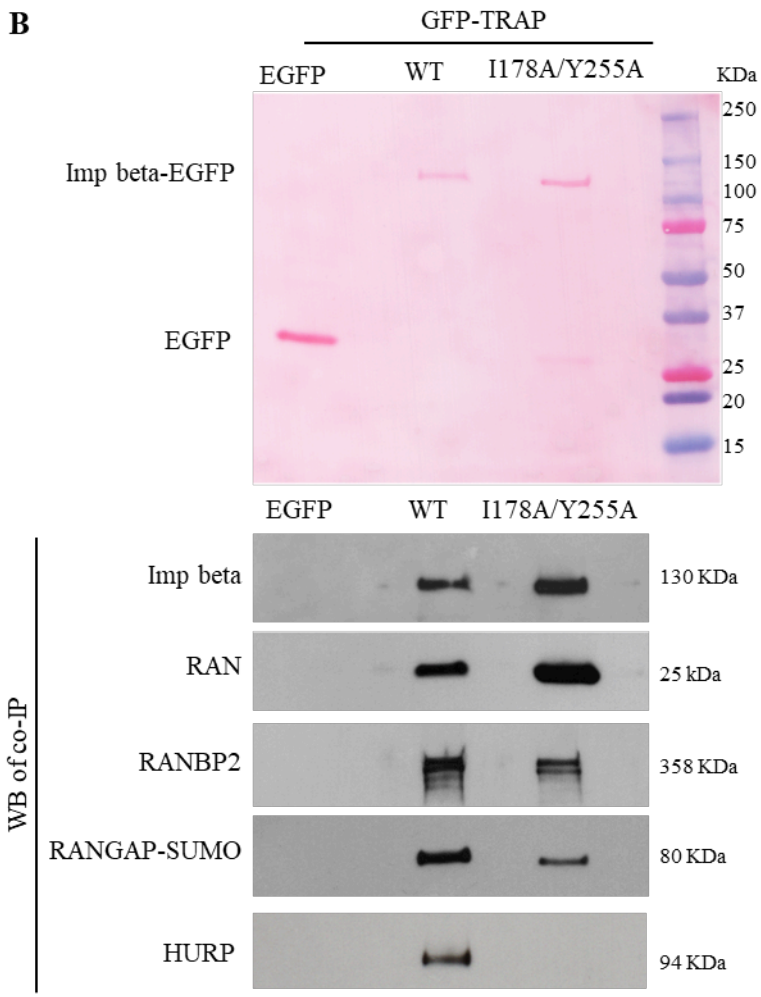

Figure 23 (continues): B. The eluted fractions from the GFP-TRAP were subjected to electrophoretic separation (4-20% gradient). Western blot indicates that RAN is a common interactor of WT and I178/Y255 Importin beta, while RANPB2 and its partner SUMO-RANGAP1 bind the I178A7Y255A mutant bind with much lower affinity and HURP only binds the wild-type form.

3.4 Exploiting PLA technique to visualize protein-protein interactions in time and space.

I next confirmed these differential interactions by PLA, to gain additional information on where and when the interactions occur.
To detect Importin beta WT or I178A/Y255A interactions with specific partners, I used anti-GFP antibody, recognizing the EGFP tag fused to Importin beta, in combination with antibodies to the tested protein, to detect specifically the interaction of the chimaeric Importin beta versions.
WT and I178A/Y255A Importin beta cells were induced, and then the PLA was performed (protocol in **Figure 24A**). Interactions were screened using the automated mode (details in materials and methods): fields were acquired (40x objective) and the RED signal (PLA intensity) was quantified in each cell. I first validated NUP153: as shown in **Figure 24B**, PLA signals were abundant at the nuclear envelope in WT but not in I178A/Y255A Importin beta-overexpressing cells. The PLA intensity signal was quantified at the single cell level and plotted in the dot plot below (at least 380 cells per sample **Figure 24C);** it confirms that NUP153 interactions with I178A/Y255A Importin beta are strongly inhibited.
Similarly, interactions of the NUP-binding defective mutant with both RANBP2 (**Figure 25**) and HURP (**Figure 26**) decreased compared to Importin beta^{WT}.

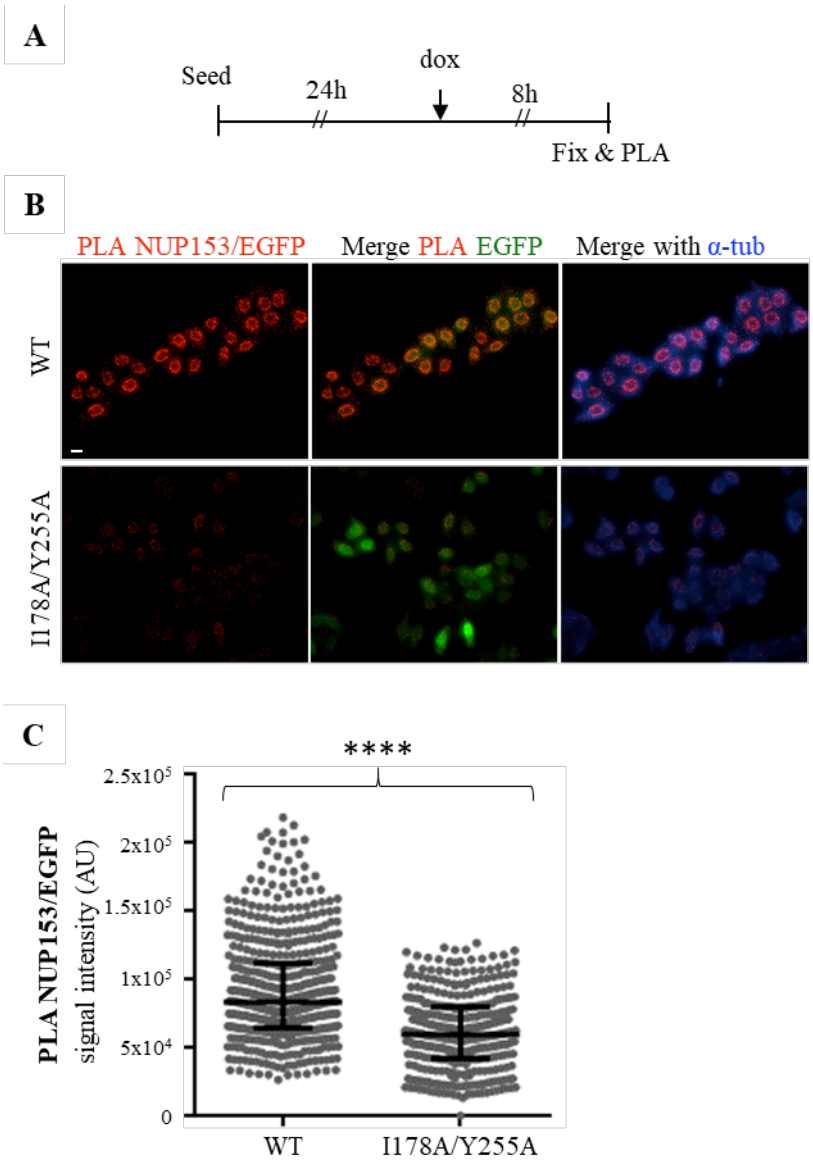

Figure 24: Validation of NUP153 differential interaction by PLA. **A.** Protocol used for the PLA assays. **B.** Exemplifying IF panels (40X fields). **C.** Quantification of red (PLA) signal in each cell. 565 and 374 cells were analyzed in WT and I178A/Y255A Importin beta respectively. Mann Whitney test, **** p<0,0001. Bar, 10μm.

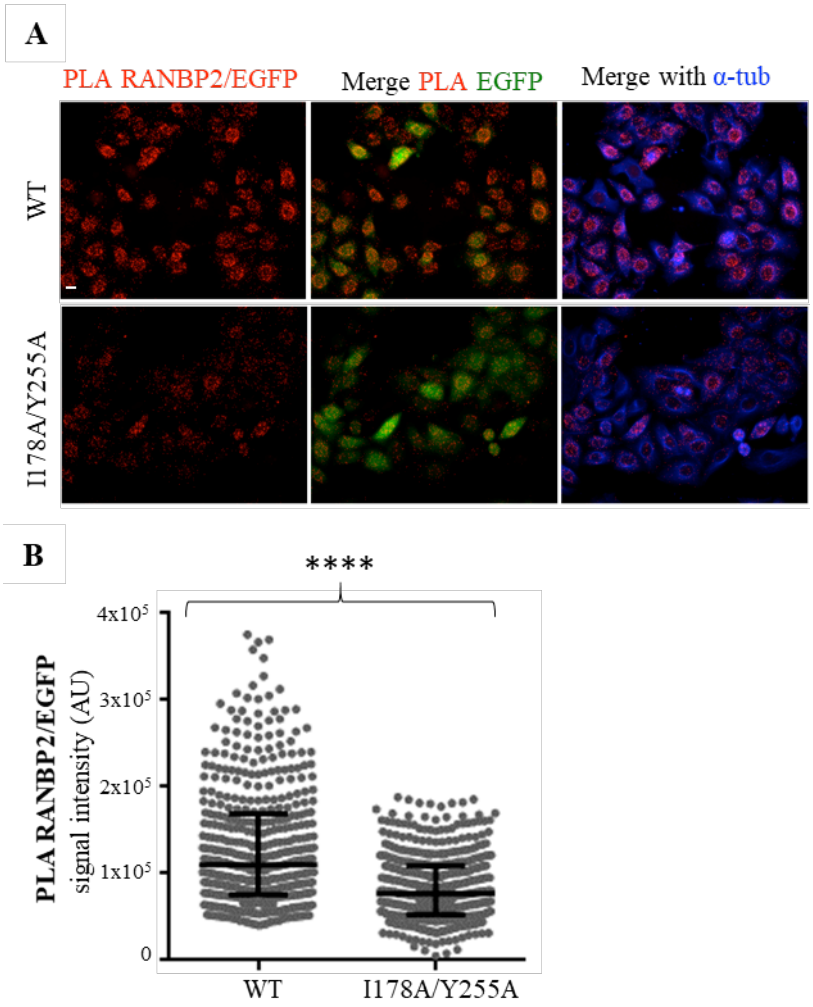

Figure 25: Validation of RANBP2 differential interaction by PLA. A. Exemplifying IF panels (40 X fields). **B.** Quantification of red (PLA) signal in each cell. 491 and 508 cells were analyzed in WT- and I178/Y255-Importin beta induced cells respectively. Mann Whitney test, **** p<0,0001. Bar, 10μm.

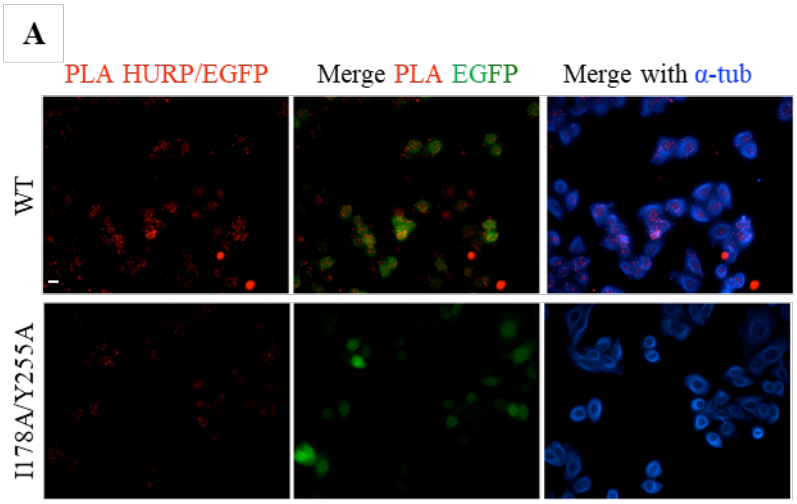

Figure 26: Visualization of HURP differential interaction by PLA. A. Exemplifying IF panels taken from 40x fields. This interaction is taken into more depth in the following pages.

Figure 27 displays exemplificative PLA images for the interactions of Importin beta^{WT} with these three partners. PLA signals for NUP153 interaction with Importin beta^{WT} move from the interphase nuclear envelope to mitotic cytosol; in late telophase, PLA signals are again visualized to the reforming nuclei (**Figure 27A**). Importin beta^{WT} PLA interaction with RANBP2 were already described: PLA spots are abundant in interphase around NE; in mitosis, PLA signals localize in cell and in the spindle area (**Figure 27B)**. PLA signals for HURP/Importin beta^{WT} interaction, more abundant in mitosis compared to interphase, are enriched in the spindle area (**Figure 27C)**.

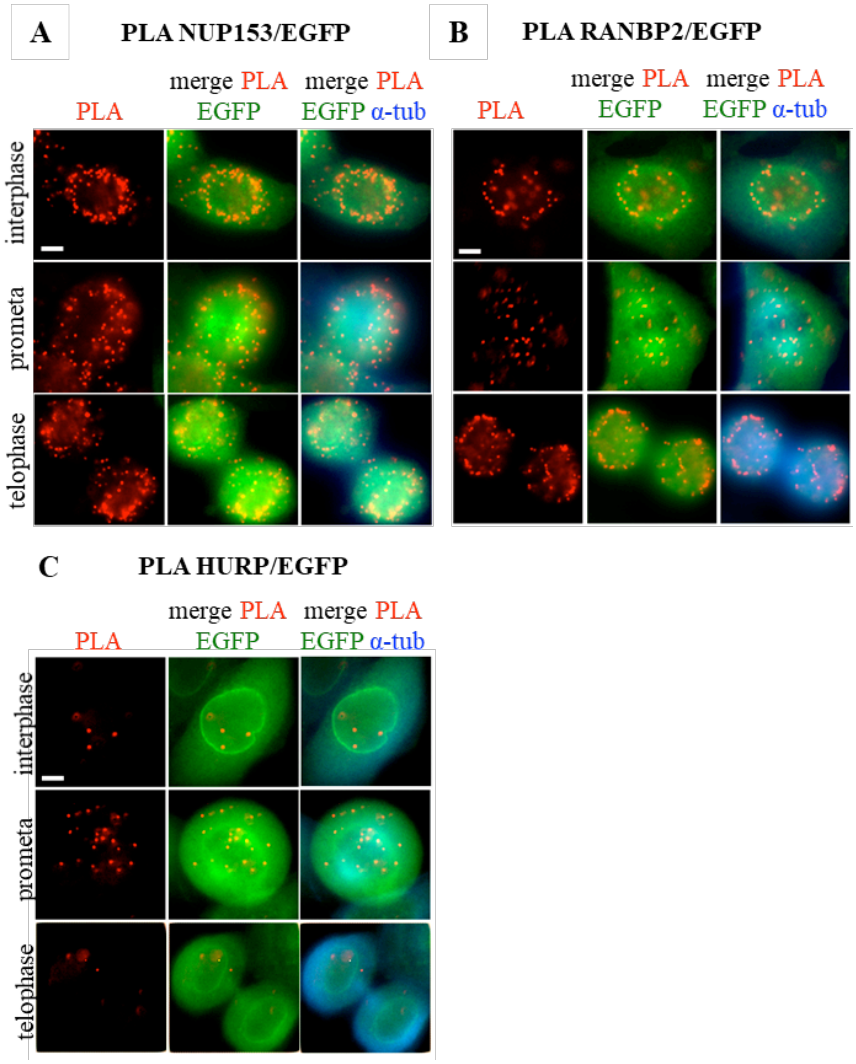

Figure 27: Detail on PLA localization. Exemplifying IF panels display where PLA reactions localize in cells in interphase, prometaphase and telophase. **A.** NUP153/Importin beta^{WT}; **B.** RANBP2/Importin beta^{WT} **C.** HURP/Importin beta^{WT}. Bars, 5 µm.

3.5 Overexpressed Importin beta impairs mitotic progression in living cells.

I then characterized the cell lines by time lapse-microscopy, which provides a faithful analysis of dynamic processes during mitotic division, and depicts dynamic defects that could not be visualized otherwise. Cells were video-recorded immediately after dox-induction over the following 26 hours (this time covers one entire cell cycle, allowing the analysis of the first mitosis after Importin beta overexpression). Some examples are displayed in **Figure 28.**

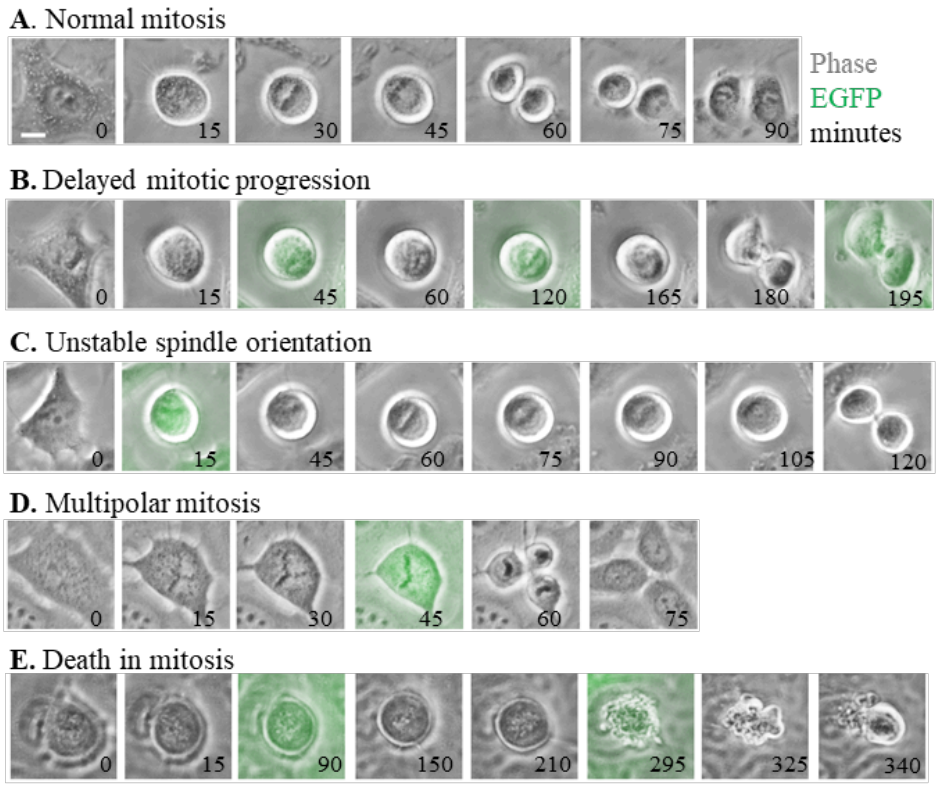

Figure 28: see legend in the following page.

Figure 28: Examples of mitotic abnormalities visualized by *time-lapse*. A. The top row displays a cell undergoing a normal mitotic division. Going down, panels **B-E** show representative abnormal phenotypes: **B**, a cell delayed in mitotic progression, arrested in a prometaphase-like state for several hours before reaching telophase; **C,** cell with unstable spindle orientation: the metaphase plate rotates in successive time frames. **D**, multipolar mitotic division, a cell aligns its chromosomes in a Y-shaped figure, then divides in three daughter cells. In **E**, the most severe phenotype, is death during prolonged mitosis. Bars, 10 μm.

The top row (**A**) represents a normal mitotic division: a cell rounds up at minute 15, aligns chromosomes at metaphase (minute 30), segregates at anaphase (minute 45), achieves telophase (minute 60), then re-adheres. Row (**B**) shows a cell undergoing delay during mitotic progression: the cell rounds up, but then spends a prolonged length of time in a prometaphase/metaphase state, reaching telophase only after 180 minutes. Row (**C**) shows another dynamic defect observed in some cells, i.e. unstable spindle orientation: the metaphase plate rotates, entailing gradual changes in the orientation of the spindle axis in subsequent time frames. This phenotype reflects a lack of connection between the (+) ends of astral MTs and the cell cortex, such that the spindle is not anchored to the cell and rotates freely. Row (**D**) presents a multipolar division, with a cell dividing in three daughter cells. Last, in row (**E**) an example of cell undergoing death during mitosis is shown.
I followed each cell in time, and, to obtain the temporal resolution of mitotic events, I performed a single cell analysis; the behaviour of control (uninduced) cells is shown in **Figure 29A**. In the panels, each horizontal bar represents a cell; different colours depict different stages of mitosis and mitotic abnormalities are highlighted by additional colours. Moreover, the length of each bar represents the time length: the longer the bar length, the more prolonged the mitotic phase duration. The timing of appearance of the EGFP signal is also depicted (green boxes).

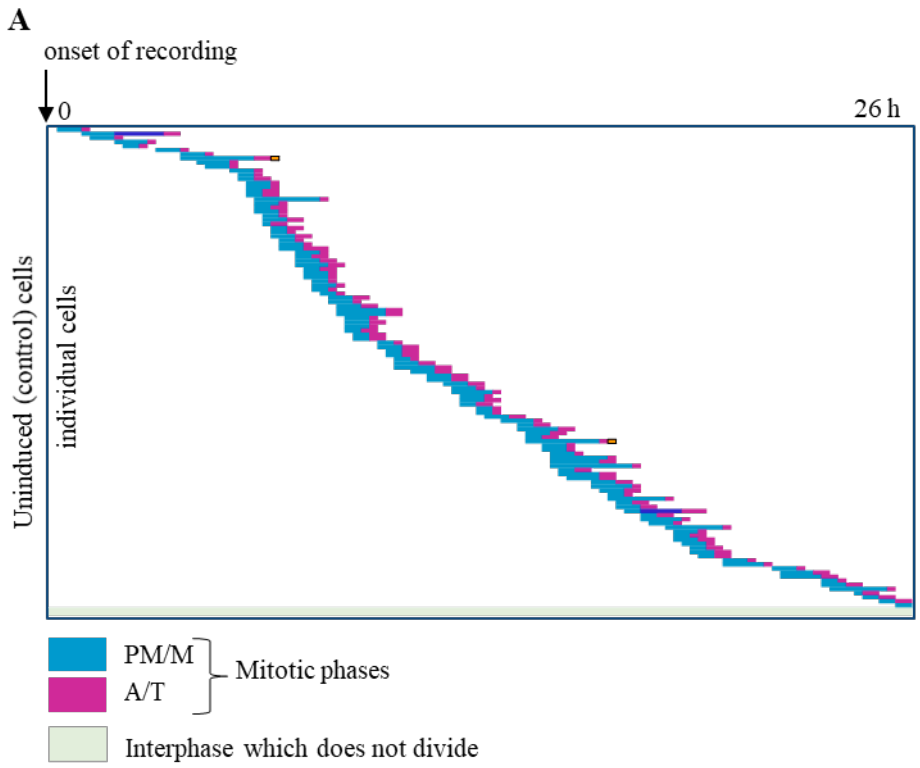

Figure 29: Single cell analysis of videorecorded mitoses. A. Control, uninduced cultures**.** Each line depicts a single cell, different colors depict different mitotic stages and mitotic abnormalities (see legends). The length of each line indicates the length of each mitotic phase. Recorded cells: n, 122.

The induction of both Importin beta^{WT} (**Figure 29B)** and Importin beta$^{I178A/Y255A}$ (**Figure 29C)** give rise to mitotic abnormalities. This kind of analysis is well suited to display the specific fate of individual recorded cells. Cells in which mitosis is abnormally prolonged are evident; as can be seen, the duration of prometaphase is especially prolonged.

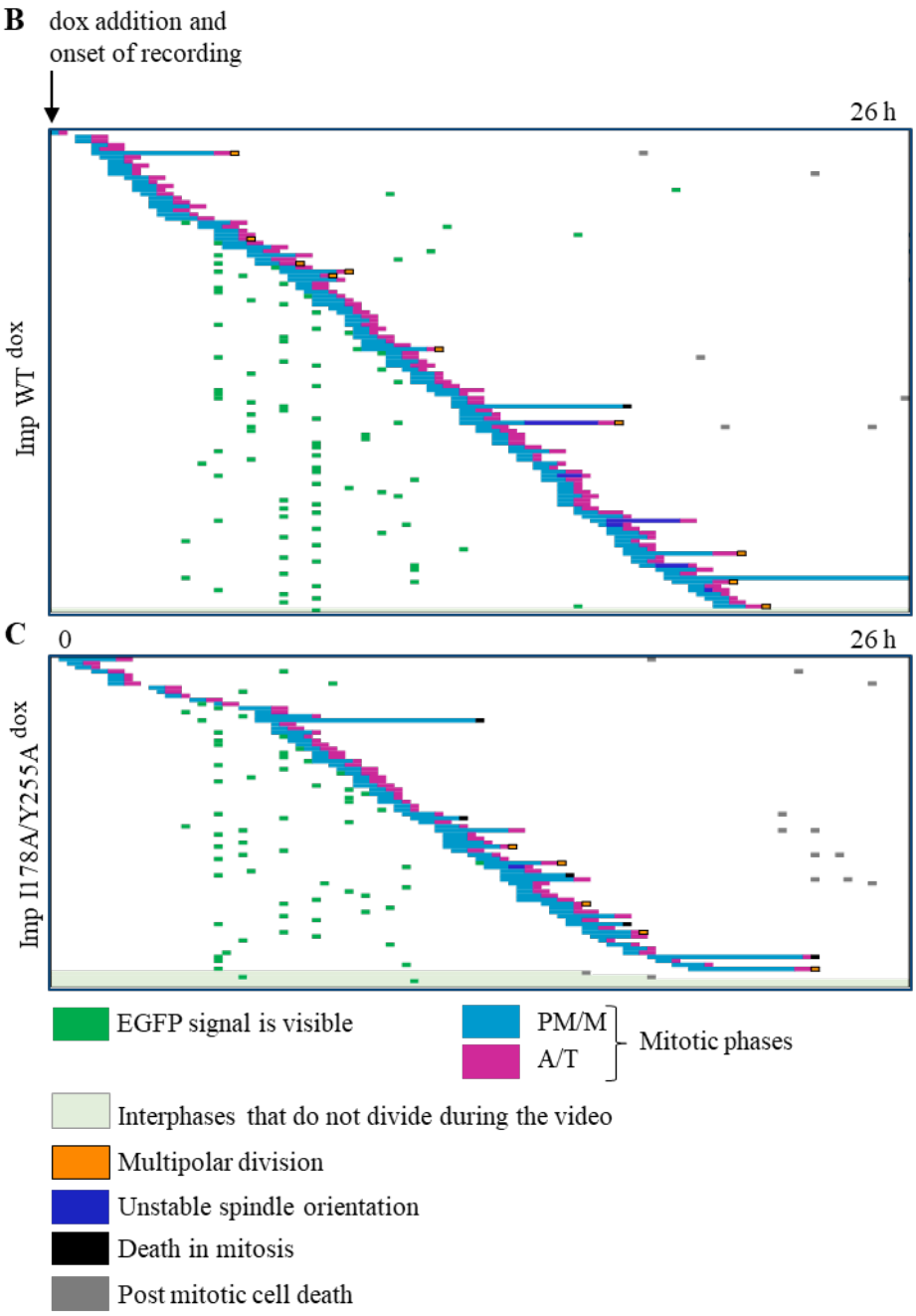

Figure 29 (continues): see legend in the following page

Figure 29 (continues): Single cell analysis of videorecorded mitoses. B. Importin beta ^{WT}-expressing cultures (n, 117 recorded cells, 3 independent experiments). **C.** Importin beta $^{I178A/Y255A}$-expressing cultures (n, 81 recorded cells, 2 independent experiments). Abnormalities arising during mitotic progression are indicated in the legend.

For ease of comparison, the histogram in **Figure 30** shows the frequency of the terminal cell fates described above. As shown, both WT and I178A/Y255A Importin beta induce multipolar divisions. Unstable spindle orientation is typically more frequent in the Importin beta^{WT}-induced cell line. Mitotic and post-mitotic cell death represent frequent phenotypes in the I178A/Y255A mutant-overexpressing cell line. These results, collectively, suggest that, although both WT and I178A/Y255A induce mitotic abnormalities, there are also specificities in the defects observed, which can be ascribed to the point mutations (I178A/Y255A) in the NUP-binding defective Importin beta mutant.

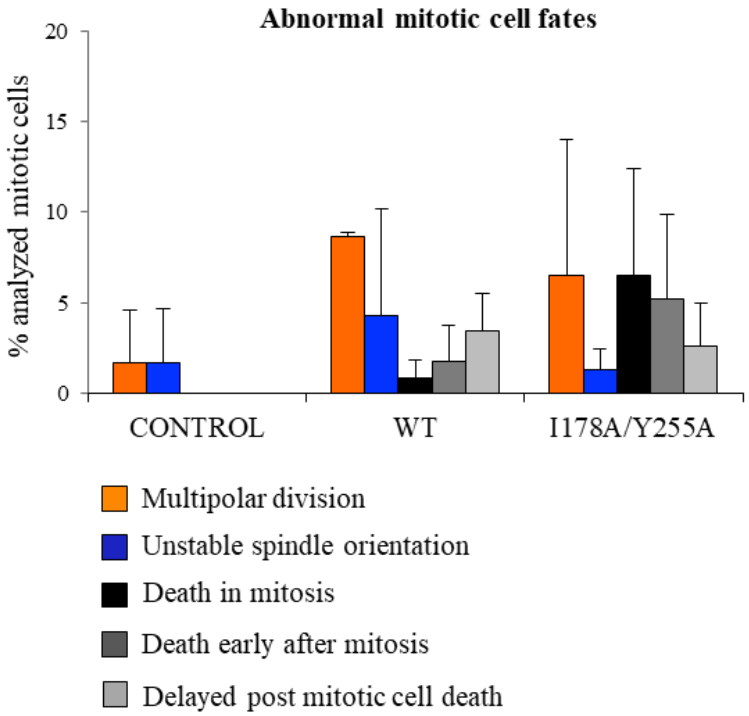

Figure 30: Mitotic fates induced by Importin beta WT and I178A/Y255A, revealed by time lapse imaging. Histograms represent the frequencies of mitotic cell fates recorded in uninduced (control) and Importin beta expressing cultures after 26 h of videorecording. Number of analyzed mitosis: Control: 119 cells, WT: 116 cells; I178A/Y255A: 77 cells.

3.6 WT and NUP-binding defective Importin beta differentially affect microtubule dynamics.

The recorded mitotic defects by time-lapse imaging, in particular the prolonged duration of prometaphase and metaphase, suggest roles of Importin beta at the MT level, with differential effects of the wild-type and I178A/Y255A forms at the level of MT (+) ends. I therefore wished to check whether Importin beta WT or I178A/Y255A mutant differentially influenced MT functional properties.

At the basis of chromosome segregation is the dynamic activity of MTs, physically measurable as the rate at which MTs switch from polymerizing to depolymerizing states. Alterations in this activity can be assessed by measuring MT resistance to cold-induced depolymerisation. By comparing control and dox-induced cell lines, the assay can reveal whether Importin beta in the wild-type or mutant form, influences the kinetics of depolymerisation, which is, in turn, a measure of MT stability.

Experimentally, cells overexpressing the construct of interest after dox treatment, are placed on ice for 20 minutes, then fixed and stained for alpha tubulin (the experimental protocol is outlined in **Figure 31 A**). After incubation on ice, a range of mitotic spindles depolymerization phenotypes is observed in mitotic cells, going from polymerized (resistant) to extensively depolymerised MTs, with growing strength of MT depolymerisation **(Figure 31B**, left to right). I quantified these phenotypes in control, WT and I178A/Y255A Importin beta-induced cells: their frequency is shown in **Figure 31C.** Control cells mostly show partially depolymerized MTs after 20 minutes of incubation on ice. In importin beta^{WT}-induced cells, MT depolymerization tends to be more extreme by comparison. In contrast, induction of Importin beta$^{I178A/Y255A}$ does not severely affect MT stability, with an overall profile of MT phenotypes comparable to that of control cells. Thus, we conclude that overexpression of wild-type Importin beta, but not the I178A/Y255A mutant, renders MT unstable. Two amino acids (I178 and Y255) are crucial to the

pathway in which Importin beta acts in the regulation of MT stability in mitosis, as their mutation abolishes this effect.

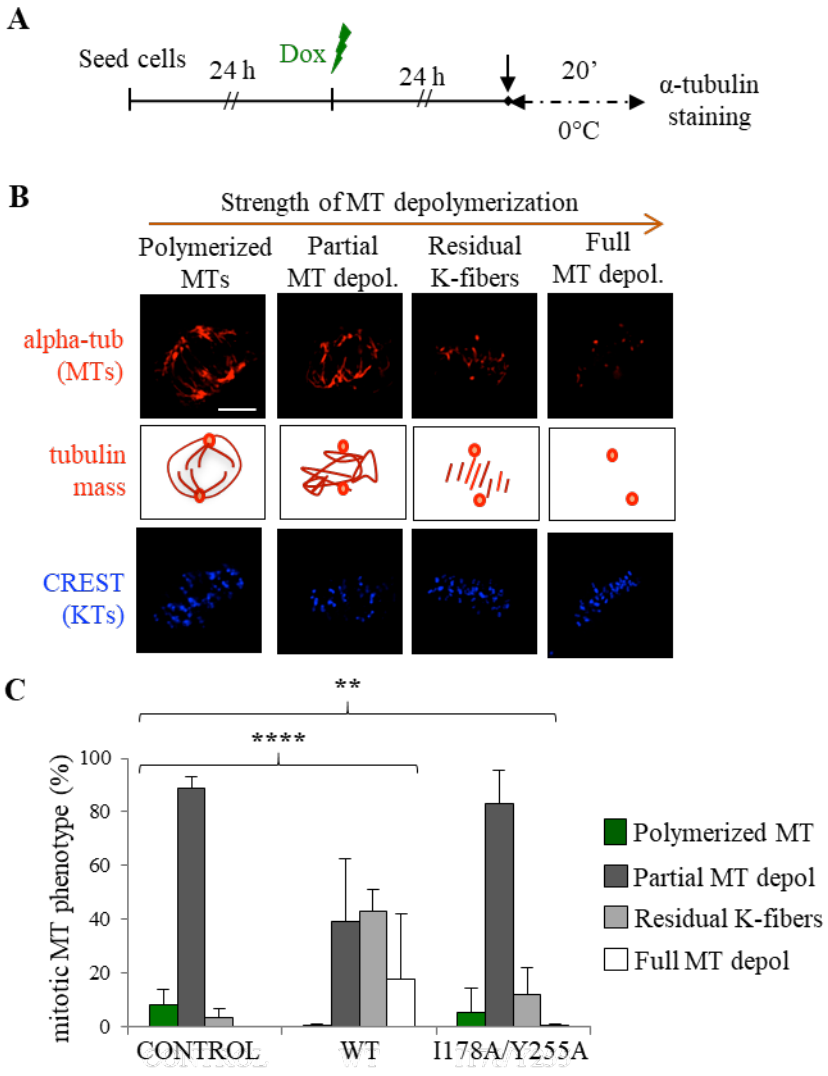

Figure 31: Ice-cold microtubule depolymerization assay: see legend in the following page

Figure 31: Ice-cold microtubule depolymerization assay. A. Protocol: cells are induced for 24 h, placed on ice for 20 minutes, then fixed and stained for alpha tubulin. **B.** Observed MT phenotypes, going from left to right, towards more complete depolymerization state. **C.** Frequencies of mitotic MT phenotypes in control, WT-and I178A/Y255A-Importin beta induced cells. At least 300 cells in 5 independent experiments were analyzed. Multiple $\chi 2$ test quantifies the distribution of MT phenotypes in Importin beta-induced cells versus control, **p<0,01, ****p<0,0001. Bar, 5μm

3.7 Both WT and NUP-binding defective Importin beta inhibit microtubule regrowth.

I then tested whether another measurable feature of MTs, i.e. their ability to regrow after extensive depolymerisation, was affected by overexpression of either WT or I178A/Y255A mutant Importin beta.
MT depolymerisation after cold treatment is a reversible process: by re-incubating the cells at 37° MT regrowth starts from kinetochores and is rapidly resumed at the spindle pole level. Thus, the nucleation capacity of MT-nucleation centers can be simply tested following a temperature shift, and the role of particular factors in the process can be evaluated. Cells overexpressing WT or I178A/Y255A mutant Importin beta were first placed on ice to promote complete MT disassembly, then shifted a 37°C for 1 or 2 minutes, fixed and stained for alpha tubulin (**Figure 32A**). **Figure 32B** shows the observed phenotypes after T° shift: after extensive incubation on ice (35') cells show a complete microtubule depolymerization; when shifted at 37°C MTs re-grow and eventually re-assemble a spindle, passing through intermediate states of MT re-polymerization.

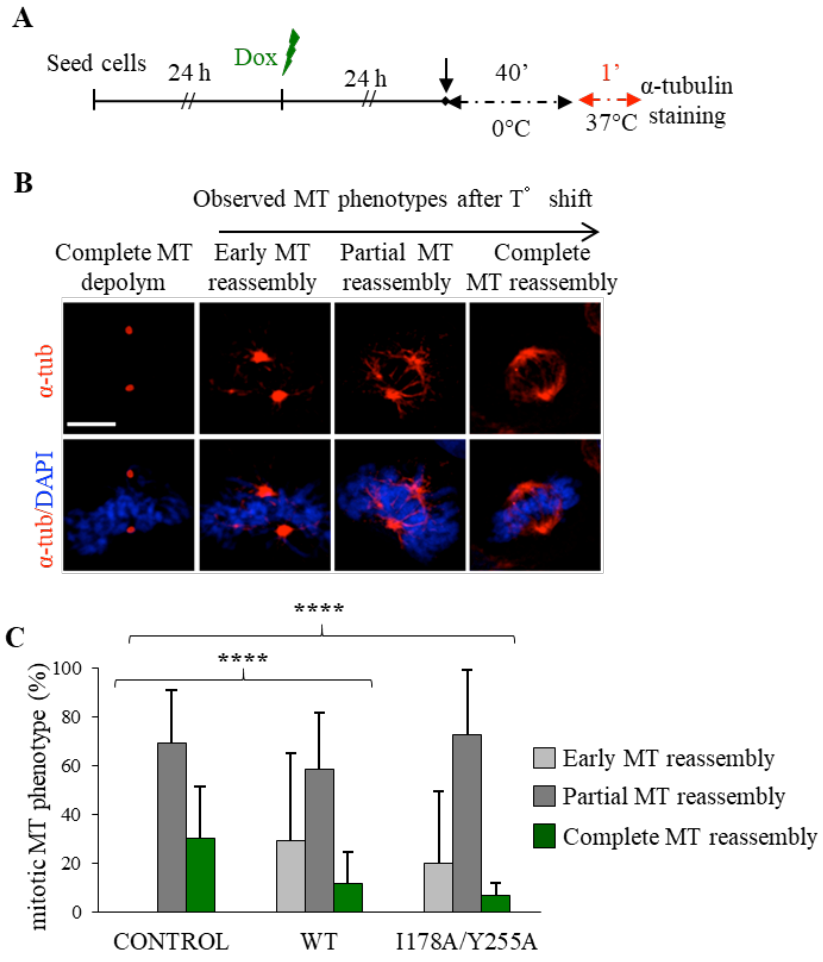

Figure 32: MT regrowth after cold induced MT depolymerization. A. Protocol: cells are induced for 24h, placed on ice for 40 minutes, shifted at 37°C for 1 minute, then fixed and stained for alpha tubulin. **B.** Observed MT phenotypes, going from left to right to progressive polymerized states. **C.** Frequencies of mitotic MT phenotypes in control, WT- and I178/Y255-Importin beta induced cells. At least 300 cells in 4 independent experiments were analyzed. Multiple $\chi 2$ test quantifies the distribution of MT phenotypes in Importin beta-induced cells versus control one, ****p<0,0001. Bar, 5μm.

Figure 32 C displays the frequencies of MT regrowth phenotypes: as can be seen, overexpression of both WT and I178A/Y255A mutant Importin beta similarly impaired MT regrowth compared to control cells. These data indicate therefore that Importin beta overexpression impairs, or delays, mitotic spindle re-assembly. The two residues I178 and Y255 are not critical for the inhibitory activity of Importin beta activity in this pathway

3.8 **Overexpression of both Importin beta WT and NUP-binding defective mutant, yield chromosome mis-alignment and mis-segregation.**

The results thus far show that Importin beta affects microtubule functions, and that the two residues at position 175 and 255, required for NUP binding, are crucial for MT stability but not for MT regrowth after depolymerization.
Because MT functions underlie the processes of MT/KT attachment and chromosome segregation, I wished to assess whether differentially proficient Importin beta forms affected chromosome alignment or segregation.
I performed an immunofluorescence staining to depict the configuration of chromosomes and the mitotic apparatus in WT and I178A/Y255A Importin beta-overexpressing cells compared to control cells, 14 or 24 hours after of dox induction; analysed figures would correspond to cells reaching mitosis after dox exposure for half (14 hours) or the entire (24 hours) cell cycle (**Figure 33**). The results indicate that, by and large, overexpression of both wild-type and I178A/Y255A Importin beta versions induce abnormal mitotic figures: in addition to multipolar spindles, already visualized in time-lapse recording, metaphases with misaligned chromosomes and ana-telophases with mis-segregating and lagging chromosomes are also seen, in statistically significant manners compared to controls.

WT Importin beta overexpression yielded initially (14 hours after dox) a remarkable frequency of multipolar spindles (almost 8% compared to <4% in controls), which decreased in frequency at later times. Conversely, misaligned and mis-segregating chromosomes increased over time. To understand these opposite trends, it may be considered that:
i) multipolar mitoses (especially seen at 14 hours post-dox) do not arrest nor experience delay during mitosis, as recorded in the time-lapse experiments; they progress past the multipolar division, either undergoing coalescence of fragmented poles, or exiting mitosis and originating an unbalanced interphase progeny, and thus are found with lower frequency after 24 hours.
ii) misalignment and/or mis-segregation of chromosomes, instead, are consistently associated with prolonged prometaphase and metaphase delay in time-lapse; therefore these cells tend to accumulate over time, resulting in a significantly increased frequency at 24 hours post-induction.
Cells overexpressing the I178A/Y255A mutant show a similar trend in accumulation of chromosome misalignment and/or mis-segregation, yet develop fewer multipolar spindles compared to cells overexpressing wild-type Importin beta.
Collectively the data indicate that:
1. elevated levels of Importin beta give rise to mitotic defects, which, in turn, can originate genomic instability;
2. both WT and mutant Importin beta hinder MT nucleation, chromosome alignment in metaphase and chromosome segregation in anaphase and telophase, regardless of the nucleoporin-binding residues;
3. wild-type Importin beta specifically impairs establishment of the spindle bipolar organization, MT stability, and MT (+) ends. These activities are abolished by mutagenizing two key amino acids in the NUP-binding domain.

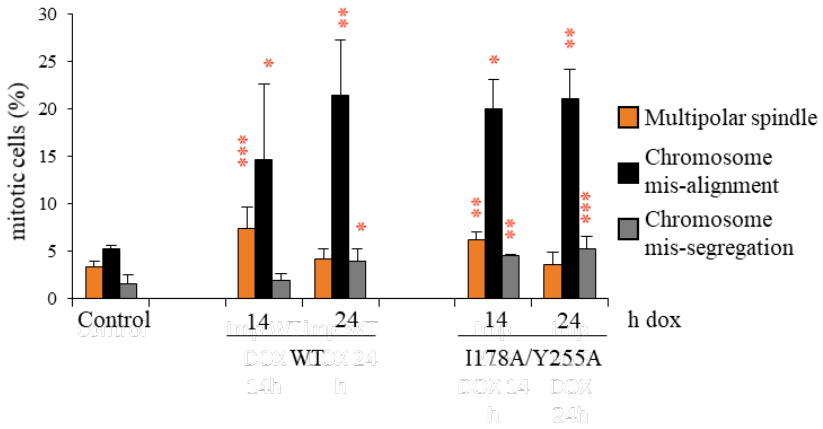

Figure 33: Mitotic abnormalities revealed by IF analysis.
Frequency of mitotic abnormalities in control, WT, and I178A/Y255A-Importin beta induced cells. At least 500 cells in 3 independent experiments were analyzed. $\chi 2$ test compares each class vs its respective in control: *p<0,05; **p<0,01; ***p<0,001. Bars, 5μm.

3.9 WT, but not the NUP-binding defective Importin beta, binds and displaces HURP from MT (+) ends.

HURP is a well-known MT-associated protein; it localizes at MT (+) ends in metaphase, near the KT outer plate, and is known to stabilize MTs. It binds directly Importin beta until RANGTP binding dissociates the complex. The Importin beta region responsible for HURP interaction is not identified yet.
Given that only wild-type but not I178A7Y255A mutant binds HURP in the mitotic interactome, and concomitantly regulates MT stability, it was interesting to assess whether wild-type and I78A7Y255A affect the mitotic pattern of HURP.
To that aim, I performed PLA assays with high resolution (100x objective). As **Figure 34A** shows, PLA products for Importin WT and HURP are abundant in late PM/M cells, and localized along MTs, including at MT (+) ends. Instead, very few PLA signals are seen with the I178A/Y255A mutant (the scatter plot in **Figure 34B** indicates the number of PLA signals per cell).
I then asked whether Importin beta^{WT}, or Importin$^{I178/Y255}$ for comparison, affected HURP localization by staining with anti-HURP antibody dox-induced cells. In **Figure 35**, the canonical HURP localization is shown (*Sillje et al., 2006*). When Importin beta^{WT}, but not the I178A/Y255A mutant, is overexpressed, HURP is largely displaced away from MT (+) ends and distributes throughout MT length, up to the spindle poles (middle row). Thus, Importin beta^{WT} prevents HURP accumulation at MT (+) ends and displaces it towards the poles, where Importin beta, via its binding to dynein, is directed (*Ciciarello et al., 2004*).
This suggests that Importin beta-dependent inhibition of HURP is achieved via displacing it from its sites of action.

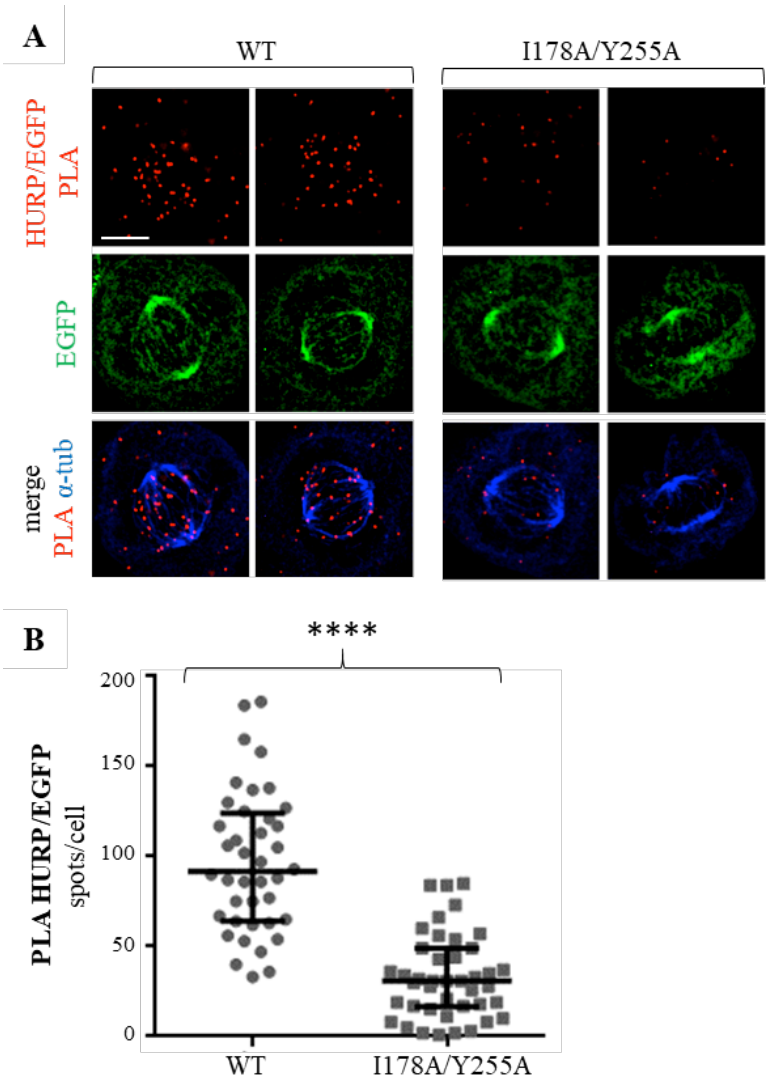

Figure 34: HURP interacts with WT-importin beta at MT (+) ends. A. PLA analysis reveals the sites of HURP-WT Importin beta interactions (100x) in mitotic cells (left panels). On the right, examples of PLA reactions for HURP and Importin beta $^{I178A/Y255A}$. **B.** PLA spots were counted in each cell in the spindle area. N, 40 and 42 analyzed cells in WT and I178A/Y255A samples, respectively. Mann Whitney test, **** p<0,0001. Bar, 5μm.

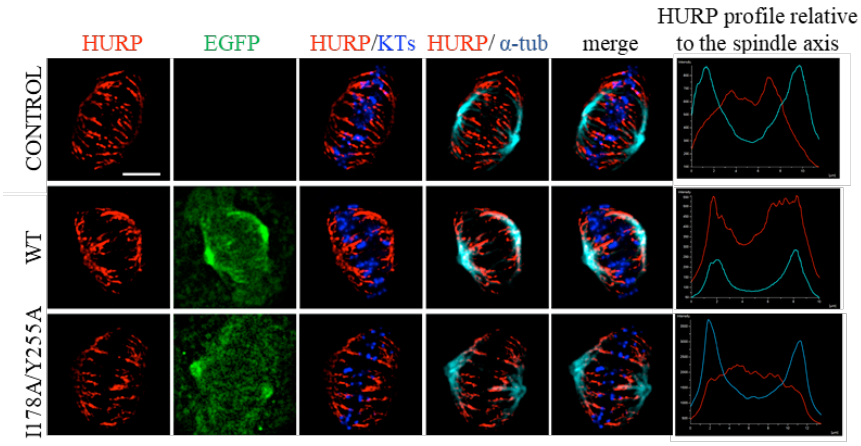

Figure 35: HURP localization is altered upon WT-importin beta overexpression. HURP (red signal) is depicted by staining with an anti-HURP antibody in control, imp-WT and Imp-I178A/Y255A overexpressing cells. Rightmost panels show HURP profile relative to the spindle axis. Bar, 5μm.

3.10. TPX2 localization is not altered by Importin beta overexpression.

A best known Importin beta partner is TPX2, a major RAN-dependent spindle organizer. It was previously demonstrated that the balance between Importin beta and free (unbound) TPX2 is crucial to spindle formation (*Ciciarello et al., 2004*).
I exploited the PLA assay to visualize TPX2 interaction with both WT and I178A/Y255A Importin beta *in-situ* in mitosis. PLA signals are abundant for both WT and I178A/Y255A Importin beta, localizing on mitotic spindle (**Figure 36A**). The graph below (**Figure 36B**) quantifies the frequency of PLA signals per cell,

confirming that interactions have similar abundance with both WT and I178A/Y255A Importin beta.

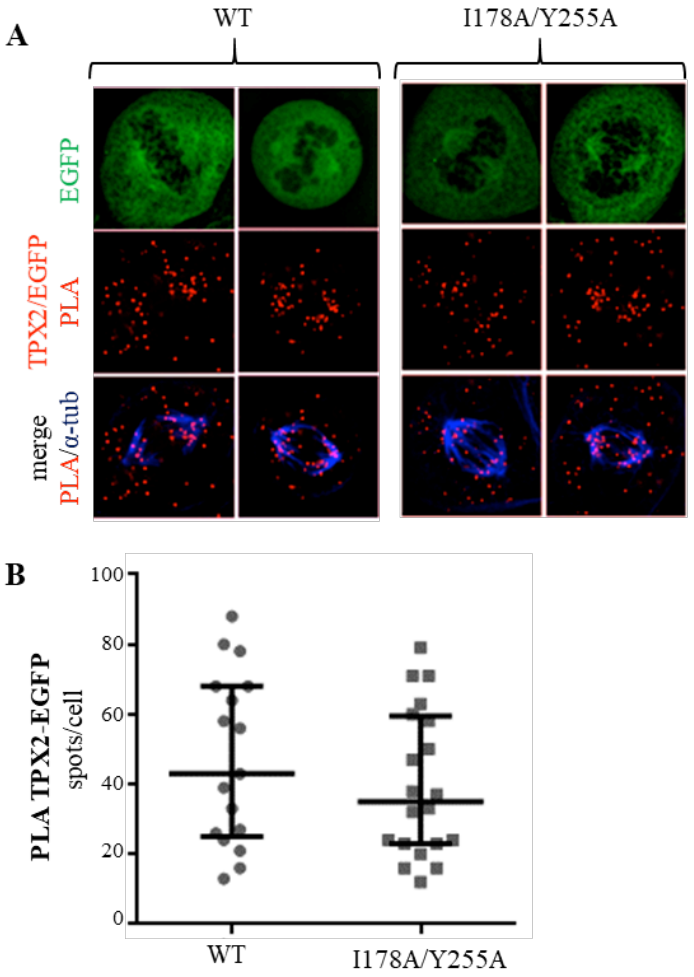

Figure 36: TPX2 interacts with both WT and I178A/Y255A Importin beta. A. PLA analysis reveals the sites of TPX2-Importin beta interactions (100x) in mitotic cells. **B.** PLA spots were counted in each cell in the spindle area. N 16 and 21 cells were analyzed in WT and I178A/Y255A respectively. Mann Whitney test, ns. Bar, 5μm.

To assess whether TPX2 localization was influenced by Importin beta overexpression, WT and I178A/Y255A Importin beta-induced cells were stained for TPX2. As **Figure 37** shows, TPX2 localization at spindle poles is not altered in induced cells, showing the same localization pattern as in non-induced controls. Thus, i) TPX2 binding is not sensitive to mutations in residues I178 and Y255, as expected from its characterized binding to Importin alpha adapters in classical trimeric import complexes; ii) Importin beta inhibitory activity on TPX2 operates via "sequestering" it in situ and rendering it inactive at its sites of action.

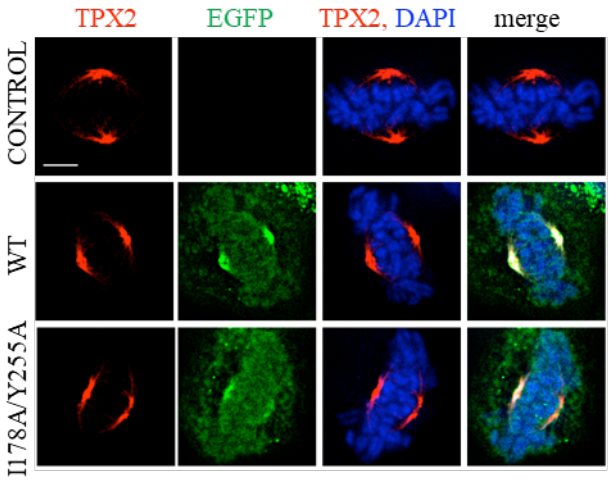

Figure 37: TPX2 localization in mitosis is not affected by Importin beta overexpression. TPX2 (red signal) is depicted by staining with an anti-TPX2 antibody in control, Importin beta^{WT} - and Importin beta$^{I178A/Y255A}$ -overexpressing cells. Bar, 5μm.

DISCUSSION

1. Investigating Importin beta control of mitosis by proteome-wide search of its mitotic partners.

As recalled in the Introduction to this Thesis, Importin beta is overexpressed in many cancer types characterised by high genetic instability. Importin beta was demonstrated to act in control of mitotic division in various studies, but the precise mechanisms were only partially clarified. To begin to unravel these mechanisms, here I have sought to identify Importin beta mitotic interactors.

A recent proteomic study identified Importin beta partners in transport pathways including, in addition to RAN network members and nucleoporins, several nuclear import cargoes, as well as ribosomal proteins and nuclear RNPs (*Kimura et al., 2013*). These studies did not address mitotic processes.

Our data on mitotic interactors highlight the versatile ability of Importin beta to interact with a broad array of mitotic factors. We have identified 272 potential hits. Search in the Mitocheck database confirmed that most identified interactors in our screening were actually required for mitosis, as their inactivation by RNA silencing generated mitotic phenotypes of varying severity. We further confirmed factors with established roles in mitosis by Pubmed search (**Table 1**).

Among previously known mitotic Importin beta interactors, we have identified all components of the RRSU SUMO ligase complex, which is emerging as a temporal regulator of KT functions in mitosis (*Joseph et al., 2004; Gilistro et al., 2017* and also this Thesis). Other important mitotic Importin beta partners identified here are NuSAP and HURP, both MT-associated proteins, involved in MT formation and elongation (*Ribbeck et al., 2006, 2007*) and in the stabilisation of K-fibres (*Sillje et al., 2006*), respectively. Very interestingly, a recent study published while this Thesis was being written indicates that NuSAP

interacts with the RRSU complex in mitosis, but the functional implication of this interaction are not clarified yet (*Mills et al., 2017*). We also find BUB3, a mitotic spindle checkpoint factor, which monitors the stabilisation of correct MT-KT attachments. It was previously shown that Importin beta interaction with BUB3 shields the latter from ubiquitination and proteasome-dependent degradation (*Jiang 2015*). This hints at an additional layer of control of Importin beta/RAN on the spindle assembly checkpoint (SAC).

Among Importin beta interactors which were not necessarily expected in mitosis, we also found many ribonucleoproteins, ribosomal proteins, RNA-binding, splicing and processing factors, and even components of the "translasome" (translation initiation and elongation factors). This is interesting, since RNAs are part of the mitotic apparatus (*Alliegro, 2011*). Some of these proteins were previously reported to play roles in mitotic entry, mitotic spindle regulation, centrosome function, MT/KT regulation or mitotic exit. Interestingly, many of them were never reported to interact with Importin beta.

Following this "classic" approach to protein identification by co-immunoprecipitation of partners and mass spectrometry analysis, I aimed to study these interactions beyond the in vitro level, in mitotic cells. During the dynamic process of mitosis, interactions may change and collecting mitotic cells by synchronisation and mitotic shake off may still be insufficient to get a complete picture including transient, low-abundance interactions. Interactions that vary in abundance in different mitotic stages may be over- or under-represented in our interactomic list. It was therefore important to validate the identified interactions with spatiotemporal resolution in mitotic cells.
We chose the PLA method to validate interactions in intact mitotic cells. PLA provides the temporal and spatial resolution on where and when interactions occur. Indeed, the visualization of Importin

beta interactions with selected partners (RAN, RANBP2, BUB3 and HURP) in intact cells detects their temporal and spatial regulation. These data indicate that PLA provides a highly informative tool that complements that derived from biochemical assays, where detection methods depict the average behaviour of a bulk cell population or cell extract.

2. Generation of stable cell lines for the inducible overexpression of Importin beta.

To address the mechanism(s) through which Importin beta acts with its interactors, I generated stable cell lines in which Importin beta overexpression could be induced. This system should eliminate the problem of technical variability occurring with transient overexpression, used in all previous studies (*Nachury et al., 2001; Ciciarello et al., 2004; Kalab et al., 2006; Roscioli et al., 2012*).

Importin beta, as reported, has a modular structure, which enables it to interact with different protein groups. Given the roles of RANBP2 described in this Thesis, we focused our attention on the NUP-binding domain of Importin beta. I initially attempted to study this domain in two complementary systems. On the one hand, I wanted to study the isolated NUP-binding domain (45-462 region of Importin beta). On the other hand, I used a mutant defective for NUP binding, Importin beta$^{I178A/Y255A}$ (*Bayliss et al 2000*). Importin beta$^{45-462}$ however proved unstable and subjected to proteasome degradation. I therefore continued with Importin beta$^{I178A/Y255A}$ to study the consequences of disrupting the NUP-binding domain.

Stable and inducible cell lines were exploited for most of the experiments here reported; results obtained will be discussed in detail in the following pages.

3. Importin beta controls KT functions via the RRSU complex.

As above, we used the PLA technique to gain temporal and spatial information on Importin beta interactions in mitosis, and, in particular, to assess Importin beta activity on KTs.
RANBP2 normally localizes at KTs after MT attachment *(Joseph et al., 2002 and 2004*). At this time, CRM1, which comprises a KT-associated fraction, normally helps recruiting RANBP2 and the RRSU complex to KTs. We found that Importin beta overexpression leads to defective recruitment of RANBP2 (and the RRSU complex) to KTs at metaphase, due to an increased retention, in the interaction with Importin beta, along MTs in metaphase. When Importin beta is overexpressed, KT-associated CRM1 is evidently not sufficient to balance the Importin beta excess, underlying the failed recruitment of the RRSU to KTs (*Gilistro et al., 2017*).
The RRSU multisubunit SUMO ligase regulates SUMOylation at KTs. Indeed, a growing number of KT proteins, in addition to RANGAP1, are reported to be conjugated with SUMO. Altering the timing, and/or the amount, of KT-associated RRSU might perturb the SUMOylated status of these proteins, and hence the processes in which they operate. An excellent example is Topoisomerase II alpha (TOP2A). TOP2A recruitment to KTs is known to require SUMOylation, in a manner dependent on RANBP2 activity. This modification is involved in TOP2A centromere decatenation functions. I show here that Importin beta overexpression, by impairing RRSU recruitment at KTs in metaphase, also hinders TOP2A SUMO-conjugation and accumulation at centromeres (*Gilistro et al., 2017*). This, and the ensuing impairment in sister centromere decatenation, can contribute to the segregation defects observed in Importin beta overexpressing cells.

4. Importin beta controls MT functional properties via different pathways.

We identified both common and specific partners of Importin beta^{WT} and NUP-binding defective mutant:

1) nuclear import factors, RAN GTPase network components and several more partners identified as partners of endogenous Importin beta in this Thesis (**Table 1**) are also found in the co-IP of Importin beta^{WT}-EGFP (**Table 2**). This indicates that Importin beta^{WT}-EGFP reproduces the same interactions as the endogenous; in other words, addition of the EGFP tag does not alter the profile of interaction of Importin beta;
2) nuclear import factors and RAN GTPase network components interact equally well with Importin beta$^{I178A/Y255A}$-EGFP
3) Importin beta$^{I178A/Y255A}$-EGFP does neither interact with NUP153 nor NUP50 (**Table 2**), as expected for the mutations introduced in the NUP-binding domain. Importin beta$^{I178A/Y255A}$ also shows a substantially reduced interaction with RANBP2 and RANGAP1-SUMO.
4) some mitotic non-nucleoporin factors, e.g. HURP, BUB3, HNRPU and HNRPK, preferentially bind Importin beta^{WT} but not, or very weakly, Importin beta$^{I178A/Y255A}$.

We reasoned that differences in WT and NUP-binding defective Importin beta protein partners might yield different consequences of their overexpression in mitosis. Indeed, in time-lapse videorecording assays, both WT and I178A/Y255A induce an increase in multipolar spindles, but specificities are also observed: namely, Importin beta$^{I178A/Y255A}$ overexpression yields higher mitotic and post-mitotic cell death, while affecting spindle orientation to a lower extent compared to Importin beta^{WT}.
Interestingly, in both WT and I178A/Y255A Importin beta-induced cells mitoses undergo prolonged duration of prometaphase and metaphase.

I therefore assessed MT functional properties in the presence of Importin beta, both WT and NUP binding-defective.
Measuring MT resistance to cold-induced depolymerisation reflects the kinetics of depolymerisation, which is, in turn, a measure of MT dynamic instability (*Cassimeris et al., 1993; Margolis and Wilson, 1998*). In this assay, Importin beta^{WT}, but not the NUP-binding defective, dramatically accelerates cold-induced MT depolymerisation.
On the other hand, both WT and I178A/Y255A Importin beta have a similar inhibitory effect (impairment or delay) when KTs resume MT regrowth after extensive depolymerisation.
These data suggest that Importin beta acts in MT stability and MT nucleation via distinct pathways: two residues, I178 and Y255, required to bind NUPs, are crucial to the former, whereas their mutation is neutral to the latter.
Importin beta^{WT}, which affects MT stability, interacts with HURP (whereas the NUP-binding defective mutant differs in both of these features): it might be speculated, therefore, that the effects of Importin beta overexpression on the MT stability pathway involve, at least in part, the inhibition of HURP activity.

HURP is a well-known MT-associated factor, which binds and stabilises MT (+) ends (*Sillje et al., 2006*). It binds Importin beta directly. Where the RANGTP concentration is high, i.e. in the vicinity of chromosomes, its binding to Importin beta dissociates the complex and releases free HURP in the functional form: indeed, HURP concentrates at the MT plus ends.

Data presented in this Thesis indicate that overexpression of Importin beta results in HURP displacement from its physiological sites to the overall length of MTs. HURP delocalization by Importin beta^{WT} suggests that HURP displacement is due to direct binding.
Importin beta regions involved in HURP binding have not been identified yet. The lack of HURP binding to I178A/Y255A

Importin beta is intriguing and could help to elucidate the mechanisms and domains of their interaction.

5. Importin beta and cancer

As recalled in the introduction, Importin beta, as well as other components of the nuclear transport network, is overexpressed in many cancer types that display high genomic instability. In this field, the most traditionally researched area is nuclear transport dysregulation in cancer.

Indeed, many steps in nuclear transport may be dysregulated in cancer. The most frequently observed include: (i) the altered expression of the nuclear transporters, (ii) altered localisation of nuclear transporters, (iii) the disruption of endogenous nuclear transport inhibitors and (iv) the mechanistic implications of nuclear transporters in mitotic division and genetic instability (*Stelma et al., 2016*).

Importin beta overexpression is proposed to increase the rate of nuclear import. This could help cancer cells to cope with their increased metabolic and proliferative demands compared to non-cancer cells. It may also allow increased nuclear entry of proteins with oncogenic functions.

Alterations in nuclear transport, however, can hardly explain the genomic instability observed in cancer. Moreover, several studies indicate that subtle dysregulation of Importin beta expression readily affects mitotic division and causes significant abnormalities, whereas nucleo-cytoplasmic transport is a more robust process (*Gorlich et al., 2003; Smith et al., 2002*).

Since mitosis is the most sensitive process affected by Importin beta overexpression, it is likely the most sensitive cell cycle stage

in which the pro-tumorigenic effect of Importin beta is exerted. The role of Importin beta as a regulator of spindle formation and function is well described (*Forbes et al., 2015*), in terms of control of the activity of certain SAFs, but also in terms of control of their stability (*Song et al., 2014*). Data in this Thesis highlight Importin beta involvement in the generation of chromosome mis-segregation, which, in turn, can lead to aneuploidy.

The potential of Importin beta in causing genomic instability has generated increasing interest in Importin beta as a potential therapeutic target and in the design of selective inhibitors. This is supported by the observation that cancer cells that overexpress Importin beta, are sensitive to its depletion, displaying reduced proliferation and increased apoptosis when importin beta is silenced or inhibited (*Angus et al., 2014*). These data suggest that cancer cells may be addicted to Importin beta overexpression, identifying the latter as an attractive target for cancer therapies.

Therefore, recent studies are focusing on the synthesis of specific Importin beta inhibitors. One of the best known is importazole (*Soderholm et al., 2011*), designed to impair importin beta interaction with RANGTP. However, no inhibitor to date is free of off-target effects.

More recently, Virna Leaner and colleagues have identified a novel Importin beta inhibitor: INI-43. It proved an effective inhibitor of Importin beta-mediated import; moreover it displayed anticancer activity in vitro and in vivo (*van der Watt et al., 2016)*.
It will be of great interest to develop research into potential therapeutic applications, in which Importin beta-inhibitors could be used in combination with “classical” antimitotic agents.

It is also worth noting that Importin beta overexpression, by altering MT stability, may also sensitise cancer cells to spindle

poisons used in cancer therapy, with MT-stabilizing activity, such as Taxol.

Recent data have demonstrated that RANBP2-depleted cells treated with Taxol had substantially reduced numbers of cells in the G2/M phase, suggesting a defect of these cells in maintaining their mitotic arrest in response to checkpoint activation. Consistent with induced slippage through mitosis, authors observed also a reduction of surviving cells (*Mills et al., 2017*).

A similar behaviour was described for NuSAP depletion, which renders cells highly sensitive to treatment with Taxol (*Okamoto et al., 2015*). This finding suggests that the presence of NuSAP1 renders cells more resistant to the toxic effects of anti-tubulin chemotherapeutics and might predict Taxol sensitivity in tumours deleted for NuSAP1 (*Emanuele et al., 2011*).

Finally, a similar trend was reported for RANBP1, a major RANGTP regulator overexpressed in cancer (*Rensen et al., 2008*), the depletion of which results in increased MT stabilization (*Tedeschi et al., 2007*) and confers increased sensitivity to Taxol (*Rensen et al., 2009*).

These studies provide examples of the functional interaction between Importin beta (or RAN-network members or effectors) and spindle poisons. They suggest that the elevated levels of these factors in cancer cells, though being tumorigenic, might confer at the same time a molecular "vulnerability" that can be exploited to increase the selectivity and effectiveness of MT-targeting drugs in those cancers. Indeed, this has been experimentally demonstrated for the association between high RANBP2 and Vinorelbine in a subset of colon cancers (*Vecchione et al., 2016*).

We therefore speculate that Importin beta overexpression might “sequester” factors (like RANBP2 or NuSAP), mimicking the

effects of depletion of those factors, and confer sensitivity to MT drugs. Indeed, preliminary data (P. Rovella, A, Verrico and P. Lavia, in preparation) are in agreement with this hypothesis, and show that Importin beta overexpressing cells exposed to Taxol undergo increased mitotic cell death.

Overall, therefore, the data obtained in this thesis suggest that Importin beta overexpression is not only a cancer marker and an initiator of genomic instability, but may also be viewed as an "Achille's heel" in cancer therapy.

MATERIALS AND METHODS

Cell culture, synchronization and treatments

Human HeLa epithelial cells (American Tissue Culture Collection, CCL-2) were grown in DMEM supplemented with 10% fetal bovine serum, 2% l-glutamine, 2.5% HEPES and 2% penicillin/streptomycin at 37°C in 5% CO_2. Where indicated, cells were synchronized in 9μM RO3306 (SML0569, Sigma) for 20 hours to induce G2 arrest, then released for 30-60 minutes in fresh medium to progress synchronously towards mitotic phase.

Generation of stable cell lines for importin beta derivatives

Inducible expression vectors for importin beta-EGFP and its derivatives were derived from the enhanced piggyBac (ePiggyBac) vector. The vector carries a tetracycline-responsive promoter element (TRE Tight) followed by a multicloning site. To generate epB-Bsd-TT- importin beta-EGFP, the importin beta-EGFP sequence was PCR- amplified from the pIB-GFP construct (*Ciciarello et al., 2004*) using the oligos pEGFP-N1_Fw_ClaI (GGCATCGATAGCGCTACCGGACTC) and pEGFP-N1_Rv (ACCTCTACAAATGTGGTATGGC). The PCR fragment was digested and cloned between the ClaI and NotI sites in the epB- Bsd-TT plasmid, in which the Puromycin resistance gene in the original epB-Puro-TT (*Rosa et al., 2014*) was replaced with a Blasticidin resistance gene (Bsd R). In addition to the WT importin beta, we generated vectors for importin beta mutants: I178A/Y255A (NUP binding-defective), 45-462(N/C del, also called "beta star"), 1-462 (C-del) and 45-876 (N-del). The vector scaffold and importin beta constructs are presented in **Figure 38.** HeLa cells were co-trasfected with vector and hypb7 (encoding the transposase gene) using Lipofectamine (Invitrogen). 24 hours after transfection, the medium was replaced with Tet-free DMEM supplemented with 3μg/ml blasticidine-S hydrochloride (Sigma). Blasticidine-S-resistant foci were expanded and tested for expression after

administration of 1 μg/ml doxycyline hyclate (dox, Santa Cruz Biotechnology).
For most functional experiments in this thesis cells were induced for 14 or 24 hours; for PLA assays 8 hour-dox induction was chosen, due to the amplification step the technique includes.

Immunofluorescence (IF)
For immunofluorescence assays, cells were grown on coverslips coated wit poly-L-lysine (Sigma) and fixed in 3.7% paraformaldehyde/30 mM sucrose for 10 minutes, permeabilized with 0.1% Triton X-100 for 5 minutes and incubated with Glycine 0.1 M for 10 minutes. Alternatively, cells were fixed in ice-cold methanol (-20°C) for 6 minutes.
Blocking and incubation with primary antibodies (in PBS, 0.05% Tween-20, 3% bovine serum albumin) were at room T°. Primary antibodies are listed in **Table 3**. Secondary antibodies were conjugated to fluorescein isothiocyanate (FITC), Cy3, Alexa-Fluor 647 (Cy5), 7-amino-4-methylcoumarin-3- acetic acid (AMCA) (Jackson Immunoresearch Laboratories), or Texas Red (Vector Laboratories). DNA was stained with 0.1 μg/ml 4,6-diamidino-2-phenylindole (DAPI, Sigma Aldrich) and coverslips were mounted in Vectashield (Vector Laboratories).

MT depolymerisation and regrowth assays
For MT stability studies cells were placed on ice for 20 minutes; at the end of incubation on ice they were washed twice in PTEMF buffer (20 mM PIPES, 10mM EGTA, 1mM $MgCl_2$ in dH_2O) to preserve resistant MTs, fixed (3.7% paraformaldehyde, 0.2% Triton X-100 in PTEMF), then processed for IF as described above. In MT regrowth assays, after depolymerization, cells were incubated for 35 minutes on ice, pre-warmed media was then added, and cells were incubated at 37°C for 1 minute. At the end of incubation at 37°C they were fixed as described above.

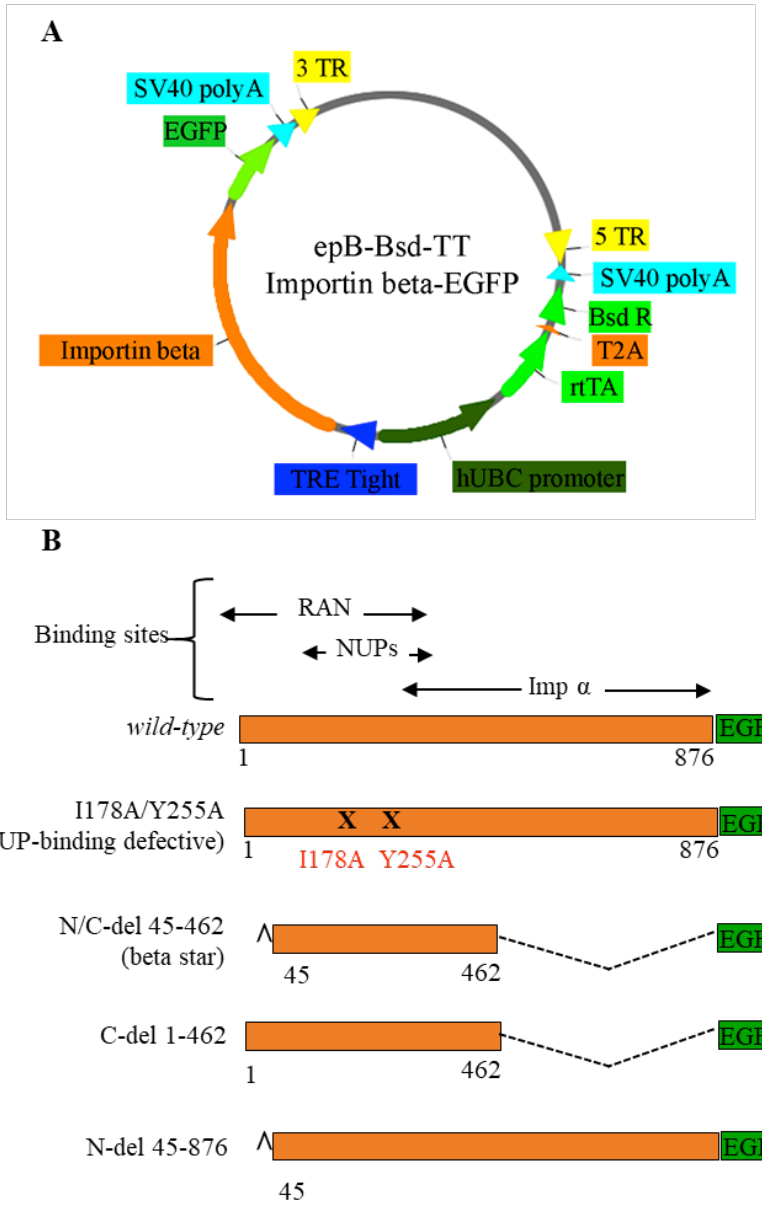

Figure 38: Construction of stable cell lines. **A**. The epB-BSD-TT vector. **B**. Importin beta constructs used to generate stable cell lines.

Protein	Host	Source	Catalog #	Dilution (IF and PLA)	Dilution (WB)
BUB3	rabbit	Abcam	ab133699	1:250	1:10000
CREST	human	Antibodies Inc.	15-234-0001	1:20	-
CRM1	mouse	Santa Cruz	sc-74455	1:100	-
CRM1	rabbit	Santa Cruz	sc-5595	1:50	-
GFP	rabbit	Abcam	ab6556	1:1000	1:500
GFP	mouse	Roche	11 814 460 001	1:1000	1:1000
HURP	rabbit	Abcam	ab70744	1:100	1:500
Importin beta	mouse	Abcam	ab2811	1:2000	1:2000
Importin beta	mouse	Sigma	I2534	-	1:4000
Importin beta	mouse	Becton Dickinson	610560	-	1:250
NuSAP	rabbit	Abcam	ab93779	1:500	1:1000
NUP 153	mouse	Abcam	(ab24700	1:500	1:500
RAN	mouse	Becton Dickinson	61034	-	1:1000
RAN	rabbit	Santa Cruz	SC-20802	1:50	1:200
RANBP1	rabbit	Santa Cruz	SC-28576	1:100	1:200
RANBP2	rabbit	Santa Cruz	ab64726	1:2000	1:1000
RanGAP1	mouse	Santa Cruz	sc-28322	1:100	1:500
SUMO 2-3	mouse	MBL	M114-3	1:200	-
TopoIIalpha	rabbit	TopoGEN	TG2011-1	1:300	-
TPX2	mouse	Abcam	ab32795	1:250	1:250
alpha-tubulin	chicken	Abcam	ab89984	1:50	-
alpha-tubulin	mouse	Sigma	T5168	1:3000	-

Table 3: List of primary antibodies.

Proximity ligation assay (PLA)

Cells grown on coverslips or 4-chamber Culture Slides (Falcon), fixed and blocked as for IF, were processed for PLA in four steps: i) incubation of fixed cell slides with primary specific antibodies for the proteins under examination; ii) incubation with secondary antibodies conjugated with complementary oligonucleotide tails (PLA probes, conventionally called PLUS and MINUS); iii) ligase addition; when the target proteins interact or are very close, the ligation step will produce a DNA circle; iv) rolling circle amplification. PLA steps are schematized in **Figure 39**. All steps were performed using the Duolink® In Situ Detection Reagents Red DUO92008 (Sigma-Aldrich). Cells were fixed, blocked, and incubated with primary antibodies as for conventional IF; our chosen combination of primary antibodies were mouse and rabbit IgGs for each protein pair (all the antibodies used are listed in **Table 3**). Anti-mouse MINUS and anti-rabbit PLUS PLA probes (PLA Duolink In Situ PLA Probe Anti-Rabbit PLUS, DUO92002, and Duolink In Situ PLA Probe Anti-Mouse MINUS, DUO92004, respectively, Sigma-Aldrich) were then added (diluted 1:5 in PBS containing 0.05% Tween-20 and 3% bovine serum albumin) and incubated in a pre-heated humidity chamber (60 minutes, 37°C). Subsequent ligation (30 minutes, 37°C) and amplification (60 minutes, 37°C) steps were performed following the Olink Bioscience protocol. To localize PLA signals, cells were co-stained using DAPI or chicken anti-alpha tubulin antibody, followed by AMCA-conjugated anti-chicken IgG.

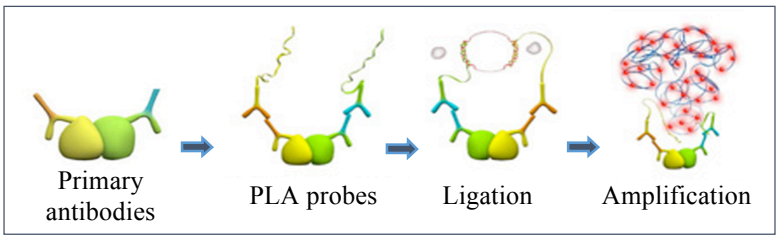

Figure 39: Proximity ligation assay (PLA) steps. See text for details.

Time-lapse imaging
Cells were seeded in 4/8 wells μ-Slide (chambered coverslip, 80426/ 80821, IbiTreat; Ibidi). During recording, cultures were kept at 37°C in a T°- and CO_2-controlled stage incubator (Okolab). Cultures were recorded under a Ti Eclipse automated inverted microscope (Nikon) equipped with a DS-Qi1MC camera, an Intensilight C-HGFIE lamp, and the NIS-Elements 3.1 software (Nikon). Images were taken using a 60x, 0.7 NA objective: phase every 15 min, GFP-fluorescence every 60 minutes.

High resolution image acquisition
Fixed samples were analyzed under a Nikon Eclipse 90i microscope equipped with a Qicam Fast 1394 CCD camera (Qimaging). Single-cell images were taken using an immersion oil 100x objective (NA 1.3) using NIS-Elements AR 3.2 and 4.0 software (Nikon); three-dimensional deconvolution of 0.3-0.4 μm z-serial optical sections was performed using the "AutoQuant" deconvolution module of NIS-Element AR 3.2/4.0. Creation of image projections from z-stacks was performed using the Maximum Intensity Projection (MIP, for quantitative analyses), and Extended Depth of Focus (EDF) functions of NIS-Element AR 3.2/4.0. IF signals were quantitatively analyzed using NIS-Element AR 3.2/4.0 (nd2file format); external background correction was applied and the sum intensity of signals on indicated selected areas was measured. PLA spots were counted on images acquired on three dimensions. Images were processed using the MIP method and activating the "spot detection" and “count objects” tools of NIS-Element AR 3.2/4.0. All figures shown in this work represent MIP images unless specified otherwise. Images were processed with Adobe Photoshop CS 8.0.

Automated PLA images acquisition, segmentation and measurement

Automated PLA analysis workflow is schematized in **Figure 40**. Images from cell samples processed for PLA in 4-chamber culture slides were acquired under a Nikon Eclipse Ti microscope equipped with the Perfect Focus System, a Nikon DS-Qi1 Cooled Digital Monochrome Camera and a 40x objective (PlanFuor, N.A. 0,75, Nikon), using the Nis-Elements AR 3.2 software. A grid (15 fields per well) was generated, saved and re-loaded for all acquisitions, with a focus adjustment step performed for each new slide. In order to collect the whole spindle-associated signal from rounded-up mitoses, images were acquired over an 8µm range along the z-dimension (z-step: 0.8 µm). An *ad-hoc* macro was then applied for the automated generation of 2D projection (Maximum Intensity Projection) of all acquired images within a single .nd2 file at the end of the acquisition process.

Segmentation is used to partition a digital image to identify objects or extract relevant information. After a background subtraction step, image segmentation on Maximum Intensity Projections was performed using Nis-Elements HC 4.2 (Nikon). We used the Threshold function of the Nis-Elements HC 4.2 software to define the regions in the images where we intended to perform the analysis (nuclei, mitotic chromosomes, mitotic spindles), based on signal intensity, size and circularity. Segmentation masks for mitotic chromosomes and spindles were saved and automatically reloaded for each new image set. All steps were performed on a single .nd2 file for the whole experiment acquisition. For the automated analysis of the PLA signals, the "Automated measurements results" function of the software was used: Sum Intensity values for PLA signals within the selected masks were obtained and exported to Excel. Data were statistically analyzed using Graph Pad Prism 6.

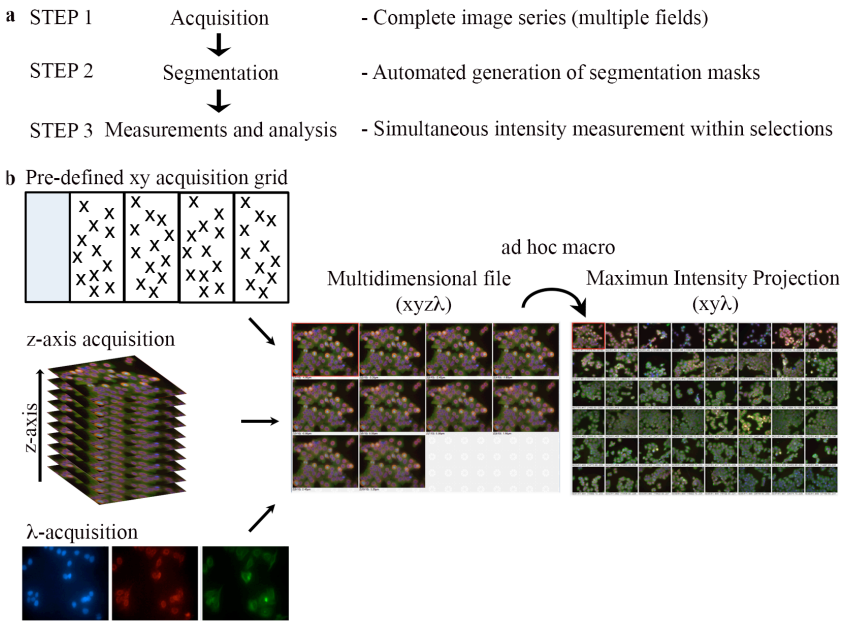

Figure 40: Automated image acquisition and analysis. **A.** The diagram shows the development of a three-step protocol for automated microscopy acquisition and analysis: 1) acquisition of complete image series, giving one multidimensional file as the output; 2) segmentation step, enabling the automated generation of the regions of interest; 3) simultaneous measurements of segmented images in one step. **B.** Image acquisition protocol. For each PLA combination, a single file is composed of 60 xy points (acquired using a pre-defined xy acquisition grid), each containing the information from 10 z-stacks and 3 wave-lengths (λ: DAPI; FITC; TRITC). The generated multidimensional file (xyzλ) is processed using an ad-hoc macro for the automated generation of the Maximum intensity projection (xyλ), which is then analyzed as described in step 2 and 3

Western immunoblotting (WB)
Cells were lysed in RIPA buffer (50 mM Tris-HCl pH 8, 150 mM NaCl, 1% NP40, 1 mM EGTA, 1 mM EDTA, 0.1% SDS, 0.25% sodium deoxycholate) supplemented with protease (05892791001, Roche) and phosphatase (PhoSTOP, 04906837001, Roche) inhibitors. 40 μg extract per lane were separated through SDS-PAGE and transferred to nitrocellulose filters (Protran BA83, Whatman) in a semi-dry system (BIO-RAD). Blocking and antibody incubations were in TBS (10 mM Tris-HCl pH 7.4, 150 mM NaCl) containing 0.1%Tween 20 and 5% low fat milk (1 hour, room T°). Primary antibodies are listed in **Table 3**. HRP-conjugated antibodies (Santa Cruz Biotechnology) were revealed using the ECL system (GE Healthcare) on Hyperfilm-ECL films (GE Healthcare).

Endogenous importin beta co-immunoprecipitation.
The importin beta-1 interactome was captured from mitotic HeLa cells using anti-Importin beta-1 antibody (Sigma-Aldrich I2534). Mouse IgG antibodies (Santa Cruz Biotechnology sc-2025) were used as a control for non-specific binding proteins. RO336-released mitotic cells were centrifuged at low speed, washed twice at 4°C in cold PBS/0.5 mM PMSF and resuspended in lysis buffer (50 mM Tris HCl (pH 8.0), 150 mM NaCl, 1% NP40) containing protease (05892791001, Roche) and phosphatase (PhoSTOP, 04906837001, Roche). After incubation on ice for 30 minutes, cells were gently homogenized using a Dounce homogenizer. After centrifugation (14000 rpm, 4°C, 20 minutes), the supernatant was quantified by Bradford assay and 1 mg of lysate was immediately precleared with Protein G-Sepharose at 4°C for 1 hour (15 μl of resin slurry per mg total protein). Importin beta-1 interacting partners were co-immunoprecipitated overnight on a rotating wheel at 4°C from the precleared mitotic supernatant with anti-importin-beta-1 antibody covalently coupled to Protein G-Sepharose (1 mg protein sample: 2μg covalent immune-conjugate, home made). For control, the same amount of precleared mitotic

extract was incubated with mouse non-specific IgG covalently coupled with Protein G-Sepharose. The mixture was then centrifuged at 3000 rpm, 4°C for 15 minutes and the pellet was washed 5x in lysis buffer and again centrifuged as above. After the last centrifugation step, protein complexes were eluted from the beads by a gentle 3x washing cycle in 15 µl of 0.1 M glycine buffer (pH 2.5) at RT. After centrifugation (3000 rpm, RT, 5 minutes), the pH of the eluted proteins was neutralized by adding 1.5 M Tris HCl pH 8.0.

GFP-TRAP

RO3306-synchronyzed stable cell lines, induced for 16 hours with dox, were collected by mechanical shake off 1 hour after RO3306 wash out. Cells were then centrifuged at low speed, washed twice at 4°C in cold PBS/0.5 mM PMSF and resuspended in lysis buffer (50 mM Tris HCl (pH 8.0), 150 mM NaCl, 1% NP40) containing protease (05892791001, Roche) and phosphatase (PhoSTOP, 04906837001, Roche). After incubation on ice for 30 minutes, cells were gently homogenized using a Dounce homogenizer; the extent of mechanical disruption of the cells was checked by microscopic observation. After centrifugation (14000 rpm, 4°C, 20 minutes), the supernatant was quantified by Bradford assay and 1 mg of lysate was immediately precleared with blocked agarose beads (bab-20) at 4°C for 1 hour (15 µl of resin slurry per mg total protein). EGFP-interacting partners were co-immunoprecipitated overnight on a rotating wheel at 4°C from the precleared mitotic supernatant with GFP-TRAP beads (Chromoteck) (1 mg protein sample: 15 µl GFP-TRAP beads), also recognizing the EGFP version. The mixture was then centrifuged at 3000 rpm, 4°C for 15 minutes and the pellet was washed 5x in lysis buffer and again centrifuged as above. The supernatant constitutes the SUP fraction. After the last centrifugation step, protein complexes were eluted from the beads by a gentle 3x washing cycle in 15 µl of 0.1 M glycine buffer (pH 2.5) at RT. The 3 washing cycles yielded the 3 elution fractions (E1, E2, E3), in which the first (E1) has the

highest amount of eluted proteins. After centrifugation (3000 rpm, RT, 5 minutes), the pH of the eluted proteins was neutralized by adding 1.5 M Tris HCl pH 8.0.

Proteomics and data analysis

The co-IP material was processed by Orbitrap MS analysis, by the group of Prof. Eugenia Schininà (Sapienza University of Rome). Aliquots of co-immunoprecipitates were diluted in Laemmli buffer and fractionated through SDS-PAGE on 4-20% Mini-PROTEAN TGX™ gel (Bio-Rad). After colloidal Coomassie staining, gel slices were processed as described and tryptic peptide mixtures extracted and desalted. LC-MS/MS analyses were performed by reverse phase chromatography (C_{18}, 5 µm particle size, 200 Å pore size; Magic C18 AQ, Michrom), on an Ultimate3000 system (Dionex, Sunnyvale, CA, USA). Peptides eluted by a two-step gradient of ACN containing 0.1% FA (5-40% in 120 minutes, and 40-85% in 15 minutes) at 300 nl/minute flow rate, were directly injected into an LTQ-Orbitrap XL mass spectrometer (Thermo-Fisher Scientific). Data-dependent tandem MS were performed with full precursor ion scans (MS1) collected at 30,000 resolution, with an automatic gain control (AGC) of 1×10^6 ions, and maximal injection time of 1000 ms. The five most intense (>200 counts) ions with charge states ≥+2 were selected for collision-induced dissociation (CID). Dynamic exclusion was active with 90 ms exclusion for ions selected twice within a 30 ms window. For MS/MS scanning, the minimum MS signal was set to 500, activation time to 30 ms, target value to 10,000 ions, and injection time of 100 ms. All MS/MS spectra were collected using a normalized collision energy of 35% and an isolation window of 2 Th. Spectra were searched against the *Homo sapiens* UniProtKB database (release 2016-07-09, 20154 sequences) and common contaminant proteins using the software package MaxQuant (version 1.5.5.1, Max Planck Institute of Biochemistry, Martinsried, Germany). We set oxidation (methionine) and acetylation (protein N-terminus) as variable modifications,

carbamidomethylation (cysteine) as fixed modification, mass tolerance of 20 ppm for the precursor ion (MS) and of 0.5 Da for the fragment ions (MSMS). High-confidence peptide-spectral matches were filtered at <1% false discovery rate.
Due to the high sensitivity and resolving power of the mass spectrometric platform used here, together with the high power of the Andromeda search engine in assigning peptide sequences from tandem MS data, the MaxQuant platform yielded a large set of starting data. As a first step of our established proteomic pipeline in data analysis of the original outputs, we discarded identifications for all annotated potential laboratory contaminants (i.e. keratins from experimenters, proteins from reagents etc.), and for hits that the search engine identified in a reverse decoy database used as a false negative control. To extract meaningful information from this cleaned data, a higher confidence matrix was set up by filtering out protein groups recognized with a low confidence level. In particular, we removed proteins which the Andromeda algorithm identified based on an extremely limited number of assigned peptide sequences (i.e.: i) number of unique peptides ≤0, ii) number of peptides ≤1, and iii) only by a peptide carrying a post-translational modification, or iv) through less than 3 MS/MS spectra), or v) presenting an ambiguous association, e.g. associated with multiple genes). Finally, mass spectra intensity difference values between the pulled-down proteins by anti-importin beta and by a non-specific mouse IgG were statistically compared using the Perseus software package (version 1.5.5.3, Max Planck Institute of Biochemistry, Martinsried, Germany) (p-value <0.05). The resultant list of the 272 high confidence hits was analyzed by data mining against the interphase list, the Mitocheck database version 2.1 (based on EnsEMBL v89, http://www.mitocheck.org/gene.shtml), and the latest releases of UNiProt http://www.uniprot.org/, Biogrid https://thebiogrid.org/, MiCroKITS http://microkit.biocuckoo.org/ and Pubmed https://www.ncbi.nlm.nih.gov/pubmed.

REFERENCES

- Alliegro M.C. The centrosome and spindle as a ribonucleoprotein complex. (2011). *Chromosome Res.* 19:367-76.
- Arnaoutov A, Azuma Y, Ribbeck K, Joseph J, Boyarchuk Y, Karpova T, McNally J, Dasso M. (2005). Crm1 is a mitotic effector of Ran-GTP in somatic cells. *Nat Cell Biol*. 7:626-32.
- Azuma Y, Arnaoutov A, Anan T, Dasso M. (2005). PIASy mediates SUMO-2 conjugation of Topoisomerase-II on mitotic chromosomes. EMBO J. 24:2172-82.
- Azuma Y, Arnaoutov A, Dasso M. (2003). SUMO-2/3 regulates topoisomerase II in mitosis. *J Cell Biol*. 163(3):477-87.
- Bachant J, Alcasabas A, Blat Y, Kleckner N, Elledge SJ. (2002). The SUMO-1 isopeptidase Smt4 is linked to centromeric cohesion through SUMO-1 modification of DNA topoisomerase II. *Mol Cell.* 9:1169-82.
- Bayliss R, Littlewood T, Stewart M. (2000) Structural basis for the interaction between FxFG nucleoporin repeats and importin-beta in nuclear trafficking. *Cell* 102(1):99-108.
- Bednenko J, Cingolani G, Gerace L. (2003) Importin beta contains a COOH-terminal nucleoporin binding region important for nuclear transport. *J Cell Biol.* 162(3):391-401.
- Carazo-Salas RE, Guarguaglini G, Gruss OJ, Segref A, Karsenti E, Mattaj IW. (1999). Generation of GTP-bound Ran by RCC1 is required for chromatin-induced mitotic spindle formation. *Nature.* 400:178-81.
- Cassimeris. (1993). Regulation of microtubule dynamic instability. *Cell Motil Cytoskeleton.* 26:275-81.
- Caudron M, Bunt G, Bastiaens P, Karsenti E. (2005) Spatial coordination of spindle assembly by chromosome-mediated signaling gradients. *Science.* 309:1373-6.
- Cavazza T, Vernos I. (2016). The Ran GTPase pathway: from nucleo-cytoplasmic transport to spindle assembly and beyond. *Front Cell Dev Biol*. 11;3:82.
- Chi NC, Adam SA. (1997). Functional domains in nuclear import factor p97 for binding the nuclear localization sequence receptor and the nuclear pore. *Mol Biol Cell*. 8:945-956.
- Chook YM, Süel KE. (2011). Nuclear import by karyopherin-βs: recognition and inhibition. *Biochim. Biophys. Acta.* 1813:1593-606.
- Christensen MO, Larsen MK, Barthelmes HU, Hock R, Andersen CL, Kjeldsen E, Knudsen BR, Westergaard O, Boege F, Mielke C. (2002).

Dynamics of human DNA topoisomerases IIalpha and IIbeta in living cells. *J Cell Biol*. 157(1):31-44.

- Ciciarello M, Mangiacasale R, Lavia P. (2007). Spatial control of mitosis by the GTPase Ran. *Cell Mol Life Sci.* 64:1891-914.
- Ciciarello M, Mangiacasale R, Thibier C, Guarguaglini G, Marchetti E, Di Fiore B, Lavia P. (2004). Importin β is transported to spindle poles during mitosis and regulates Ran-dependent spindle assembly factors in mammalian cells. *J Cell Sci*. 117, 6511-6522.
- Cingolani G, Petosa C, Weis K, Müller CW. (1999) Structure of importin-beta bound to the IBB domain of importin-alpha. *Nature.* 399(6733):221-229.
- Cingolani G, Bednenko J, Gillespie MT, Gerace L. (2002) Molecular basis for the recognition of a nonclassical nuclear localization signal by importin beta. *Mol Cell.* 10(6):1345-1353.
- Clarke PR, Zhang C. (2008) Spatial and temporal coordination of mitosis by Ran GTPase. *Nat Rev Mol Cell Biol*. 9:464-77.
- Cubeñas-Potts C, Srikumar T, Lee C, Osula O, Subramonian D, Zhang XD, Cotter RJ, Raught B, Matunis MJ. (2015) Identification of SUMO-2/3 modified proteins associated with mitotic chromosomes. *Proteomics.* 15: 763–772.
- Cubeñas-Potts C, Goeres JD, Matunis MJ. (2013). SENP1 and SENP2 affect spatial and temporal control of sumoylation in mitosis. *Mol Biol Cell*. 24:3483-95
- Dawlaty MM, Malureanu L, Jeganathan KB, Kao E, Sustmann C, Tahk S, Shuai K, Grosschedl R, van Deursen JM. (2008). Resolution of sister centromeres requires RanBP2-mediated SUMOylation of topoisomerase IIalpha. *Cell.* 133:103-15.
- Debec A, Detraves C, Montmory C, Geraud G, and Wright M. (1995). Polar organization of gamma-tubulin in acentriolar mitotic spindles of Drosophila melanogaster cells. *J Cell Sci*. 108(Pt 7), 2645–2653.
- Dou H, Huang C, Van Nguyen T, Lu LS, Yeh ET. (2011). SUMOylation and de-SUMOylation in response to DNA damage. *FEBS Lett.* 585:2891-6.
- Eifler K, Vertegaal AC. (2015) SUMOylation-mediated regulation of cell cycle progression and cancer. *Trends Biochem Sci*. 40:779-93.
- Emanuele M J, Elia AE, Xu Q, Thoma CR, Izhar L, Leng Y, Guo A, Chen Y-N, Rush J, Hsu PW, Yen H-C, and Elledge SJ. (2011). Global identification of modular cullin-RING ligase substrates. *Cell* 147,459–474.

- Flotho A., Werner, A. (2012). The RanBP2/RanGAP1*SUMO1/Ubc9 complex: a multisubunit E3 ligase at the intersection of sumoylation and the Ran GTPase cycle. *Nucleus*. 3:429-32.
- Forbes DJ, Travesa A, Nord MS, Bernis C. (2015). Nuclear transport factors: global regulation of mitosis. *Curr Opin Cell Biol*. 35:78-90.
- Gilistro, E., de Turris V, Damizia M, Verrico A, Moroni S, De Santis R, Rosa A, Lavia P. (2017). Importin beta and CRM1 control a RANBP2 spatiotemporal switch essential for mitotic kinetochore function. *J. Cell Sci.* 130:2564-2578.
- Görlich D, Seewald MJ, Ribbeck K. (2003). Characterization of Ran-driven cargo transport and the RanGTPase system by kinetic measurements and computer simulation. EMBO J. 22(5):1088-100.
- Görlich D, Kostka S, Kraft R, Dingwall C, Laskey RA, Hartmann E, Prehn S. (1995). Two different subunits of importin cooperate to recognize nuclear localization signals and bind them to the nuclear envelope. *Curr Biol* 5:383 – 392.
- Goshima G, Mayer M, Zhang N, Stuurman N, Vale D. (2008). Augmin: a protein complex required for centrosome-independent microtubule generation within the spindle. *J Cell Biol.* 181:421-9.
- Hashizume C, Kobayashi A, Wong RW. (2013). Down-modulation of nucleoporin RanBP2/Nup358 impaired chromosomal alignment and induced mitotic catastrophe. *Cell Death Dis*. 4:e854.
- Harel A, Chan RC, Lachish-Zalait A, Zimmerman E, Elbaum M, Forbes DJ. (2003). Importin beta negatively regulates nuclear membrane fusion and nuclear pore complex assembly. *Mol Biol Cell*. 14:4387-4396.
- Hay RT. (2006). Role of ubiquitin-like proteins in transcriptional regulation. *Ernst Schering Res Found Workshop.* (57):173-92.
- He S, Miao, X, Wu Y, Zhu X, Miao X, Yin H, He Y, Li C, Liu Y, Lu X, Chen Y, Wang Y, Xu X. (2016). Upregulation of nuclear transporter, Kpnβ1, contributes to accelerated cell proliferation- and cell adhesion-mediated drug resistance (CAM-DR) in diffuse large B-cell lymphoma. *J. Cancer. Res. Clin. Oncol.* 142(3):561-72.
- Heald R and Khodjakov A. (2015). Thirty years of and search capture: the complex simplicity of mitotic spindle assembly. *J Cell Biol*. 211(6):1103-11.
- Holland AJ, Cleveland DW. (2012) Losing balance: the origin and impact of aneuploidy in cancer. *EMBO Rep*. 13(6):501-14.

- Hsia KC, Wilson-Kubalek EM, Dottore A, Hao Q, Tsai KL, Forth S, Shimamoto Y, Milligan RA, Kapoor TM. (2014). Reconstitution of the augmin complex provides insights into its architecture and function. *Nat Cell Biol.* 16:852-63.
- Izaurralde E, Kutay U, von Kobbe C, Mattaj IW, Görlich D. (1997). The asymmetric distribution of the constituents of the Ran system is essential for transport into and out of the nucleus. *EMBO J.* 16: 6535 – 6547.
- Jiang H, He X, Feng D, Zhu X, Zheng Y. (2015). RanGTP aids anaphase entry through Ubr5-mediated protein turnover. *J. Cell Biol.* 211:7-18.
- Johnson ES. (2004) Protein modification by SUMO. *Annu Rev Biochem.* 73:355-82.
- Joseph J, Liu ST, Jablonski SA, Yen TJ, Dasso M. (2004). The RanGAP1-RanBP2 complex is essential for microtubule-kinetochore interactions in vivo. *Curr Biol*.14:611-7.
- Joseph J, Tan SH, Karpova TS, McNally JG, Dasso M. (2002). SUMO-1 targets RanGAP1 to kinetochores and mitotic spindles. *J Cell Biol*. 156:595-602.
- Kalab P, Heald R. (2008). The RanGTP gradient - a GPS for the mitotic spindle. *J Cell Sci.* 121:1577-86.
- Kaláb P, Pralle A, Isacoff EY, Heald R, Weis K. (2006). Analysis of a RanGTP-regulated gradient in mitotic somatic cells. *Nature*. 440:697-701.
- Keryer G, di Fiore B, Celati C, Lechtreck KF, Mogensen M, Delouvée A, Lavia P, Bornens M and Tassin AM. (2003). Part of Ran is associated with AKAP450 at the centrosome. Involvement in microtubule organizing activity. *Mol. Biol. Cell* 14, 4260-4271.
- Khodjakov AL, Cole R. W, Oakley BR., and Rieder CL. (2000). Centrosome-independent mitotic spindle formation in vertebrates. Curr. Biol. 10, 59–67.
- Kimura M, Imamoto N. (2014). Biological significance of the importin-β family-dependent nucleocytoplasmic transport pathways. *Traffic.* 15:727-48
- Kimura M, Okumura N, Kose S, Takao T, Imamoto N. (2013). Identification of cargo proteins specific for importin-β with importin-α applying a stable isotope labeling by amino acids in cell culture (SILAC)-based in vitro transport system. *J. Biol. Chem.* 288:24540-9.

- Kutay U, Izaurralde E, Bischoff FR, Mattaj IW, Görlich D. (1997) Dominant-negative mutants of importin-beta block multiple pathways of import and export through the nuclear pore complex. *EMBO J.* 16(6):1153-1163.
- Lawo S, Bashkurov M, Mullin M, Ferreria MG, Kittler R, Habermann B, Tagliaferro A, Poser I, Hutchins JR, Hegemann B, Pinchev D, Buchholz F, Peters JM, Hyman AA, Gingras AC, Pelletier L. (2009). HAUS, the 8-subunit human Augmin complex, regulates centrosome and spindle integrity. *Curr Biol.* 19:816-26.
- Lee MT, Bachant J. (2009). SUMO modification of DNA topoisomerase II: trying to get a CENse of it all. *DNA Repair* 8:557-68.
- Mahajan R, Delphin C, Guan T, Gerace L and Melchior F. (1997). A small ubiquitin-related polypeptide involved in targeting RanGAP1 to nuclear pore complex protein RanBP2. *Cell*. 88:97–107.
- Margolis and Wilson. (1998). Microtubule treadmilling: what goes around comes around. *Bioessays.* 20:830-6.
- Martens-de Kemp SR, Nagel R, Stigter-van Walsum M, van der Meulen IH, van Beusechem VW, Braakhuis BJ, et al. (2013) Functional genetic screens identify genes essential for tumor cell survival in head and neck and lung cancer. *Clin Cancer Res*. 19(8):1994–2003.
- Matunis, M.J., Coutavas, E., Blobel, G. (1996). A novel ubiquitin-like modification modulates the partitioning of the Ran-GTPase-activating protein RanGAP1 between the cytosol and the nuclear pore complex. *J Cell Biol*. 135:1457-70.
- Matunis, M.J., Wu, J., Blobel, G. (1998) SUMO-1 modification and its role in targeting the Ran GTPase-activating protein, RanGAP1, to the nuclear pore complex. *J Cell Biol.* 140:499-509.
- Meunier S., Vernos I. (2016). Acentrosomal microtubule assembly in mitosis: the where, when and how. *Trends Cell Biol* 26:80-7.
- Meunier, S., and Vernos, I. (2011). K-fibre minus ends are stabilized by a RanGTP-dependent mechanism essential for functional spindle assembly. Nat. Cell Biol.13, 1406–1414.
- Mills CA, Suzuki A, Arceci A, Mo JY, Duncan A, D, Emanuele MJ. (2017). Nucleolar and spindle-associated protein 1 (NuSAP1) interacts with a SUMO E3 ligase complex during chromosome segregation. *J Biol Chem*. 292(42):17178-17189.
- Morris JR. (2010). More modifiers move on DNA damage. *Cancer Res.* 70:3861-3.

- Mishra, R. K., Chakraborty, P., Arnaoutov, A., Fontoura, B. M. A.,and Dasso, M. (2010). The Nup107-160 complex and gamma-TuRC regulate microtubule polymerization at kinetochores. *Nat. Cell Biol.* 12, 164–169.
- Moschos SJ., Mo YY. (2006) Role of SUMO/Ubc9 in DNA damage repair and tumorigenesis. *J Mol Histol.* 37 (5-7):309-19.
- Nachury, M.V., Maresca, T.J., Salmon, W.C., Waterman-Storer, C.M., Heald, R., Weis, K. (2001). Importin beta is a mitotic target of the small GTPase Ran in spindle assembly. *Cell* 104:95-106.
- Okamoto A, Higo M, Shiiba M, Nakashima D, Koyama T, Miyamoto I, Kasama H, Kasamatsu A, Ogawara K, Yokoe H, Tanzawa H, Uzawa K. (2015). Down-regulation of Nucleolar and Spindle-Associated Protein 1 (NUSAP1) expression suppresses tumor and cell proliferation and enhances anti-tumor effect of paclitaxel in oral squamous cell carcinoma. *PLoS One.* 10:e0142252
- Ohtsubo M, Okazaki H, Nishimoto T. (1989). The RCC1 protein, a regulator for the onset of chromosome condensation locates in the nucleus and binds to DNA. *J Cell Biol.* 109:1389-1397.
- Otsuka S, Iwasaka S, Yoneda Y, Takeyasu K, Yoshimura SH. (2008) Individual binding pockets of importin-beta for FG-nucleoporins have different binding properties and different sensitivities to RanGTP. *Proc Natl Acad Sci U S A* 105(42):16101-16106.
- Petry S., Groen A.C., Ishihara K., Mitchison T.J., Vale R.D. (2013). Branching microtubule nucleation in Xenopus egg extracts mediated by augmin and TPX2. *Cell* 152:768-77.
- Petry S., Pugieux C., Nédélec F.J., Vale R.D. (2011). Augmin promotes meiotic spindle formation and bipolarity in Xenopus egg extracts. *Proc Natl Acad Sci USA.* 108:14473-8.
- Pichler A, Gast A, Seeler JS, Dejean A, and Melchior F. (2002). The nucleoporin RANBP2 has SUMO E3 ligase activity. *Cell* 108: 109-120.
- Porter A.C., Farr C.J. (2004). Topoisomerase II: untangling its contribution at the centromere. *Chromosome Res.* 12(6):569-83.
- Potts PR. (2009). The Yin and Yang of the MMS21-SMC5/6 SUMO ligase complex in homologous recombination. *DNA Repair* 8:499-506.
- Rensen, W.M., Mangiacasale, R., Ciciarello, M., Lavia, P. (2008). The GTPase Ran: regulation of cell life and potential roles in cell transformation. *Front Biosci*. 1;13:4097-121.

- Rensen, Roscioli E, Tedeschi A, Mangiacasale R, Ciciarello M, Di Gioia SA, Lavia P. (2009). RanBP1 downregulation sensitizes cancer cells to taxol in a caspase-3-dependent manner. *Oncogene*. 28:1748-58
- Ribbeck, K., Groen, A. C., Santarella, R., Bohnsack, M. T., Raemaekers, T., Kcher,T., et al. (2006). NuSAP, a mitotic RanGTP target that stabilizes and cross-links microtubules. *Mol. Biol. Cell* 17, 2646–2660.
- Ribbeck, K., Raemaekers, T., Carmeliet, G., and Mattaj, I. W. (2007). A role for NuSAP in linking microtubules to mitotic chromosomes. *Curr. Biol.* 17,230–236.
- Ritterhoff, T., Das, H., Hofhaus, G., Schröder, R.R., Flotho, A., Melchior, F. (2016). The RanBP2/RanGAP1*SUMO1/Ubc9 SUMO E3 ligase is a disassembly machine for Crm1-dependent nuclear export complexes. *Nat Commun.* 10;7:11482.
- Rosa A, Papaioannou MD, Krzyspiak JE and Brivanlou AH (2014). miR-373 is regulated by TGFβ signaling and promotes mesendoderm differentiation in human Embryonic Stem Cells. *Dev Biol* 391: 81-88
- Roscioli E, Bolognesi A, Guarguaglini G, Lavia P. (2010). Ran control of mitosis in human cells: gradients and local signals. Biochem Soc Trans. 38(6):1709-14.
- Roscioli E, Di Francesco L, Bolognesi A, Giubettini M, Orlando S, Harel A, Schininà ME, Lavia P. (2012) Importin beta negatively regulates multiple aspects of mitosis including RANGAP1 recruitment to kinetochores. *J Cell Biol.* 196:435-50.
- Ryu H., Furuta M., Kirkpatrick D., Gygi S.P., Azuma Y. (2010). PIASy-dependent SUMOylation regulates DNA topoisomerase IIalpha activity. *J Cell Biol.* 191(4):783-94.
- Salina, D., Enarson, P., Rattner, J.B., Burke, B. (2003). Nup358 integrates nuclear envelope breakdown with kinetochore assembly. *J Cell Biol.* 162:991-1001.
- Schellhaus, A.K., De Magistris, P., Antonin, W. Nuclear reformation at the end of mitosis. *J. Mol. Biol.* 428:1962-85 (2016).
- Sillje, H. H., Nagel, S., Korner, R., and Nigg, E. A. (2006). HURP is a Ran-importin beta-regulated protein that stabilizes kinetochore microtubules in the vicinity of chromosomes. *Curr. Biol*. 16, 731–742.
- Söderberg O, Gullberg M, Jarvius M, Ridderstråle K, Leuchowius KJ, Jarvius J, Wester K, Hydbring P, Bahram F, Larsson LG, Landegren U. (2006) Direct observation of individual endogenous protein complexes in situ by proximity ligation. *Nat Methods*. 3(12):995-1000.

- Söderberg O, Leuchowius KJ, Gullberg M, Jarvius M, Weibrecht I, Larsson LG, Landegren U. (2008) Characterizing proteins and their interactions in cells and tissues using the in situ proximity ligation assay. *Methods*. 45(3):227-32.
- Soderholm JF, Bird SL, Kalab P, Sampathkumar Y, Hasegawa K, Uehara-Bingen M, Weis K, Heald R. (2011) Importazole, a small molecule inhibitor of the transport receptor importin-β. *ACS Chem Biol*. 6(7):700-8
- Song L, Craney A, Rape M. (2014). Microtubule-dependent regulation of mitotic protein degradation. *Mol Cel*l. 53(2):179-92.
- Sorokin, A. V., Kim, E. R., and Ovchinnikov, L. P. (2007). Nucleocytoplasmic transport of proteins. Biochemistry 72, 1439–1457.
- Stelma, T., Chi, A., van der Watt, P.J., Verrico, A., Lavia, P., Leaner V.D. (2016) Targeting nuclear transporters in cancer: Diagnostic, prognostic and therapeutic potential. *IUBMB Life.* 68:268-80.
- Ström, A.C., and Weis, K. (2001). Importin-beta-like nuclear transport receptors. *Genome Biol.* 2:S3008.
- Swaminathan, S., Kiendl, F., Körner, R., Lupetti, R., Hengst, L., Melchior, F. (2004). RanGAP1*SUMO1 is phosphorylated at the onset of mitosis and remains associated with RanBP2 upon NPC disassembly. *J Cell Biol.* 164:965-71
- Tedeschi A, Ciciarello M, Mangiacasale R, Roscioli E, Rensen WM, Lavia P. (2007). RANBP1 localizes a subset of mitotic regulatory factors on spindle microtubules and regulates chromosome segregation in human cells. *J Cell Sci.* 120(Pt 21):3748-61.
- Torosantucci, L., M. De Luca, G. Guarguaglini, P. Lavia, and F. Degrassi. (2008). Localized RanGTP accumulation promotes microtubule nucleation at kinetochores in somatic mammalian cells. *Mol. Biol. Cell*. 19:1873–1882.
- Tulu, U.S., C. Fagerstrom, N.P. Ferenz, and P. Wadsworth. (2006). Molecular requirements for kinetochore-associated microtubule formation in mammalian cells. *Curr. Biol.* 16:536–41.
- Uehara R., Nozawa R.S., Tomioka A., Petry S., Vale R.D., Obuse C., Goshima G. (2009). The augmin complex plays a critical role in spindle microtubule generation for mitotic progression and cytokinesis in human cells. *Proc Natl Acad Sci USA*. 106:6998-7003.
- Ungricht, R., Kutay, U. (2017). Mechanisms and functions of nuclear envelope remodelling. *Nat. Rev. Mol. Cell Biol.* 18:229-45.

- van der Watt PJ, Chi A, Stelma T, Stowell C, Strydom E, Carden S, Angus L, Hadley K, Lang D, Wei W, Birrer MJ, Trent JO, Leaner VD. (2016) Targeting the Nuclear Import Receptor Kpnβ1 as an Anticancer Therapeutic. *Mol Cancer Ther*. 15(4):560-73.
- van der Watt, P.J., Stowell, C.L., Leaner, V.D. (2013) The nuclear import receptor Kpnβ1 and its potential as an anticancer therapeutic target. Crit Rev Eukaryot Gene Expr 23:1-10
- van der Watt, P.J., Maske, C.P., Hendricks, D.T., Parker, M.I., Denny, L., Govender, D., Birrer, M.J., Leaner, V.D. (2009). The Karyopherin proteins, Crm1 and Karyopherin beta1, are overexpressed in cervical cancer and are critical for cancer cell survival and proliferation. *Int J Cancer.* 124:1829-40.
- Vecchione, L., Gambino, V., Raaijmakers, J., Schlicker, A., Fumagalli, A., Russo, M., Villanueva, A., Beerling, E., Bartolini, A., Mollevi, D.G., et al. (2016). A vulnerability of a subset of colon cancers with potential clinical utility. *Cell.* 165:317-30.
- Vetter IR, Nowak C, Nishimoto T, Kuhlmann J, Wittinghofer A. (1999) Structure of a Ran-binding domain complexed with Ran bound to a GTP analogue: implications for nuclear transport. *Nature* 398(6722):39-46.
- Walther TC, Askjaer P, Gentzel M, Habermann A, Griffiths G, Wilm M, Mattaj IW, Hetzer M. (2003). RanGTP mediates nuclear pore complex assembly. Nature. 424:689-694
- Wan, J., Subramonian, D., Zhang, X.D. (2012). SUMOylation in control of accurate chromosome segregation during mitosis. *Curr Protein Pept Sci*. 13:467-81.
- Weaver L.N., Walczak C.E. (2015). Spatial gradients controlling spindle assembly. *Biochem Soc Trans.* 43(1):7-12.
- Werner A, Flotho A, Melchior F. (2012) The RANBP2/RanGAP1*SUMO1/Ubc9 complex is a multisubunit SUMO E3 ligase. *Mol Cell*. 46:287-98.
- Wollman, R., Cytrynbaum, E. N., Jones, J. T., Meyer, T., Scholey, J.M., and Amogilner, A. (2005). Efficient chromosome capture requires a bias in the 'search-and-capture' process during mitotic-spindle assembly. Curr. Biol. 15,828–832.
- Wu, J., Matunis, M.J., Kraemer, D., Blobel, G., Coutavas, E. (1995). Nup358, a cytoplasmically exposed nucleoporin with peptide repeats, Ran-GTP binding sites, zinc fingers, a cyclophilin A homologous domain, and a leucine-rich region. *J Biol Chem*. 270:14209-13.

- Yan W, Li R, He J, Du J, Hou J. (2015) Importin β1 mediates nuclear factor-κB signal transduction into the nuclei of myeloma cells and affects their proliferation and apoptosis. *Cell Signal*. 27(4):851-9.
- Yang L, Hu B, Zhang Y, Qiang S, Cai J, Huang W, Gong C, Zhang T, Zhang S, Xu P, Wu X, Liu J. (2015). Suppression of the nuclear transporter-KPNβ1 expression inhibits tumor proliferation in hepatocellular carcinoma. *Med Oncol*. 32(4):128
- Yokoyama, H., Nakos, K., Santarella-Mellwig, R., Rybina, S., Krijgsveld, J., Koffa, M. D., et al. (2013). CHD4 Is a RanGTP-Dependent MAP that Stabilizes microtubules and regulates bipolar spindle formation. Curr. Biol. 23,2443–2451.
- Zhu, J., Wang, Y., Huang H, Yang Q, Cai J, Wang Q, Gu X, Xu P, Zhang S, Li M, Ding H, Yang L. (2016) Upregulation of KPNβ1 in gastric cancer cell promotes tumor cell proliferation and predicts poor prognosis. *Tumour Biol.* 37:661-72.
- Zuccolo, M., Alves, A., Galy, V., Bolhy, S., Formstecher, E., Racine, V., Sibarita, J.B., Fukagawa, T., Shiekhattar, R., Yen, T., Doye, V. (2007). The human Nup107-160 nuclear pore subcomplex contributes to proper kinetochore functions. *EMBO J.* 26:1853-64.

LIST OF PUBLICATIONS

- Di Francesco L[*], **Verrico A**[*], Asteriti IA, Rovella P, Cirigliano P, Guarguaglini G, Schininà ME and Lavia P. (2018) Visualization of human karyopherin beta-1/importin beta-1 interactions with protein partners in mitotic cells by co-immunoprecipitation and proximity ligation assays. *Sci Rep*. 8(1):1850. doi: 10.1038/s41598-018-19351-9.
  * first co-authors
- Gilistro E, de Turris V, Damizia M, **Verrico A**, Moroni S, De Santis R, Rosa A and Lavia P. (2017). Importin beta and CRM1 control a RANBP2 spatiotemporal switch essential for mitotic kinetochore function. *J Cell Sci* 130(15):2564-2578. doi: 10.1242/jcs.197905.
- Di Cesare E, **Verrico A**, Miele A, Giubettini M, Rovella P, Coluccia A, Famiglini V, La Regina G, Cundari E, Silvestri R, and Lavia P. (2017). Mitotic cell death induction by targeting the mitotic spindle with tubulin-inhibitory indole derivative molecules. *Oncotarget* 8(12):19738-19759. doi: 10.18632/oncotarget.14980.
- Stelma T, Chi A, van der Watt PJ, **Verrico A**, Lavia P, and Leaner VD. (2016). Targeting nuclear transporters in cancer: Diagnostic, prognostic and therapeutic potential. *IUBMB Life* 68(4):268-80. doi: 10.1002/iub.1484.
- La Regina G, Bai R, Coluccia A, Famiglini V, Pelliccia S, Passacantilli S, Mazzoccoli C, Ruggieri V, **Verrico A**, Miele A, Monti L, Nalli M, Alfonsi R, Di Marcotullio L, Gulino A, Ricci B, Soriani A, Santoni A, Caraglia M, Porto S, Da Pozzo E, Martini C, Brancale A, Marinelli L, Novellino E, Vultaggio S, Varasi M, Mercurio C, Bigogno C, Dondio G, Hamel E, Lavia P, Silvestri R. (2015). New Indole Tubulin Assembly Inhibitors Cause Stable Arrest of Mitotic Progression, Enhanced Stimulation

of Natural Killer Cell Cytotoxic Activity, and Repression of Hedgehog-Dependent Cancer. *J Med Chem*. 58(15):5789-807. doi: 10.1021/acs.jmedchem.5b00310.

Invited reviews

- **Verrico A,** Schininà ME, Di Francesco L, Ilari A, Morea V and Lavia P. (2016). Nuclear Transport Receptors: Moonlighting Proteins Aberrantly Expressed in Cancer. *EC Proteomics and Bioinformatics* 1.1: 01-03.
- Giubettini M, van der Watt P, **Verrico A**, de Turris V, Leaner V, Lavia P. KPNB1 (karyopherin (importin) beta 1). 2013. *Atlas Genet Cytogenet Oncol Haematol.* 17(10):689-698.

Submitted manuscripts

- La Regina G, Bai R, Coluccia A, Naccarato V, Famiglini V, **Verrico A**, Rovella P, Mazzoccoli C, Da Pozzo E, Cavallini C, Martini C, Vultaggio S, Dondio G, Varasi M, Mercurio C, Hamel E, Lavia P, Silvestri R. New 6- and 7-Heterocyclyl-1H-indole Derivatives as Potent Tubulin Assembly and Cancer Cell Growth Inhibitors with Potential to treat Human Liver Carcinoma and Glioblastoma. Manuscript submitted.